CASPASE-3 PROMOTES CELL PROLIFERATION AND INHIBITS DNA-DAMAGE INDUCED NECROSIS IN COLORECTAL CANCER

by

Matthew Francis Brown

B.S., California State University: Sacramento, 2007

Submitted to the Graduate Faculty of

School of Medicine in partial fulfillment

of the requirements for the degree of

Doctor of Philosophy

University of Pittsburgh

2013

UNIVERSITY OF PITTSBURGH

SCHOOL OF MEDICINE

This dissertation was presented

by

Matthew Francis Brown

It was defended on

December 3, 2013

and approved by

Satdarshan P.S. Monga, M.D., Professor, Pathology and Medicine

Robert Sobol, Ph.D., Associate Professor, Pharmacology and Chemical Biology

Gutian Xiao, Ph.D., Associate Professor, Microbiology and Molecular Genetics

Reza Zarnegar, Ph.D., Professor, Pathology

Dissertation Advisor: Jian Yu, Ph.D., Associate Professor, Pathology and Radiation Oncology

Copyright © by Matthew Francis Brown

2013

CASPASE-3 PROMOTES CELL PROLIFERATION AND INHIBITS DNA-DAMAGE INDUCED NECROSIS IN COLORECTAL CANCER

Matthew Francis Brown, Ph.D.

University of Pittsburgh, 2013

Colorectal cancer leads to over 50,000 deaths in the United States each year. Many colon cancer patients are diagnosed at late stages where surgical options are limited and require chemo- and or radiotherapy. A hallmark of cancer is the accumulation of genetic mutations resulting in dysfunction of the apoptotic response, which can lead to reduced sensitivity to chemo- and radiotherapy. Damaged cells can also die through necrosis, previously thought to be an unregulated process. Recent studies have begun to suggest that necrosis is an orderly event that occurs in cells when apoptosis is blocked, and kinases, rather than p53, play a critical role in activating downstream necrotic machinery. The high incidence of p53 mutation and apoptotic dysfunction in cancer requires development of new treatment strategies, with activation of necrosis a potentially beneficial option. However, little is known about the relationship between different forms of cell death and how it is regulated.

Caspases are cysteine proteases best known to play a pivotal role in the execution of apoptosis. However, recent studies indicate roles beyond apoptosis. Interestingly, Caspase-8 inhibits autophagy and necrosis, whereas caspase-3 promotes survival of cancer cells following radiation therapy. In an effort to determine the role of caspase-3 in colon cancer cell survival and proliferation, we generated caspase-3 knockout HCT-116 colon cancer cells using recombinant adeno-associated virus (AAV)-mediated gene targeting. Interestingly, we observe an unexpected decrease in proliferation and altered mitochondrial morphology in caspase-3

knockout cells, compared to wild-type cells. Furthermore, caspase-3 knockout cells exhibit reduced oxidative phosphorylation and increased glutamine dependence. In addition to altered metabolism, caspase-3 knockout cells are more sensitive to DNA damaging agents, including 5-FU, etoposide and camptothecin due to an increase in programmed necrosis. This is in stark contrast to wild-type cells that die largely via apoptosis. Having shown that caspase-3 promotes survival and proliferation of colon cancer cells and reduces sensitivity to multiple DNA damaging agents we hypothesize that targeting its non-apoptotic functions may improve the effectiveness of chemotherapeutic agents.

TABLE OF CONTENTS

LIST OF TABLES

LIST OF FIGURES

PREFACE

Acknowledgements

It has been a long road getting to this point and I could not have made the journey alone. Thank you to all that have helped me along the way. To my family and friends: Spencer, Leslie, Cole, Sam, Ed, Patrick, Rachael and Liz, you have been what kept me going when the road got rough. I would like to thank my partner in crime, Dana and her amazing family. Mark, Laverne, Marissa and Molly have been incredible from day one. Their love and support is appreciated beyond words. I could not have achieved this goal without the tireless guidance of my mentors, Jian and Lin. They have been unbelievable throughout this journey.

Above all else, this is for my father, who would be proud to know I never stopped reading brochures.

1.0 COLORECTAL CANCER

1.1 ABSTRACT

Colorectal cancer (CRC) is one of the predominant cancers worldwide, annually affecting 1.23 million new patients, resulting in the death of 500,000 and accounting for 10% of all human cancers [1, 2]. In the United States it stands as the fourth most common cancer and the second leading cause of cancer related death [3]. The current five year survival rate for all CRC patients is 60% with only 6% of metastatic patients, indicating the need for improved therapeutic options [4].

1.1.1 Risk factors

Similar to other cancers, colorectal cancer incidence seems to be intimately tied to both environmental and genetic factors. CRC risk increases by age with 80% of patients being between the age of 55 and 85 years old. [5-7]. Other common risk factors include excess body weight, lack of physical activity and first-degree relatives with CRC (Table 1).

Table 1: Colon Cancer Risk Factors

Colorectal Cancer Risk Factors	
Non-preventable Factors	**Preventable Factors**
Age older than 50 years	High-fat diet
Previous CRC diagnosis	Low consumption of fruits & vegetables
Polyps	Lack of physical activity
First degree relative with CRC	Obesity
Ulcerative colitis	Smoking
Crohn's disease	Alcohol consumption

1.1.2 Evolution of CRC

Colorectal tumors are found in a number of different forms ranging from benign tumor to invasive cancer, with the majority of tumors arising from epithelial tissue. Newly discovered colorectal tumors within a patient are classified as nonneoplastic polyps, neoplastic polyps or cancer. Upwards of 30% of Americans will develop polyps in their lifetime and 70-90% of CRCs arise from adenomatous polyps [8]. Roughly 30% of all polyps are hyperplastic and at no risk for future malignancy. However, others are adenomatous and considered premalignant [9]. Half of polyps greater than 2 cm in diameter ultimately advance to malignant tumors. Currently the best method for polyp treatment is surgical removal [10].

1.1.3 Multiple gene mutations lead to CRC

The advancement of normal epithelial tissue to CRC is associated with multiple molecular events. Although CRC can be caused by a single gene mutation, it is predominately initiated as the result of multiple genetic mutations (average of 5-7) in genes that regulate cell cycle and/or apoptosis including tumor suppressor, oncogenes and genes associated with repair/stability [11-13]. Tumor suppressor

mutations are the most common mutations found in hereditary CRC and are the causative mutations behind both Familial Adenomatous Polyposis (FAP) and Juvenile Polyposis Syndrome (JPS). Mutation in stability genes, including mismatch repair genes are another large contributor to hereditary CRC and are the causative mutation behind Lynch syndrome. Table 2 summaries current knowledge of genetic mutations found in CRC and their corresponding diseases [11, 12].

Table 2: Known gene mutations in CRC

Gene	Function	Syndrome	Hereditary Pattern	Predominant Cancer
APC	Tumor Suppressor	FAP	Dominant	Colon, intestine
AXIN2	Tumor Suppressor	Attenuated polyposis	Dominant	Colon
TP53	Tumor Suppressor	Li-Fraumeni	Dominant	Multiple
STK11	Tumor Suppressor	Peutz-Jeghers	Dominant	Multiple
PTEN	Tumor Suppressor	Cowden	Dominant	Multiple
BMPR1A	Tumor Suppressor	Juvenile polyposis	Dominant	Gastrointestinal
SMAD4	Tumor Suppressor	Lynch	Dominant	Gastrointestinal
MLH1	Repair/Stability	Lynch	Dominant	Multiple
MSH2	Repair/Stability	Lynch	Dominant	Multiple
MSH6	Repair/Stability	Lynch	Dominant	Multiple
PMS2	Repair/Stability	Lynch	Dominant	Multiple
EPCAM	Repair/Stability	Lynch	Dominant	Multiple
MYH	Repair/Stability	Attenuated polyposis	Recessive	Colon
BLM	Repair/Stability	Bloom	Recessive	Multiple
KIT	Oncogene	Familial GIST	-	GIST
PDGFRA	Oncogene	Familial GIST	-	GIST

Adapted from http://www.cancer.gov/cancertopics/pdq/genetics/colorectal/healthprofessional/page2

1.1.4 Prevention and treatment

Observational studies of the average risk population has shown that the use of multiple drugs including Non-steroidal Anti-inflammatory Drugs (NSAIDs), estrogens, folic acid and calcium might help prevent the development of CRC [10, 14]. Additional approaches to reduce risk of developing CRC include eating a low fat diet, exercising regularly and limiting alcohol/tobacco use [6, 10]. In the event of CRC diagnosis there are currently six standard treatments widely used. The first line of therapeutic intervention is surgery including both local excision and surgical resection of the colon. In addition to surgical removal of malignant tissue, patients are concurrently treated with radiofrequency ablation, cryosurgery, chemotherapy, radiation therapy or targeted therapies. Historically, chemotherapy has been the most commonly used approach. Currently there are 28 CRC approved chemotherapeutic drugs. Targeted therapy has gained significant momentum in recent years due to optimism that it might provide greater therapeutic response with fewer side effects than are generally associated with chemotherapy. Currently monoclonal antibodies and Vascular Endothelial Growth Factor (VEGF) inhibitors are the only FDA approved targeted therapies for CRC. Unfortunately while targeted therapies have shown great efficacy in initial response, a large proportion of patients will develop resistance within two years of initial treatment. Despite our best efforts, the current five year survival rate for all colorectal cancer patients is 60% with 6% of metastatic patients surviving that period. Clearly new therapeutic approaches are urgently needed [10, 11].

1.2 MOLECULAR ALTERATIONS IN COLORECTAL CANCER

The hallmarks of cancer are composed of eight biological abnormalities acquired during the multistep development of malignant tumors. They include: sustained proliferative signaling, evasion of growth suppression signaling, cell death resistance, acquired replication immortality, increased angiogenesis, reprogramming of energy metabolism, evasion of immune destruction and activation of invasion and metastasis [15]. The underlining of these hallmarks is genetic instability which allows for the acquisition of advantageous phenotypes and inflammation which fosters multiple hallmark functions.

1.2.1 Cancer cells demonstrate unregulated proliferation

Cell proliferation is a vital function for mammals and is required for normal development, repair and general maintenance of tissue. However, uncontrolled cell proliferation is a major cause behind tumorigenesis. Progression of normal tissue to malignant tumor is a stepwise process composed of acquisition of genetic mutations leading to altered phenotype. In the context of CRC, one of the most common first steps towards malignancy is loss of Wingless-type MMTV Integration Site Family (Wnt) signaling regulation. The Wnt/β-catenin pathway is responsible for directing growth and patterning during embryonic development. Additionally, the pathway directs postembryonic regulation of stem cell populations in the intestine [16]. A common mutation acquired by CRC patients is inactivation of the Adenomatous Polyposis Coli (APC) tumor suppressor. APC is responsible for down-regulation of transcriptional activation mediated by the β-catenin and T Cell Transcription Factor 4 (TCF4). Mutant APC is defective in this

activity resulting in unchecked activation of β-catenin signaling and increased cell proliferation (Figure 1) [17].

V-Ki-ras2 Kirsten Rat Sarcoma Viral Oncogene Homolog (KRAS) is a GTPase responsible for down regulating the v-raf-1 Murine Leukemia Viral Oncogene/Mitogen-activated Protein Kinase (RAF/MAPK) proliferative pathways (Figure 1). A single amino acid substitution most commonly occurring in codons 12 and 13 is responsible for constitutive activation. The transformed protein that results is implicated in various malignancies, including lung adenocarcinoma, mucinous adenoma, ductal carcinoma of the pancreas and colorectal carcinoma [18-21]. Current estimates suggest that KRAS is mutated in 35-45% of CRCs [22]. In addition to increased cell proliferation KRAS mutation is an indicator of resistance to Epithelial Growth Factor Receptor (EGFR) based therapies [20].

Transforming Growth Factor Beta (TGFβ) is a member of the transforming growth factor family of cytokines which are multifunctional peptides that regulate proliferation, adhesion, differentiation, migration and other functions in a large number of cell types. Many cells contain TGFβ receptors and ligation of the receptor is able to both positively and negatively regulate many other growth factors [23]. In the context of CRC, TGFβ is a potent inhibitor of epithelial cell growth. CRC cells with high rates of microsatellite instability were found to harbor mutations in TGFβ leading to its inability to inhibit cell growth (Figure 1) [24-26].

Tumor Protein p53 (p53) is one of the most commonly mutated proteins in all malignancies [27, 28]. p53 is stabilized in response to a number of stimuli including DNA damage, hypoxia, viral infection or oncogenic activation. Activation of p53 results in a number of diverse manners including cell cycle arrest, apoptosis, senescence, differentiation and antiangiogenesis. p53 activity is highly regulated by post translational modifications including

phosphorylation, dephosphorylation and acteylation. Active p53 signals a number of downstream proteins including Cyclin-dependent Kinase Inhibitor 1 (p21), Growth Arrest and DNA-damage-inducible Protein (GADD45), 14-3-3σ, BCL2-associated X Protein (Bax), TNF Receptor Superfamily Member 6 (Fas), Death Receptor 5 (DR5), Spermatogenic Leucine Zipper 1 (Tsp1), Insulin-like Growth Factor Binding Protein 3 (IGF-BP3) and others [29]. Approximately half of all CRCs show *p53* gene mutations with greater frequencies in distal colon and rectal tumors and lower frequencies in proximal tumors and tumors harboring microsatellite instability (Figure 1) [30]. Furthermore, mutated p53 is highly overexpressed in CRC tumors [31]. Multiple point mutations have been documented and a patient's therapeutic response is strongly tied to their mutation status. Specifically, point mutations in the conserved domains of p53 were inherently more aggressive than mutations outside of them and mutations of codon 175 were highly aggressive [32, 33].

The final phase in CRC progression is metastasis. It has become increasingly clear that there are a number of molecular alterations that lead tumors to become increasingly invasive including increased matrix metalloproteinase leading to loss of basement membrane and decreased epithelial gene expression leading to epithelial-mesenchymal transition (EMT) (Figure 1) [34-36]. Progression from normal epithelium to localized colorectal carcinoma and final metastatic disease is a stepwise process composed of acquired genetic alterations leading to altered cell signaling often resulting in activation of multiple pathways that signal increased proliferation. Therapeutic targeting of such pathways is a key theme in current chemotherapeutic approaches.

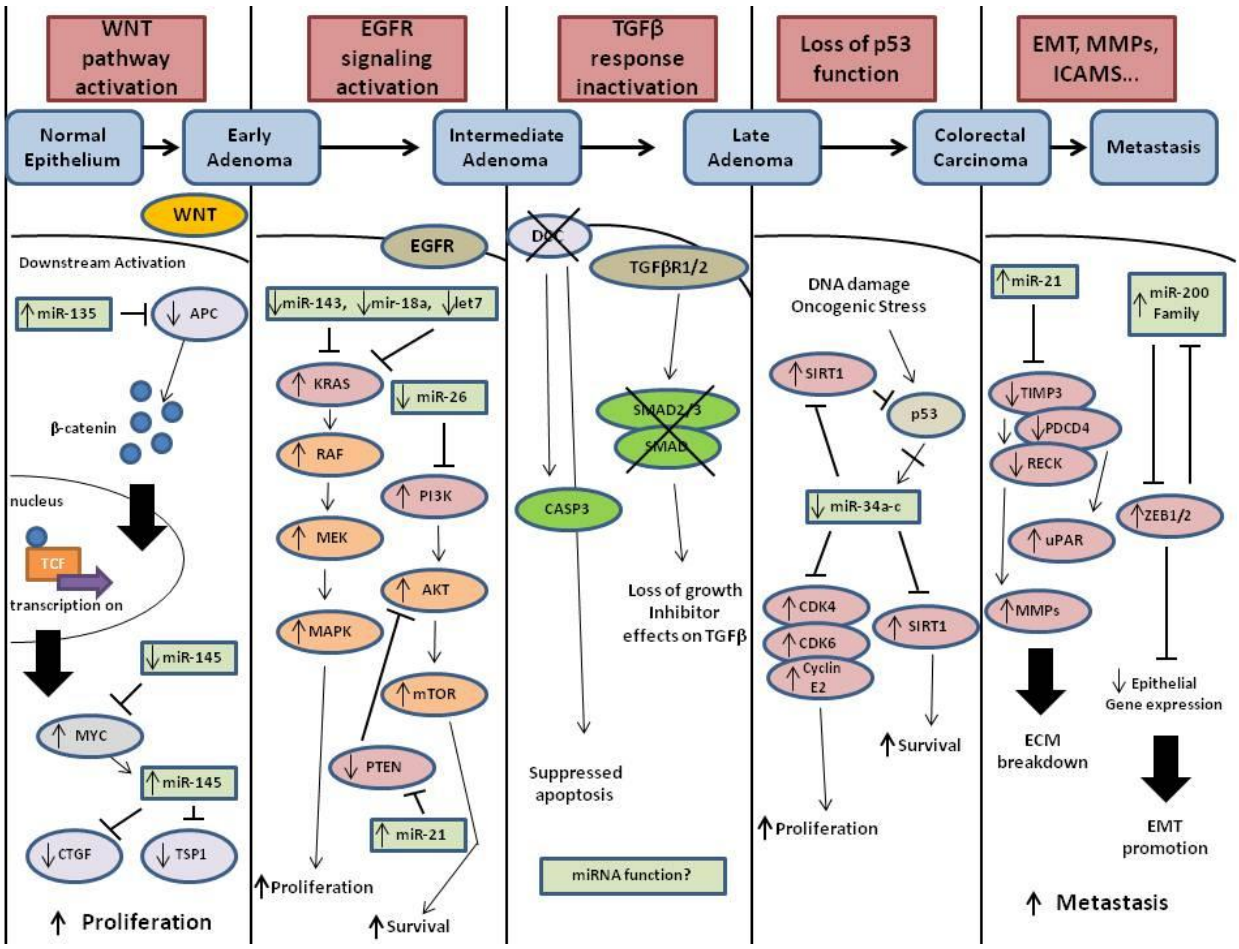

Figure 1: Progression of colorectal cancer

Known pathway alteration in CRC and resulting molecular consequences. APC - adenomatous polyposis coli, CTGF - connective tissue growth factor, TSP1 -thrombospondin 1, EGFR - epidermal growth factor receptor, mTOR - mechanistic target of rapamycin, PTEN - phosphatase and tensin homolog, DCC - deleted in colorectal carcinoma, TGFβ R1/2 - transforming growth factor, beta receptor 1/2, CASP3 - caspase 3, SIRT1 - sirtuin 1, CDK4,6 - cyclin-dependent kinase 4,6, ECM - extracellular matrix, EMT - epithelial--mesenchymal transition, ICAMs - intercellular adhesive molecules, miR – microRNA, TIMP3 - tissue inhibitor of metalloproteinase 3, PDCD4 - programmed cell death 4, RECK - reversion-inducing-cysteine-rich protein with kazal motifs, uPAR - plasminogen activator, urokinase receptor, MMPs - matrix metallopeptidases, ZEB1/2 - zinc-finger E-box binding homeobox 1). Adapted from Slaby et al. Molecular Cancer 2009 8:102 doi: 10.1186/1476-4598-8-102.

1.2.2 Cancer cells have increased metabolic demands

Otto Warburg was the first to describe a phenomenon in which cancer cells are able to suppress oxidative phosphorylation and increase glycolysis [37]. This alteration in metabolic processes allows cells to continually proliferate in situations where oxygen might be depleted. However, cancer cells often show increased glycolysis even in the presence of adequate oxygen levels [38-40]. Furthermore, tumor related metabolic abnormalities are not limited to altered balance between glycolysis and oxidative phosphorylation [41]. While p53 and V-myc Myelocytomatosis Viral Oncogene Homolog (MYC) have long been regarded as master regulators of metabolism, recent studies have uncovered a number of other proteins including Isocitrate Dehydrogenase I (IDH1), Pyruvate Kinase Muscle Form 2 (PKM2), Fumurate Hydratase (FH) and Succinate Dehydrogenase (SDH) that, when mutated, have the capability of inducing tumorigenesis [41-45]. With these advancements it is becoming increasingly clear that altered cellular metabolism is sufficient in itself to induce cancer [41].

As a consequence of increased glycolysis cancer cells often have higher dependence upon glucose to sustain continual proliferation [41, 46]. Interestingly, many cancer lines demonstrate glutamine addiction [47]. This is puzzling due to the fact that glutamine is not an essential amino acid and can be synthesized from glucose. Recent evidence suggests that glutamine addiction has more to do with glutamine's ability to activate Target of Rapamycin (TOR) and maintain mitochondrial membrane potential rather than serve as a nitrogen donor for protein synthesis [47].

1.2.3 Mitochondria are often altered in cancer

Mitochondria have multiple roles within the cell including generation of Adenosine-triphosphate (ATP), production and regulation of reactive oxygen species (ROS) and maintenance of intracellular calcium levels. In line with the observed increase in aerobic glycolysis, many cancer cells have been shown as having defective mitochondria. Tumor mitochondria are often relatively small, lack cristae, and are deficient in the β-F1 subunit of ATP synthase [48, 49]. Frequently mitochondrial DNA is mutated in carcinomas, including: breast, colon, hepatocellular, pancreatic, prostate, lung, renal, thyroid and brain among others [50]. It is still unclear whether this is a consequence of malignancy or a driving force behind it [51, 52]. In addition to increased glycolysis, faulty mitochondria drive tumorigenesis by activation of downstream proliferative pathways including the V-Akt Murine Thymoma Viral Oncogene Homolog 1 (AKT) pathway. Defects in mitochondrial respiration cause increased levels of NADH, which can subsequently inactivate Phosphatase and Tensin Homologue (PTEN), a lipid phosphatase that is vital to inhibition of Phosphoinositide-3-kinase (PI3K)/AKT signaling [53, 54].

1.2.4 Significance

Identification of highly proliferative cells has long been a therapeutic approach for cancer patients. While this strategy has shown some success, it inevitably also affects highly proliferative off target cells of the intestine, hematopoietic system, mucus membranes and hair follicles. Identification of altered metabolic strategies implored by cancer cells may provide an additional layer of therapeutic specificity. Manipulation of glucose and glutamine serum levels

has the potential to be lethal to cancerous cells but not normal tissue that would be sustained by increased levels of oxidative phosphorylation. Furthermore, identification of potentially lethal mitochondrial abnormalities specific to cancerous cells would provide additional targets for the next generation of targeted therapies.

1.3 CELL DEATH IN COLORECTAL CANCER

1.3.1 Apoptosis

Apoptosis, also known as type I cell death is initiated and executed by a series of well-ordered biochemical events and regulated by complex signaling networks. There are two major apoptotic pathways, termed as the extrinsic and intrinsic pathways, which are responsible for processing stress signals and executing cell demise [55, 56]. There is significant cross-talk in many situations among these two pathways, but each pathway has distinct regulatory processes.

1.3.2 Extrinsic pathway

The extrinsic apoptotic pathway was first found to be used by immune cells to kill infected or damaged cells, and subsequently shown to operate in many cell types [57]. This pathway is engaged upon binding of proapoptotic ligands to cell surface death receptors of the Tumor Necrosis Factor Receptor (TNFR) family. All death receptors contain a cysteine-rich extracellular domain, which is responsible for ligand binding, and an intracellular death domain

for transmitting signals through the recruitment of effectors. Proapoptotic ligands belong to the extended cytokine Tumor Necrosis Factor (TNF) super family, and are either present on the cell surface or secreted into the extracellular space [55, 56]. Upon binding of proapoptotic ligands to their respective receptors, each receptor can independently form a Death-inducing Signaling Complex (DISC) by recruiting the adapter protein Fas (TNFRSF6)-associated Via Death Domain (FADD), along with pro-caspase-8 and pro-caspase-10 [56]. FADD recruitment and DISC formation lead to proximity-induced processing and activation of caspase-8 and caspase-10, and their release into the cytoplasm triggers subsequent activation of effecter caspases to execute apoptosis.

1.3.3 Intrinsic pathway

The intrinsic apoptotic pathway is triggered by stresses such as DNA damage, deregulated oncogenes or nutrient/growth factor deprivation, and is largely regulated by the B-cell CLL/lymphoma 2 (Bcl-2) family of proteins and mitochondria [58, 59]. For example, following DNA damage and p53 activation, death signals are transmitted to Bcl-2 Homology Domain 3 (BH3)-only proteins to allow for the activation of BCL2-associated X Protein (Bax) and BCL2-antagonist/killer 1 (Bak), which leads to mitochondrial outer membrane permeabilization (MOMP) [60-62] and release of several mitochondrial apoptogenic proteins, including cytochrome c, Secondary Mitochondrial Activator of Cytochrome c (SMAC/Diablo), HtrA Serine Peptidase 2 (Omi/HtrA2), Apoptosis-inducing Factor (AIF), and Endonuclease G (EndoG) [63]. The release of cytochrome c promotes the assembly of the apoptosome and subsequent activation of caspase-9 [63]. Additionally, SMAC/Diablo and HtrA2/Omi facilitate

apoptosis by binding to Inhibitor of Apoptosis Proteins (IAPs) and relieving their inhibition of caspases [64, 65]. The release of AIF and EndoG promotes DNA degradation [66, 67]. Notably, in some cells where there are low levels of DISC, caspase-8-dependent cleavage of the BH3-only protein BH3-interacting Domain Death Agonist (Bid) generates truncated Bid (tBid) to amply apoptotic signaling via the mitochondria [68, 69].

1.3.4 Bcl-2 family proteins

The Bcl-2 family proteins are central regulators of caspase activation and their competing factions of proapoptotic and antiapoptotic members dictate a cell's decision to live or die. The BH3 family is composed of both antiapoptotic (Bcl-2, BCL2-associated Agonist of Cell Death (Bcl-XL), Myeloid Cell Leukemia Sequence 1 (MCL1) and others) and proapoptotic (Bax, Bid, Bak, BCL2-related Ovarian Killer (Bok), BCL2-associated Agonist of Cell Death (Bad), BCL2-Like 11 (Bim), Bcl2 Modifying Factor (Bmf), BCL2-interacting Killer (Bik), Phorbol-12-myristate-13-acetate-induced Protein 1 (Noxa), p53-upregulated Modulator of Apoptosis (PUMA) and others) proteins that govern mitochondrial membrane potential [70, 71].

1.3.5 Caspase activation

Both the mitochondrial dependent intrinsic and death receptor dependent extrinsic apoptotic pathways lead to the activation of initiator caspases (caspases 2, 8, 9 and 10) that will in turn activate executioner caspases (caspases 3, 6 and 7) (Figure 2) [72-74]. Caspases belong to a family of conserved aspartate-specific cysteine proteases that are initially synthesized as zymogens, also known as procaspases. A distinct difference between initiator and executioner

caspases lies in their activation. Initiator procaspases are stable monomers in the cell and upon dimerization gain enzymatic activity. Further chain cleavage of dimerized initiator caspases aids in stabilization of the active site but doesn't affect activity. In contrast, the executioner caspases have been shown to be stable dimers that do not gain enzymatic activity until after cleavage of the interdomain linker which allows for translocation of the activation loop facilitating formation of the active site (Figure 2) [75-78].

Upon initiation of the intrinsic apoptotic response, cytochrome c is released from the mitochondria. Its release prompts activation of Apoptotic Peptidase Activating Factor 1 (APAF-1) which binds to and initiates cleavage/activation of caspase-9. Caspase-9 then activates caspases 3 and 7. Caspase-3 in turn activates caspase-6 which then activates caspases 8 and 10 [79]. Studies have also shown a reduction in caspase-9 activity in cells depleted of caspase-3 suggesting that it feeds back to caspase-9 and increases activity once active itself [79, 80].

Caspase-3 has been shown to play an important role in the initiation and amplification of extrinsic apoptosis in human T lymphocytes. Prior to activation of Fas, the zymogen form as well as mature caspase-3 was found to be co-localized with FADD and caspase-8 in lipid rafts at the base of Fas. This association was amplified following activation of Fas with Fas ligand (Fas-L). In the presence of Bcl-2 over-expression caspase-3 maturation was prevented resulting in accumulation of the partially processed p20 fragment. It has been suggested that in the presence of Bcl-2, X-linked Inhibitor of Apoptosis (XIAP) is able to bind to the p20 fragment of caspase-3 and prevent removal of its prodomain. Lack of caspase-3 activation resulted in reduced caspase-8 activation and a reduction in apoptosis [81].

While caspase-3 has recently been shown to have roles in brain development, cytoskeleton remodeling, T cell activation and stem cell differentiation, among others, all

functions are dependent upon its enzymatic activity [82-86]. There currently is little knowledge of any non-enzymatic activities performed by caspase-3.

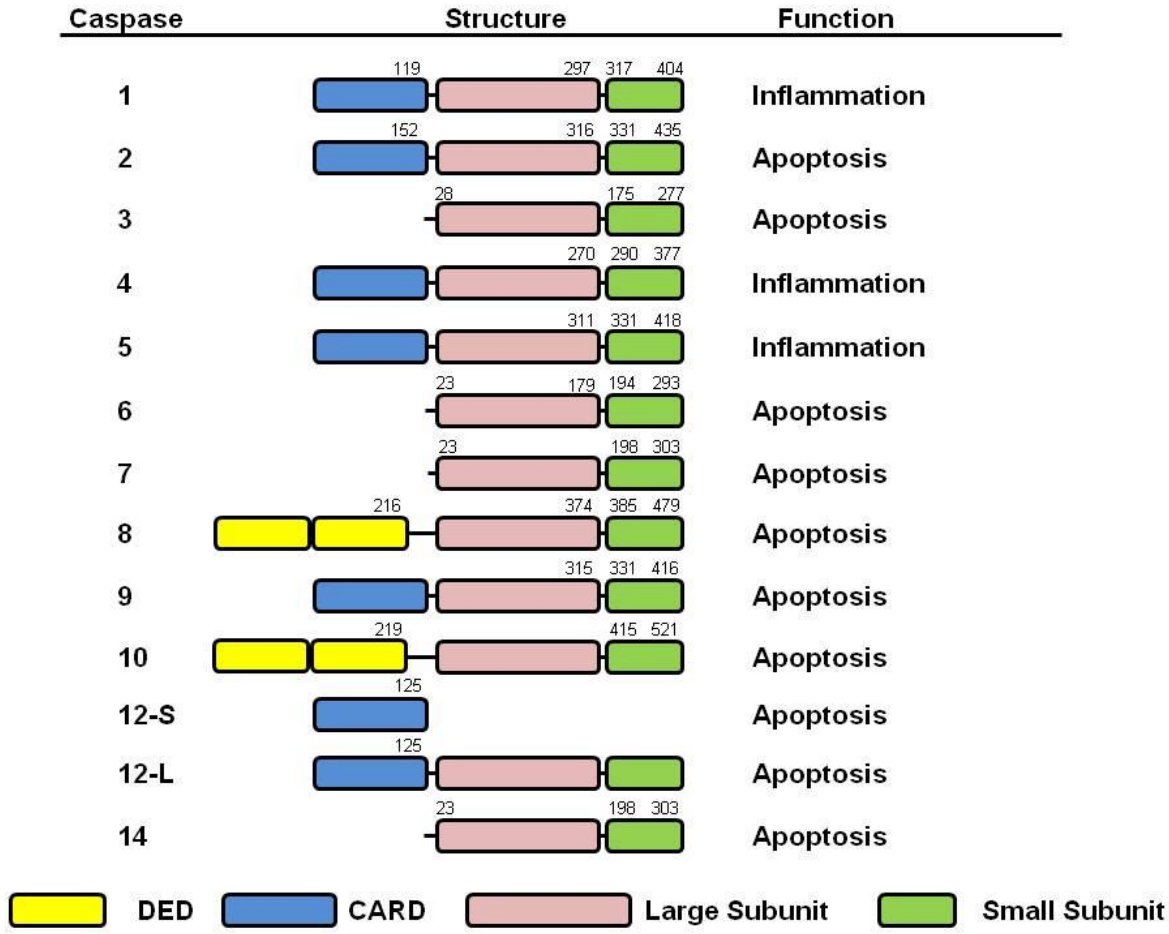

Figure 2: Known human caspases

Caspases are initially found in uncleaved "zymogen" form and have known roles in apoptosis and the inflammatory response. Caspases 2, 8, 9 and 10 are known as initiator caspases. Caspases 3, 6 and 7 are executioner caspases. DED= Death Effector Domain. CARD = Caspase Activation and Recruitment Domain. Numbers denote amino acid sequence.

1.3.6 Inhibitors of apoptosis

The inhibitor of apoptosis family of proteins was originally identified in model organisms. Endogenous inhibitors of IAPs such as SMAC and HrtA2 can directly bind to a conserved Baculovirus Interacting Repeat (BIR) within IAPs. The binding of SMAC to IAPs is mediated through a conserved tetrapeptide. Cumulative evidence in the last decade using biochemical, molecular and cellular, pharmacological, structural biology approaches and genetically modified model systems has revealed a multitude of IAP functions in cell death, survival, proliferation and immunity. Furthermore, several IAPs play a key role in regulating Nuclear Factor of Kappa Light Polypeptide Gene Enhancer in B-cells (NF-κB) activation and non-apoptotic cell death. Overexpression and genetic alterations of IAPs, as well as reduced expression of their endogenous inhibitors have been reported in solid tumors and hematological malignancies [87, 88]. In rare cases, loss of IAPs is associated with the development of certain types of hematological malignancies, suggesting a potential role as a tumor suppressor [89].

Agents targeting IAPs have been developed, with the most promising class being small molecules mimicking the IAP binding domain in SMAC, also known as SMAC mimetics. These compounds have limited toxicity to cancer cells as a single agent, while synergizing with different classes of anti-cancer agents in a wide array of cancer cell types. The use of SMAC mimetics has helped elucidate signaling functions of IAPs, particularly cIAP1 and cIAP2, independent of their ability to suppress caspase activation or apoptosis.

1.3.7 Apoptosome

APAF-1 is a key protein component of the intrinsic apoptotic response. In response to genotoxic stress, cytochrome c is released from the mitochondria. In the presence of cytochrome c and dATP, APAF-1 oligomerization occurs and the Caspase recruitment domains (CARDs) of APAF-1 and caspase-9 interact with each other to form a CARD-CARD disk which can then act as an asymmetrical proteolysis machine [90]. Two forms of the apoptosome have been described, a 700 kDa form and a 1.4 MDa form. The smaller 700 kDa form appears to be the first to form following activation of the apoptotic response and has a greater capacity for activating executioner caspases [91].

1.3.8 Death-inducing signaling complex

The DISC, also known as Complex-I, is critical for initiation of death receptor-mediated apoptosis. After FAS ligation, TNFRSF1A-associated via Death Domain (TRADD) is recruited to the base of the receptor followed by FADD, caspase-8, RIP1 and CASP8 and FADD-like Apoptosis Regulator (cFLIP), all of which complex to form the DISC (Figure 3). Complete formation of the DISC leads to activation of caspase-8 and subsequent downstream cleavage and activation of executioner caspase-3 and Bid [92].

1.3.9 PIDDosome

The PIDDosome is a relatively small (500kDa) apoptotic cell death complex that forms in response to genotoxic stress. It is comprised of the core components; caspase-2, p53-induced

Death Domain Protein (PIDD), and CASP2 and RIPK1 Domain Containing Adaptor With Death Domain (RAIDD) (Figure 4) [93]. PIDDosome activity has been shown to be p53 dependent upon treatment with DNA damaging agents, including 5-FU. Interestingly cell death is absent in p53 null cancer cells, but the PIDDosome still forms following 5-FU treatment [94].

1.3.10 Autophagy

Autophagy is an intracellular degradation system that is found ubiquitously in eukaryotes. It is responsible for the degradation of long-lived proteins and certain organelles. Cytoplasmic components, including organelles are sequestered into double membrane autophagosomes which subsequently fuse with lysosomes where their contents are degraded. Autophagy has been implicated in numerous physiological processes including protein and organelle turnover, starvation response, cellular differentiation, cell death (type II) and pathogenesis [95].

1.3.11 Necrosis

Until recently necrosis (type III cell death) was thought of as a disorganized last resort for cells unable to initiate apoptosis, autophagy or another preferred method of death. It has become increasingly evident that this is incorrect and, similar to apoptosis, necrosis is a highly ordered process comprised of multiple intracellular pathways capable of initiating it [96, 97].

The first indication that necrosis might be regulated came in 1988 when it was noted that distinct cell types died differently in response to the same trigger, TNF. Certain cell types exhibited the traditional apoptotic phenotype, others showed a “balloon-like” morphology without nuclear disintegration indicative of necrosis and others exhibited characteristics of both

avenues of cell death [98, 99]. This led to the belief that necrosis was not solely induced in situations where apoptosis was inhibited. In the decades since this first observation there have been a number of discoveries that have helped outline the induction of programmed necrosis (often referred to as necroptosis). Known activators of necrosis include the receptor-like protein kinases, Receptor (TNFRSF)-interacting Serine-threonine Kinase 1 (RIP1) and Receptor (TNFRSF)-interacting Serine-threonine Kinase 3 (RIP3) [100-104], TNFR [98], reactive oxygen species [105-107], Bcl_2 family members [108], caspase inhibitors [109], ubiquitin E3 ligases, deubiquitylating enzymes [108, 110], bioenergetic reactions [104, 111], poly (ADP-ribose) polymerase (PARP) [112], the mitochondrial permeability transition pore complex [113-115], lysosomal membrane permeabilization [116, 117] and lysosomal, mitochondrial and cytosolic hydrolases [99, 116-118]

1.3.12 Induction of necrosis occurs through death receptors and pathogen recognition receptors.

Initiation of necrosis can be triggered by ligation of a number of death receptors including FAS/CD95 [119], TNFR1 [98, 109], TNFR2 [120], TNF-related apoptosis-inducing ligand receptor 1 (TRAIL1) [121] and TRAIL2 [121]. All of these death receptors are also able to induce apoptosis and do so preferentially. In the presence of transcriptional inhibition or caspase inhibition by cIAP or exogenous caspase inhibitors, death receptors will resort to activation of necrosis [99, 122]. Additionally, recent evidence has demonstrated the ability of pathogen recognition receptors (PRRs) to initiate necrosis. Known PRRs include Toll-like receptors, NOD-like receptors and retinoic acid-inducible gene I-like receptors, all of which are expressed

by cells of the innate immune system to identify pathogen-associated molecular patterns (PAMPs) [123]. Viral double stranded RNA has been shown to induce necrosis mediated through PRRs in a number of cell types including Jurkat T Lymphocytes and murine fibrosarcoma L929 cells [124].

1.3.13 Receptor interacting protein kinase 1

Receptor-interacting protein kinase-1 was the first kinase linked to programmed necrosis [125]. Since its initial discovery RIP1 has been shown to be quite ever-present, found in all organ systems with roles in cell survival, apoptosis and programmed necrosis. In unstressed cancer cells RIP1 is found in the cytosol. Upon cellular stress and stimulation of TNFR1, RIP1 is bound and polyubiquitinated by THF receptor associated factor 2 (TRAF2) at K377 with lysine-63 linked ubiquitin. K63-linked polyubiquitination of RIP1 leads to its binding with the death receptor TNF and association with Complex-I which contains multiple adaptor proteins including NF-kappa-B essential modulator (NEMO), TGF-beta activated kinase 1/MAP3K7 binding protein 1 (TAB1), TGF-beta activated kinase 2/MAP3K7 binding protein 2 (TAB2) and Nuclear receptor subfamily 2 group C member 2 (TAK1). Association of Complex I induces rapid activation of NF-κB with subsequent activation of antiapoptotic proteins including c-FLIP and IAPs (Figure 3). Furthermore Complex-I mediates the activation of prosurvival MAPK proteins including Mitogen-activated Protein Kinase 14 (p38), MAPK, c-Jun N-terminal Kinase (JNK) and Extracellular-signal-regulated Kinase (ERK) [125-132].

RIP1 activation of NF-κB is a highly regulated process that can be inhibited at multiple levels. K63-linked polyubiquitinated RIP1 can be bound to and inhibited by Cylindromatosis (CYLD). Additionally, the K63-linked ubiquitin can be removed by TNFAIP3 Interacting

Protein 2 (A20) which then promotes K48-linked polyubiquitination at K377 which leads to RIP1 degradation by the 26S proteasome. Furthermore, in the presence of high levels of cIAP 1 or 2, RIP1 is polyubiquitinated by K48-linked ubiquitin, once again leading to its degradation by the 26S proteasome.

In the presence of prolonged cellular stress, cell survival is negated and cell death is induced. RIP1 has been shown to be an indispensable component of multiple cell death complexes including Complex-II (DISC), Complex-IIb (Necrosome) and the Ripoptosome (Figure 4).

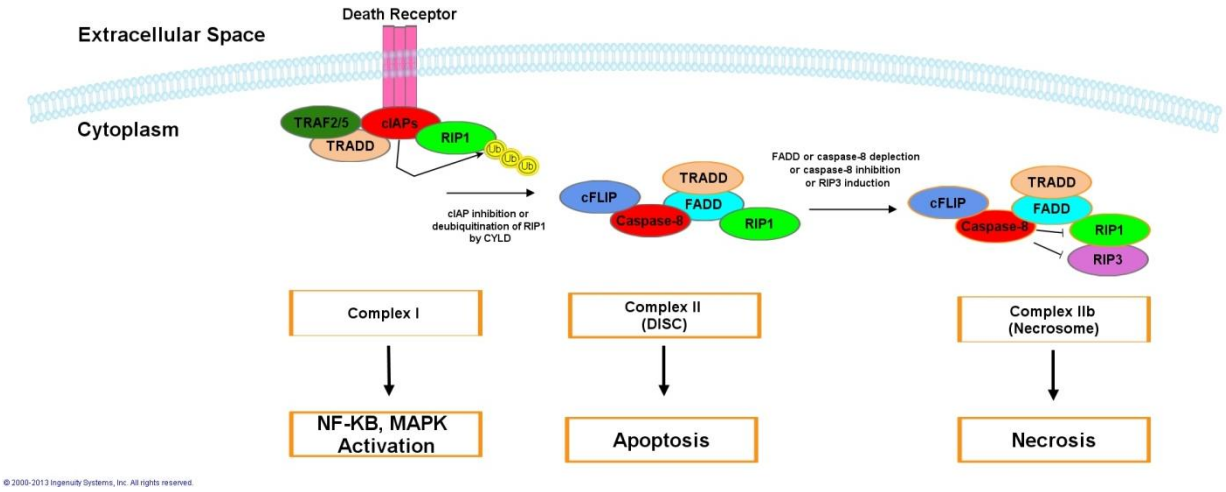

Figure 3: RIP1 activation and downstream pathway activation

1.3.14 Receptor interacting protein kinase 3

RIP3 is a member of the receptor-interacting protein family of serine/threonine protein kinases and contains a c-terminal domain that is unique from other RIP family members. It is primarily

localized to the cytoplasm in an inactive conformation. In response to ligation of TNFR, RIP3 can act in a similar fashion as RIP1 and induce apoptosis as well as activate the NF-κB signaling although to a lesser degree than RIP1 [133]. In addition to prosurvival and proapoptotic functions, RIP3 is an essential component of necrotic death. Upon induction of necrosis, RIP3 interacts with and phosphorylates RIP1 to form the necrosome [134]. RIP3 also binds to and enhances the activity of metabolic enzymes including Glutamate-ammonia Ligase (GLUL), Glutamate Dehydrogenase 1 (GLUD1) and Phosphorylase Glycogen Liver (PYGL). GLUL, GLUD1 and PYGL will in turn stimulate the oxidative phosphorylation and the tricarboxylic acid cycle (TCA) cycle leading to increased ROS production and an amplification of the necrotic response [104].

1.3.15 Reactive oxygen species

Oxygen derived species including superoxide radical, hydrogen peroxide, single oxygen and hydroxyl radical are well known to be cytotoxic and have been implicated in the etiology of a range of human diseases including cancer. Oxidative damage to cellular DNA can lead to mutations and aid in the initiation and progression from normal tissue to malignancy. Elevated levels of ROS and reduced levels of ROS scavengers and antioxidants have been identified in a number of human cancers [135]. Furthermore, there is solid evidence that cancer cells utilize ROS signaling to drive proliferation and other events for tumor progression [136]. However, cells have a threshold for elevated ROS levels and when it is met, apoptosis is induced [137]. This leaves cancer cells with elevated basal ROS levels vulnerable to chemotherapeutic agents that further augment ROS generation or that weakens antioxidant defenses of the cell [135].

Several independent studies have outlined the role of mitochondria-produced ROS in necrosis of L929 fibrosarcoma cells induced by TNFα [138, 139]. Elevated levels of ROS lead to inactivation of caspases which inhibits apoptosis leading to increased ROS and a perpetuation of the cycle [140]. After enough cellular damage, cells revert to necrotic death. ROS have also been implemented in dsRNA induced necrotic death [124, 141].

1.3.16 Necrosome

Complex-IIb, also known as the necrosome, is a large cell death complex composed of TRADD, FADD, Caspase-8, RIP1 and RIP3 (Figure 4). Formation of the necrosome is dependent upon the presence of both RIP1 and RIP3 and does not form in the absence of either component. RIP1 ubiquitination (both K63-linked and K48-linked) has also been shown to inhibit formation of the necrosome. Upon induction of necrosis by death receptor ligation, RIP1 and RIP3 interact through RIP homotypic interaction motifs (RHIMs) and initiate both auto and mutual phosphorylation at S161 (RIP1) and S199 (RIP3) [142, 143]. Phosphorylation leads to activation of both proteins and signaling of downstream targets including Mixed Lineage Kinase Domain-Like (MLKL) and Phosphoglycerate Mutase Family Member 5 (PGAM5) [96, 97].

1.3.17 Ripoptosome

The Ripoptosome is a 2MDa cell death complex that is unique in its ability to induce both caspase-8 mediated apoptosis and caspase-independent necrosis depending upon the presence/absence of certain proteins [144]. Discovered in 2011, the Ripoptosome is composed of the core components RIP1, FADD, and caspase-8 (Figure 4) [144, 145]. It forms in the

response to depletion of inhibitor of apoptosis proteins (XIAP, cIAP1 and cIAP2) as a result of genotoxic stress or use of SMAC mimetics. Unlike the necrosome, the Ripoptosome does not form in response to death receptor (TNFR, FAS, and TRAIL) or mitochondrial pathway stimulation [144]. Ripoptosome assembly is intimately linked to the kinase activity of RIP1 and is negatively regulated by cIAP mediated ubiquitination and subsequent degradation of RIP1 [144-146].

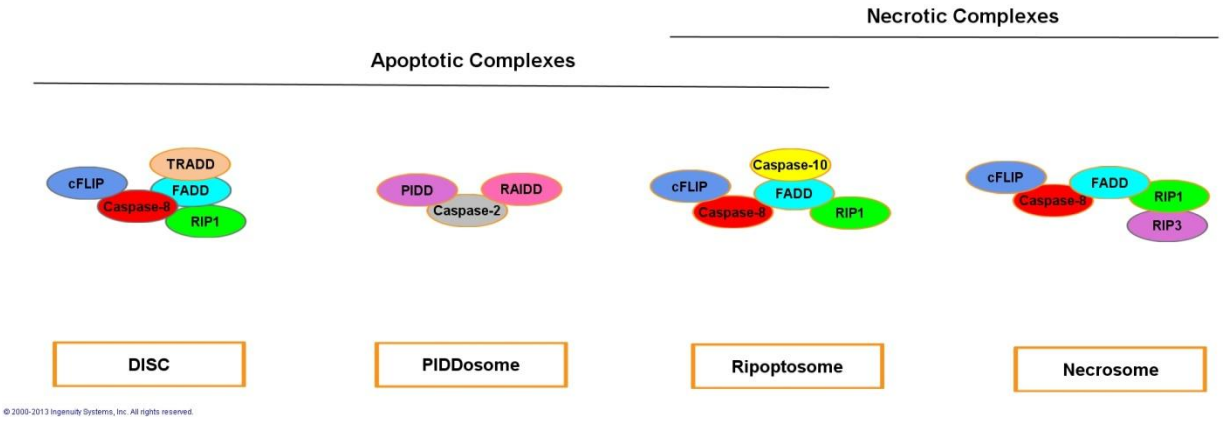

Figure 4: Apoptotic and necrotic cell death complexes.

1.3.18 Significance

A common characteristic of cancer is genetic abnormalities leading to reduced ability to initiate apoptosis. A better understanding of all the avenues in which cell death can be initiated and the protein complexes involved in each respective pathway will provide potential new

targets and approaches for tumors resistant to apoptosis. Although initially thought of as not ideal, autophagy and necrosis activation might be key mechanisms behind future chemotherapeutic options.

2.0 LOSS OF CASPASE-3 LEADS TO IMPAIRED GROWTH AND ALTERED BIOENERGENTICS IN COLORECTAL CANCER CELLS

2.1 ABSTRACT

A hallmark of cancer is the ability to proliferate uncontrollably. In the 1930s Otto Warburg discovered that cancer cell metabolism is unique from normal cells and utilizes glycolysis at a much higher rate. It was initially thought that this altered metabolism was the driving force behind the rapid proliferation of cancer cells. Emerging evidence indicates that an acidic environment resulting from increased glycolysis is detrimental to normal cells but does not affect cancer cells. Furthermore, glycolysis produces less reactive oxygen species compared to oxidative phosphorylation. While advantages of increased glycolysis have been identified, the mechanisms underlying altered energy metabolism in cancer cells are still unclear.

Caspases are cysteine proteases best known to play a pivotal role in the execution of apoptosis. In an effort to determine the role of caspase-3 in colon cancer cell survival and proliferation, we generated a *caspase-3* knockout human colorectal cancer HCT116 cell line using recombinant adeno-associated virus (AAV)-mediated gene targeting. Our studies showed an unexpected decrease in growth and colony formation in *caspase-3* knockout cells without increased cell death. The defects in cell proliferation and long-term growth were rescued by full length but not catalytically dead caspase-3. Furthermore, *caspase-3* knockout cells were

significantly smaller, had abnormally shaped mitochondria, and showed increased production of reactive oxygen species compared to their normal counterparts. Stable knockdown of *caspase-3* in HCT116 cells recapitulated the altered growth and increased ROS production. We also found a near -complete loss of mitofusin-2 expression in *caspase-3* knockout cells. The role of caspase-3 in altering cancer cell growth was investigated in xenograft and cell culture models. In summary, our data demonstrate a novel role of caspase-3 in cell proliferation and bioenergetics, and identify caspase-3 as a potential drug target in colon cancer cells.

2.2 BACKGROUND

Cell proliferation is a vital function for mammals and is required for development, repair, and general maintenance of tissue. However, uncontrolled cellular proliferation ultimately leads to cancer, a phenomenon caused by the accumulation of genetic mutations over time. Current therapeutic strategies attempt to curtail cancer development by preferentially targeting their ability to rapidly proliferate. .

Otto Warburg was the first to describe a phenomenon in which cancer cells are able to suppress oxidative phosphorylation and increase glycolysis [37]. This alteration in metabolic processes allows cells to continually proliferate in situations where oxygen might be depleted. As a consequence of increased glycolysis, cancer cells often have a higher dependence upon glucose to sustain continual proliferation. Additionally, cancer cells often show an addiction to glutamine, a paradoxical phenomenon in light of the fact that glutamine is a nonessential amino

acid that can be synthesized from glucose [47]. The current understanding of glutamine addiction suggests that it is critical for use as a nitrogen donor in nucleotide and amino acid biosynthesis as well as a regulator of (target of rapamycin) TOR activation [47].

Mitochondria have multiple roles within the cell, including the generation of ATP, the production and regulation of reactive oxygen species (ROS), and the maintenance of intracellular calcium levels. In addition to metabolic processes, mitochondria play a vital role in the activation and amplification of the apoptotic response [53]. It has been hypothesized that the altered mitochondrial function witnessed in cancer cells leads to a reduced apoptotic response and increased malignancy.

Caspase-3 is generally associated with cell death pathways rather than mitochondria and cancer cell metabolism. In light of this, we were surprised to find that caspase-3-null colon cancer cells showed reduced proliferation, altered mitochondrial morphology, and hindered oxidative phosphorylation when compared to wild-type (WT) cells. Identifying the role caspase-3 plays in these processes might prove beneficial in restoring mitochondria to a pre-malignant state.

2.3 MATERIALS AND METHODS

2.3.1 Cell Culture and Drug Treatment

Human colorectal cancer cell lines, including HCT116, RKO, and embryonic kidney 293T cells were obtained from the American Type Culture Collection (Manassas, VA, USA). RKO, HCT116, and derivative cell lines were cultured in McCoy's 5A modified media (Life

Technologies) at 37ºC/5% CO2. 293T cells were maintained in DMEM (Life Technologies) media at 37ºC/5% CO2. All media was supplemented with 10% FBS and 1% Penicillin-Streptomycin solution (Sigma). Unless otherwise noted, all drugs were reconstituted in 1% dimethyl sulfoxide (DMSO) and used as follows: 2 µM Oligomycin, 1 µM FCCP and 1 µM Na2S2O (Sigma).

2.3.2 Targeting caspase-3 in HCT116 cells

Gene-targeting vectors were constructed by using the recombinant adeno-associated virus (rAAV) system as previously described [147]. Briefly, two homologous arms (1.334 kb and 1.411 kb, respectively) flanking exons 5 and 7 of *caspase-3*, along with a neomycin-resistant gene cassette (*Neo*), were inserted between two Not I sites in the AAV shuttle vector pAAV-MCS (Stratagene, La Jolla, CA). Packaging of rAAV was performed by using the AAV Helper-Free System (Stratagene) according to the manufacturer's instructions.

HCT116 cells containing two copies of WT *caspase-3* were infected with the rAAV and selected by G418 (0.5 mg/ml, Mediatech, Manassas, VA) for 3 weeks. Drug-resistant clones were pooled and screened by PCR for targeting events. Prior to targeting the second allele, the Neo cassette, which is flanked by Lox P sites, was excised from a heterozygous clone by infection with an adenovirus expressing Cre recombinase (Ad-Cre) [147]. Single clones were screened by PCR for Neo excision, and a positive clone was infected again with the same caspase-3-targeting construct. After the second round, Neo was again excised by Ad-Cre infection, and gene-targeting in caspase-3 KO cells was verified by PCR and western blotting. All primer sequences used are listed in Table 3.

2.3.3 Reverse transcriptase polymerase chain reaction (RT-PCR)

Total RNA was isolated from cells using the RNAgents Total RNA Isolation System (Promega, Madison, Wisconsin, USA) according to the manufacturer's instructions. First strand cDNA was synthesized using Superscript Reverse Transcriptase (Invitrogen) according to the manufacturer's instructions. PCR was performed on a Thermo Scientific Hybaid MultiBlock MBS 0.2S Thermal Cycler using gene -specific primers. Primers used are listed in Table 3. PCR products were analyzed by agarose gel electrophoresis.

2.3.4 Transfection

Full-length human *caspase-3* (Addgene # 11813) and catalytically dead human C163A *caspase-3* (Addgene# 11814) were obtained from Addgene (Cambridge, MA). dsRED was a generous gift from Dr. Ben Van Houten at the University of Pittsburgh. All plasmids were transfected with Lipofectamine 2000 (Invitrogen) according to the manufacturer's instructions. Stable clones were maintained in McCoy's 5A supplemented with 0.4 mg/ml G418 (Gibco).

2.3.5 Caspase-3 Knockdown

Lentiviral particles were generated by co-transfection of 4 plasmids [Control plasmid (pLK01.GFP-puro) or the CASP3 specific shRNA plasmids pLK01.CASP3-sh1 through 5 (Sigma), together with pMD2.g (VSVG), pVSV-REV, and pMDLg/pRRE] into 293-FT cells using FuGene 6 Transfection reagent (Table 3). The collection and isolation of lentiviral

particles, and lentiviral transduction and screening of most effective CASP3 shRNA was carried out as described previously [148]. The CASP3-specific shRNA (shRNA2, Table 3) was used in HCT116 and RKO cells. In brief, cells were plated and allowed to grow until 40% confluent. Cell media was replaced with a 1:1 dilution of lentivirus containing CASP3-shRNA2 and McCoy's 5A media supplemented with 8µg/ml polybrene (Millipore). Cells were then incubated at 32°C/5% CO_2 for 16 hours. Cell media was removed and replaced with fresh McCoy's 5A, and cells were incubated for 8 hours at 37°C/5% CO_2. This process was repeated a second time before putting the cells permanently at 37°C/5% CO_2 under puromycin (2 µg/ml) selection, and single clones were isolated by limiting dilution. Knockdown of *CASP3* was determined by quantitative RT-PCR using an Applied Biosystems StepOnePlus system using the Applied Biosystems Taqman® Gene Expression Cells-to-CT kit [148] and validated by western blotting.

2.3.6 Mitochondrial fractionation

Cytoplasmic and mitochondrial fractions were separated by Mitochondrial Fractionation Kit (Active Motif, Carlsbad, CA, USA) according to the manufacturer's instructions.

2.3.7 Cell counts

$1.5*10^6$ cells per well in a 12-well tissue culture plate were plated. Following plating, cells were harvested at 24, 48, and 72 hours. At each time point, triplicate wells for each cell type were spun down and reconstituted in HBSS. Cell suspensions were then diluted 1:10 in Trypan blue (Gibco) and counted by hemacytometer.

2.3.8 Colony formation assay

200, 400, and 600 cells of each cell type were plated in 6-well tissue culture plates. Cells were maintained at 37ºC/5% CO_2 and allowed to grow for 14 days with media changed every other day. At the conclusion of 14 days, cell media was removed and cells were washed once with HBSS before staining with Crystal Violet dye for 10 minutes. Cells were then washed 3 times with HBSS. All conditions were performed in triplicate.

2.3.9 Viability assay

$8.0 * 10^3$ cells per well were initially plated in 96-well format. Cell viability was assayed using Cell-Titer 96 Aqueous One Solution Cell Proliferation Assay and Cell-Titer-GLO Luminescent Viability Assay (Promega) according to manufacturer's recommendations. Long term viability of cells was measured by plating cells the same as above but allowing them to grow for 7, 14, or 21 days before being assayed by CyQuant® (Life Technologies) according to manufacturer's suggestions.

2.3.10 Detection of reactive oxygen species

Cells were plated at 20-30% confluence. 48 hours after plating, cell media was removed and replaced with fresh media containing 2 µM mitoSox reagents (Life Technologies). Cells were then incubated for 20 minutes at 37ºC/5% CO_2. Following incubation, cells were harvested,

washed once in cold phosphate-buffered saline (PBS), and then reconstituted in cold 1% BSA PBS. Following excitation at 518nm, 580nm emission was measured on a C6 flow cytometer (Accuri Cytometers). At minimum, 30,000 events per sample were measured and all conditions were performed in triplicate.

2.3.11 Immunoblot

Cells were harvested in RIPA buffer (50 mM Tris pH 7.4, 150 mM NaCl, 1% Triton-X-100, 0.1% SDS, 1% Deoxycholate, 1 mM EDTA) supplemented with protease inhibitor cocktail (Roche Applied Sciences). Cells were rotated for one hour at 4ºC and then centrifuged at 13,000 RPM for 30 minutes. Protein concentration was determined by the Bradford assay and 40µg per well were loaded in 10% bis-tris gels (Life Technologies). Gels were run for 40minutes at 180 V in MOPS buffer (Life Technologies). Protein was then transferred to PVDF membranes using a TransBlot SD semi-dry transfer cell (Bio-Rad). Membranes were blocked for nonspecific binding with 5% non-fat milk in TBS-T for one hour at room temperature and then incubated in primary antibody overnight at 4ºC. Primary antibodies were used at a 1:1000 dilution and include DRPI (ab56788), MFN2 (ab56889) (Abcam), OPA-1 (612606) (BD Transduction Laboratories), α-Tubulin (CP06) (Oncogene Science), β-Actin (A5441) (Sigma), and Caspase-3 (AAP103E) (Stressgen). Following primary incubation, membranes were washed with TBS-T and incubated in appropriate HRP-conjugated secondary antibody for 1 hour at room temperature. Secondary antibodies used include goat-anti-rabbit (31462), goat-anti-mouse (31432), and mouse-anti-goat (31400) (Pierce). Presence of antibody binding was detected using Western Lighting - Plus ECL

(Perkin Elmer) according to manufacturer's specifications. Membranes were then exposed on blue X-ray film (Phenix Research Products)[149].

2.3.12 Transmission electron microscopy

Cells grown on tissue culture plasticware were fixed in 2.5% glutaraldehyde in 100 mM PBS (8 gm/l NaCl, 0.2 gm/l KCl, 1.15 gm/l $Na_2HPO_4 \cdot 7H_2O$, 0.2 gm/l KH_2PO_4, pH 7.4) overnight at 4^oC. Monolayers were then washed in PBS three times then post-fixed in aqueous 1% osmium tetroxide, 1% Fe_6CN_3 for 1 hour. Cells were washed 3 times in PBS then dehydrated through a 30-100% ethanol series then several changes of Polybed 812 embedding resin (Polysciences, Warrington, PA). Cultures were embedded by inverting Polybed 812-filled BEEM capsules on top of the cells. Blocks were cured overnight at 37^oC, and then cured for two days at 65^oC. Monolayers were pulled off the coverslips and re-embedded for cross section. Ultrathin cross sections (60 nm) of the cells were obtained on a Riechart Ultracut E microtome, post-stained in 4% uranyl acetate for 10 min and 1% lead citrate for 7 min. Sections were viewed on a JEOL JEM 1011 transmission electron microscope (JEOL, Peobody, MA) at 80 KV. Images were taken using a side-mount AMT 2k digital camera (Advanced Microscopy Techniques, Danvers, MA)[150].

2.3.13 Mitochondrial outer membrane potential

$1.5*10^6$ cells per well in a 12-well tissue culture plate were plated. 48 hours following plating, cells were harvested, centrifuged and washed once with HBSS. Cells were then resuspended in 400 µl full media with 100 nM MitoTracker Red CMXRos (Molecular Probe) and incubated at 37º C for 30 minutes. Cells were then analyzed for positive staining by flow cytometry.

2.3.14 Mouse xenograft studies

All animal experiments were approved by the University of Pittsburgh Institutional Animal Care and Use Committee. Female 5-6 week-old Nu/Nu mice (Charles River, Wilmington, MA) were housed in a sterile environment with micro- isolator cages and allowed access to water and chow *ad libitum*. Mice were injected subcutaneously in both flanks with 4×10^6 WT or *caspase-3*-KO HCT116 cells. After implantation, tumors were allowed to grow 21 days before being sacrificed.

2.3.15 Tissue preparation in mice

Following treatment and sacrifice of mice, tumors were dissected and fixed in 10% formalin for histological analysis. Five-micron (5µm) sections were used for tissue staining. Histological analysis was performed by hematoxylin and eosin (H&E) staining.

2.3.16 Statistical analysis

Statistical analyses were carried out using GraphPad Prism IV software. P values were calculated by the student's t-test and were considered significant if $p < 0.05$. The means ± standard error (s.e.m.) is displayed in the figures.

2.4 RESULTS

2.4.1 Loss of caspase-3 leads to reduced cell survival and proliferation

In an effort to determine the role of caspase-3 in cell survival and growth we generated caspase-3- null HCT116 colon cancer cells (C3KO) (Figure 5A). To our surprise, we saw reduced cell growth of multiple C3KO clones 72 hours after seeding when counted with a hemocytometer following Trypan blue staining.(Figure 5B). Reduced long term viability was further confirmed by CyQuant proliferation assay at 7 and 14 days after seeding (Figure 5C). In line with reduced cell adhesion C3KO cells showed significantly less colony formation 14 days after seeding (Figure 5D). Taken together these results show reduced cell proliferation and ability to form colonies in C3KO cells.

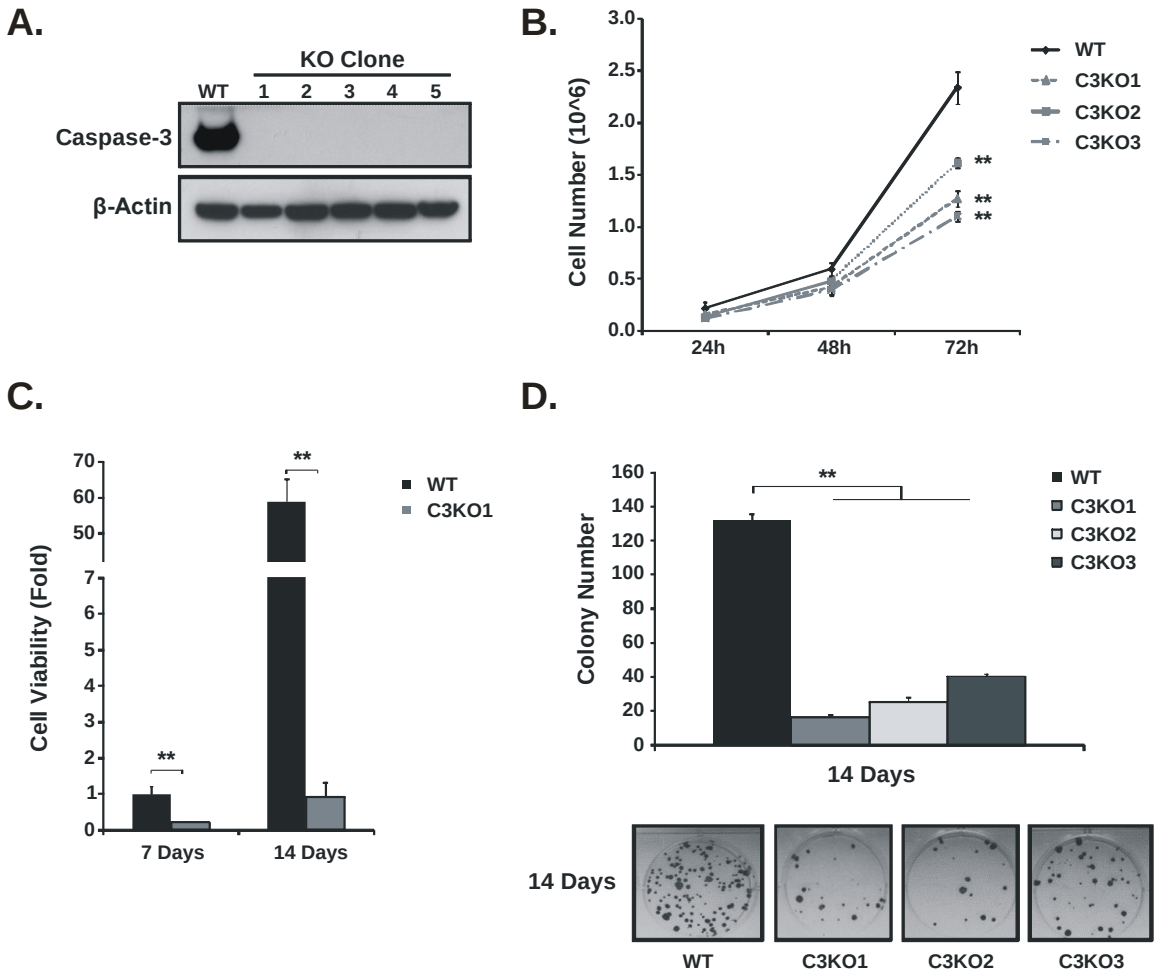

Figure 5: Caspase-3 knockout cells grow slower and form fewer colonies.

(A) Protein expression of HCT116 WT and C3KO cells. (B) WT and C3KO cell number at the indicated times. (C) WT and C3KO cell viability as measured by the CyQuant proliferation assay. (D) WT and C3KO colony formation mean values and representative images.

2.4.2 Caspase-3 catalytic activity is required to restore proliferation

Following identification that loss of caspase-3 leads to a reduction in cell proliferation, C3KO cells were transfected with either a full length capase-3 (FLC3) expression construct, or a mutated catalytically dead (C163A) construct, and stable clones were generated (Figure 6A). In FLC3 cells, there was a significant increase in colony formation when compared to C3KO cells (Figure 6B). This increased growth was not recapitulated in C163A cells, indicating that the catalytic activity of caspase-3 is required for cell proliferation.

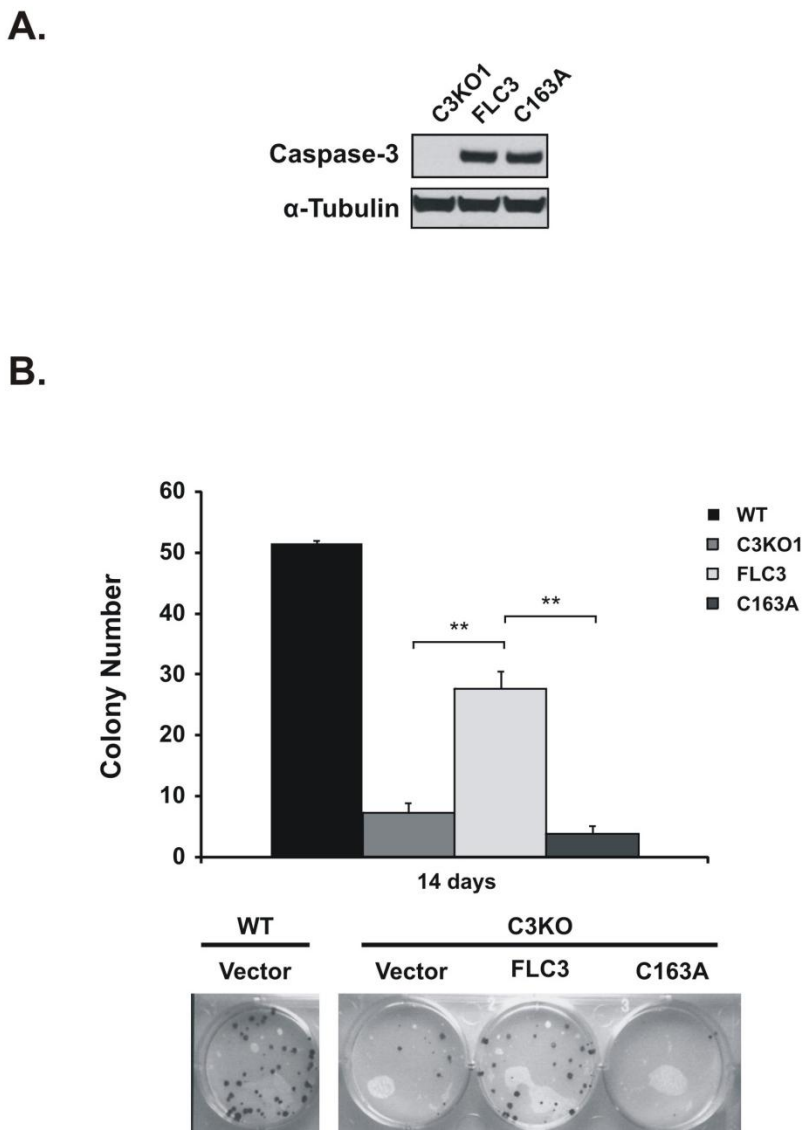

Figure 6: Caspase-3 catalytic activity is required to restore growth.

(A)Protein expression in HCT116 C3KO cells expressing a full length caspase-3 expression construct (FLC3), or a mutated catalytically- dead caspase-3 (C163A). (B) Colony formation in WT, C3KO, FLC3, and C163A cells 14 days after seeding.

2.4.3 Caspase-3 knockout cells are smaller in size and have enlarged, morphologically-different mitochondria

In order to determine the effect of caspase-3 loss on cell morphology, we utilized transmission electron microscopy. Interestingly, while C3KO cells were significantly smaller than WT cells (Figure 7A-B), they contained mitochondria that were more than twice as large as WT cells (Figure 7A, C). In order to confirm the altered mitochondrial morphology, WT and C3KO cells were transiently transfected with a dsRED expression construct that localizes to the mitochondria by virtue of being fused to the mitochondrial localization signal for subunit VIII of cytochrome c oxidase [151]. Confocal imaging of WT and C3KO cells showed less-defined mitochondria puncta in C3KO cells (Figure 7D). Further analysis using Image J [152] confirmed that mitochondria of C3KO cells have larger mean area, perimeter, and elongation among other characteristics (Figure 7E and 8).

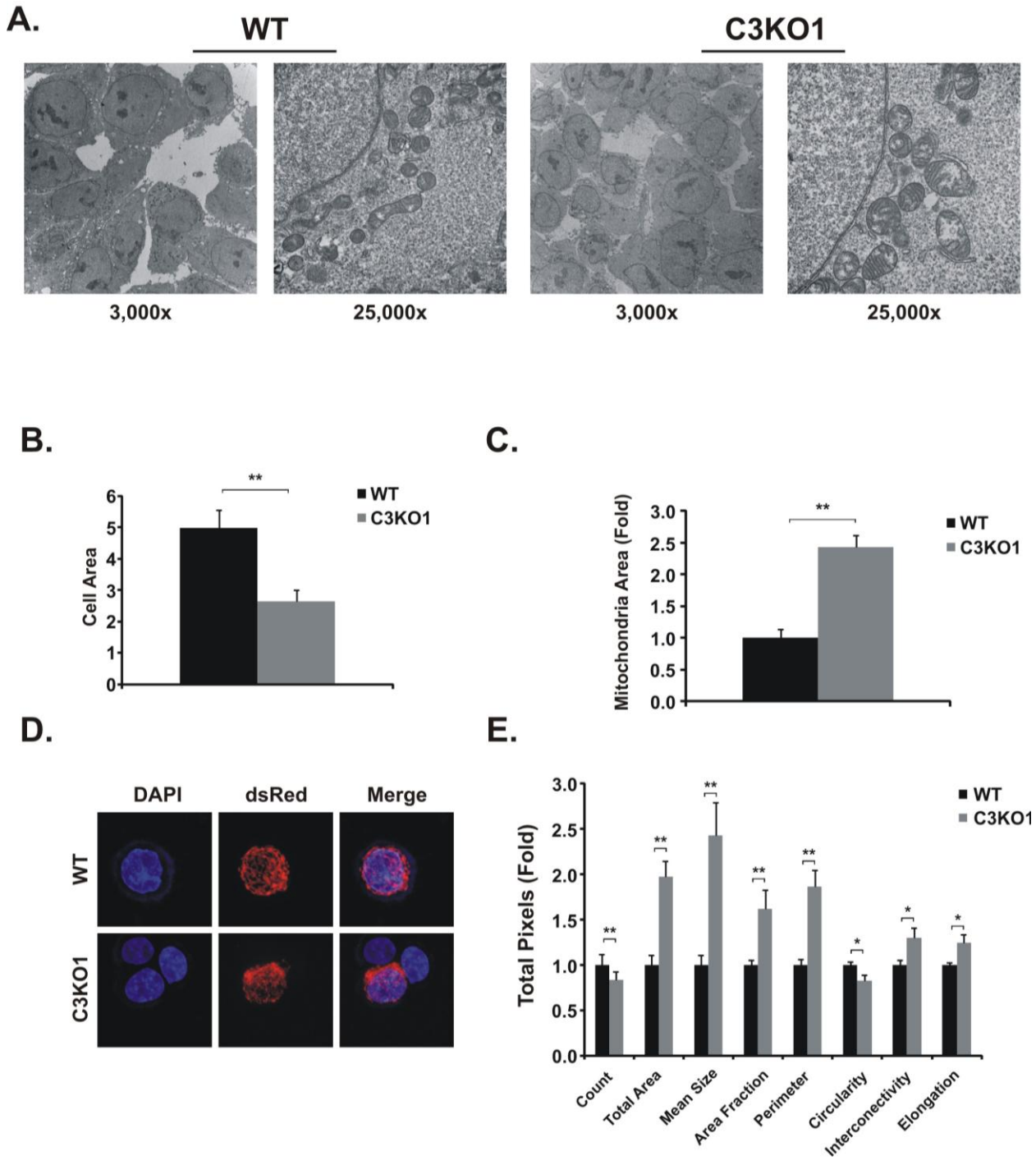

Figure 7: Caspase-3 knockout cells are smaller and have larger mitochondria.

(A) Transmission electron microscopy images of WT and C3KO cells at 3,000x and 25,000x magnification. (B) WT and C3KO mean cell size as measured from TEM images. (C) WT and C3KO mean mitochondria size as measured from TEM images. (D) Representative images of dsRED- transfected WT and C3KO cells. (E) Mean mitochondrial parameters shown in dsRED images as measured by Image J.

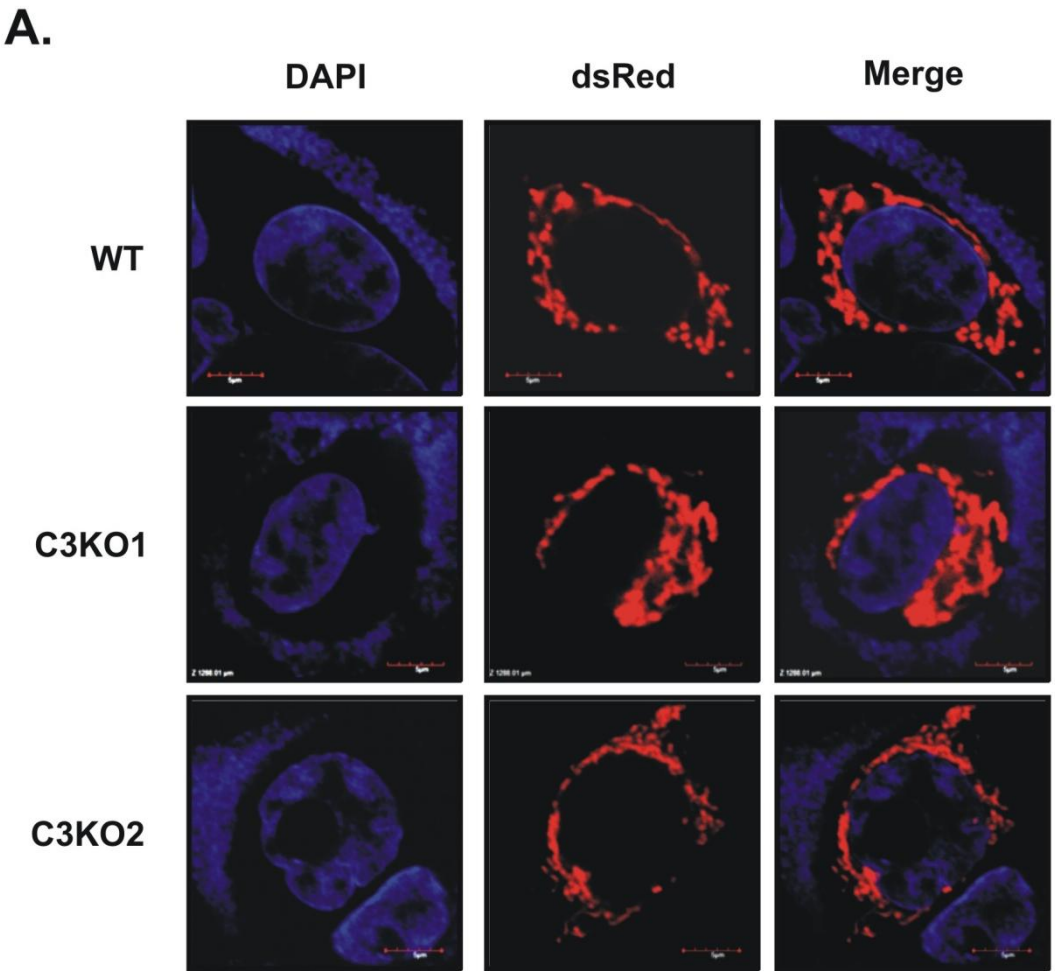

Figure 8: Caspase-3 knockout cells have altered mitochondrial morphology.

(A) Representative images of WT and C3KO mitochondria following transfection with dsRED.

2.4.4 Caspase-3 knockout cells have altered bioenergetics

Following identification of altered mitochondrial morphology, we aimed to identify the metabolic consequence of such alteration. Utilizing an Oroboros O2K respirometer to measure cellular oxidative phosphorylation capabilities, we discovered that C3KO cells consumed oxygen at a slower pace, indicating reduced metabolic activity (Figure 9A-B). Furthermore, C3KO cells showed reduced oxygen flow per cell (Figure 9C).

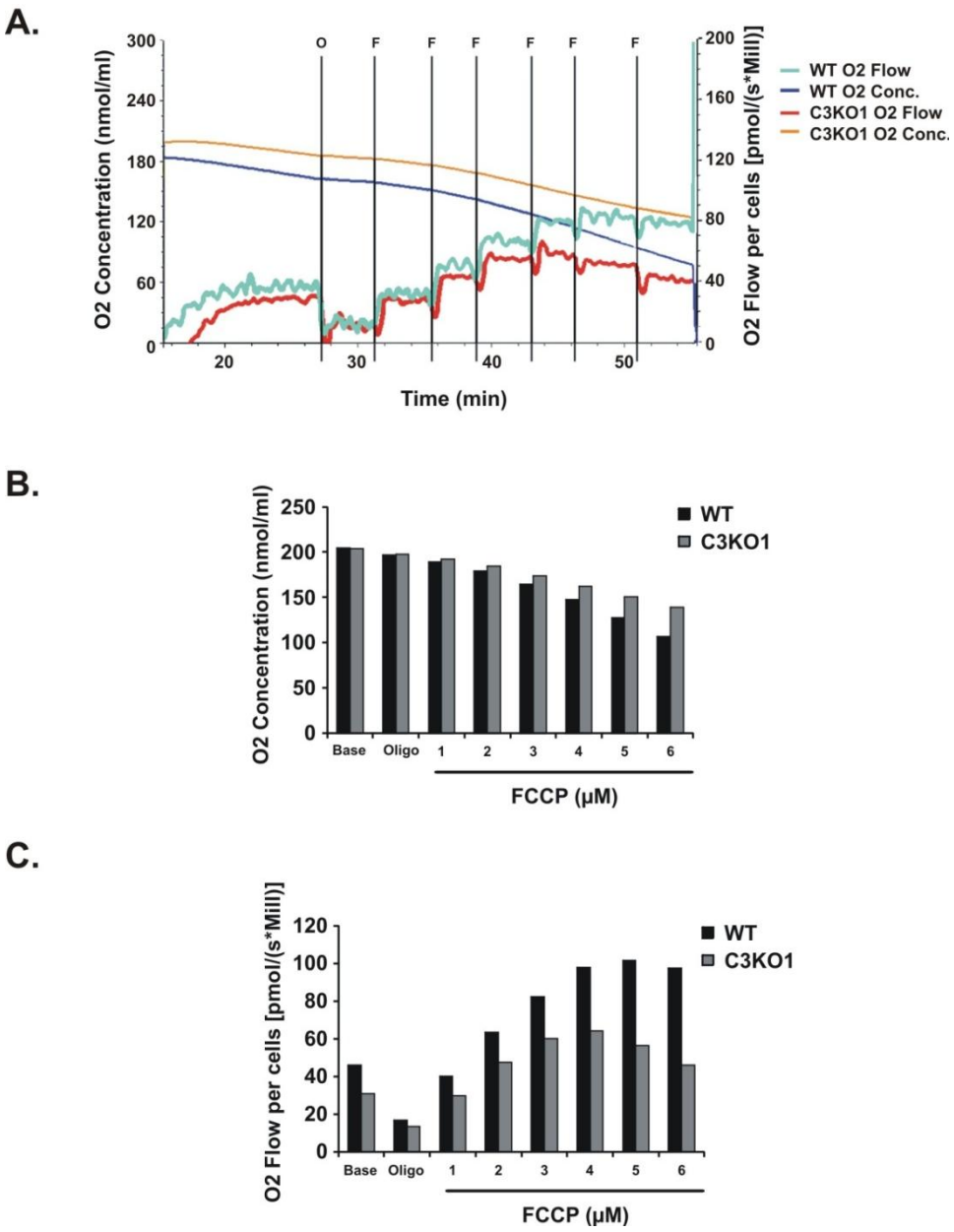

Figure 9: Caspase-3 knockout cells have altered bioenergetics.

(A) Oxygen consumption and flow of WT and C3KO cells as measured by an Oroboros machine. O = Oligomycin (2µM), F = FCCP (1µM). (B) Quantification of Oroboros chamber oxygen concentration for WT and C3KO cells treated as in A. (C) Quantification of WT and C3KO oxygen flow per cell treated as in A.

2.4.5 Caspase-3 knockout cells have increased ROS and autophagy and reduced MFN-2 levels

In order to determine the consequences of altered mitochondrial morphology and impaired cellular respiration, we examined the release of reactive oxygen species (ROS) in addition to basal autophagy levels, two indicators of overall mitochondrial health. Measurement of basal ROS levels showed a more than two-fold increase in C3KO cells (Figure 10A). To assess autophagy levels, WT and C3KO cells were transiently transfected with a GFP tagged LC3 expression construct. LC3II-GFP puncta were twice as prevalent in C3KO cells as in WT (Figure 10B). Probing for known mitochondrial -associated proteins uncovered a drastic reduction in the mitochondria fusion protein MFN-2, suggesting that C3KO cells are deficient in mitochondrial fusion and fission (Figure 10C). Treatment of C3KO cells with the proteasome inhibitor MG132 was able to rescue MFN-2 degradation (Figure 10D).

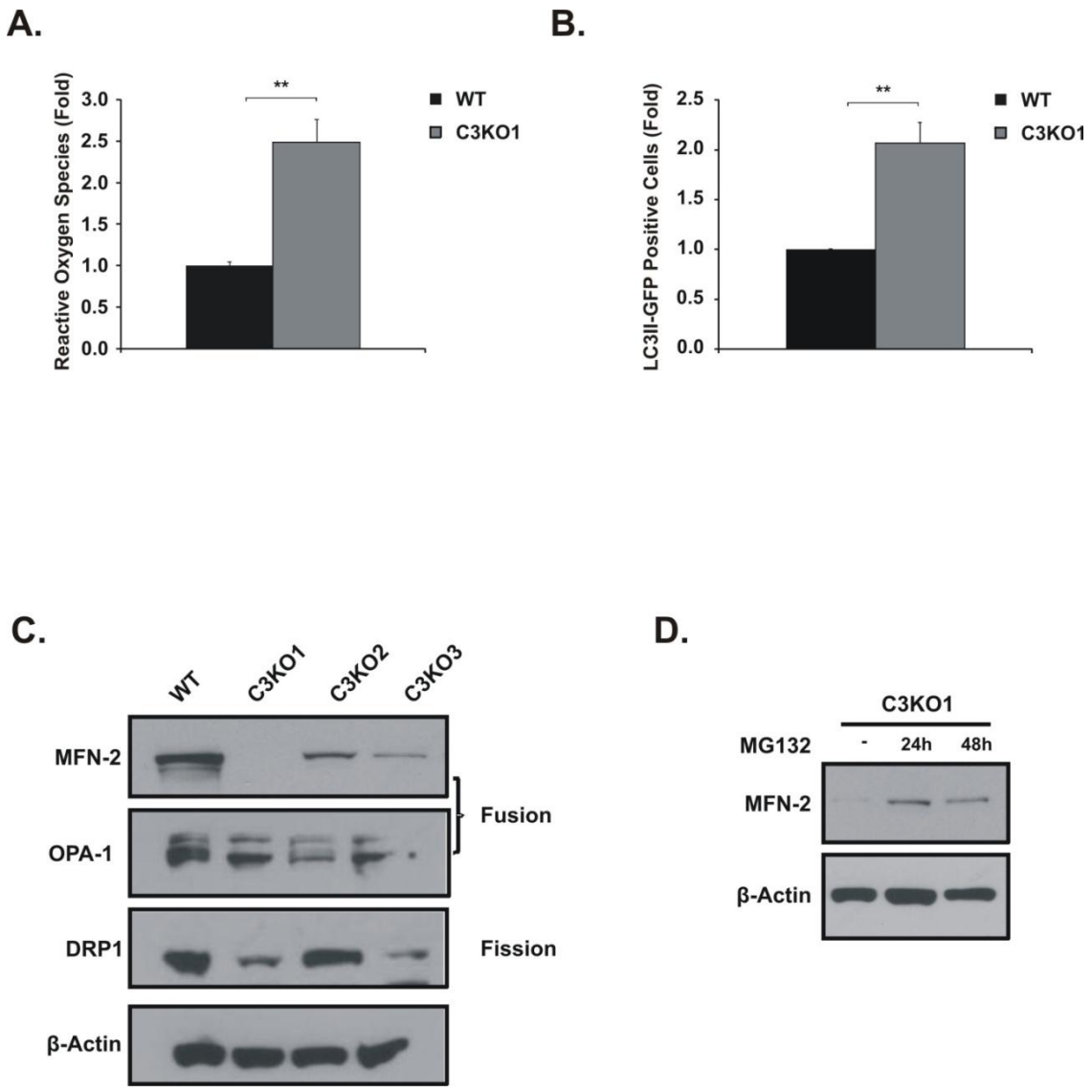

Figure 10: Caspase-3 knockout cells have increased ROS and autophagy and reduced MFN-2.

(A) Relative mitochondrial reactive oxygen species in WT and C3KO cells. (B) LC3II -GFP positive puncta in untreated WT and C3KO cells. (C) Protein expression in WT and C3KO cells. Fusion = proteins involved in mitochondrial fusion. Fission = proteins involved in mitochondrial fission. (D) Protein expression in WT and C3KO cells treated with MG132 (1μM) for the indicated times.

2.4.6 Caspase-3 knockout cells are more sensitive to glucose and glutamine deprivation

After identifying C3KO cells as having reduced levels of oxidative phosphorylation, we aimed to determine if they showed a higher reliance on glucose for survival. Reduction of glucose levels from 25 mM (what is normally provided in commercially-available media) to 5.5 mM resulted in high rates of cell death in C3KO when compared to parental lines as measured by adherent cells (Figure 11). Surprisingly, C3KO cells also showed increased sensitivity to removal of the non-essential amino acid glutamine. Glutamine is commonly found in cell culture media at a concentration of 4 mM. Combination experiments manipulating both glucose and glutamine showed loss of glutamine to be the more critical of the two for C3KO cell survival (Figure 11). These data confirm that caspase-3 knockout cells are more reliant upon glucose and glutamine to sustain cell survival and proliferation.

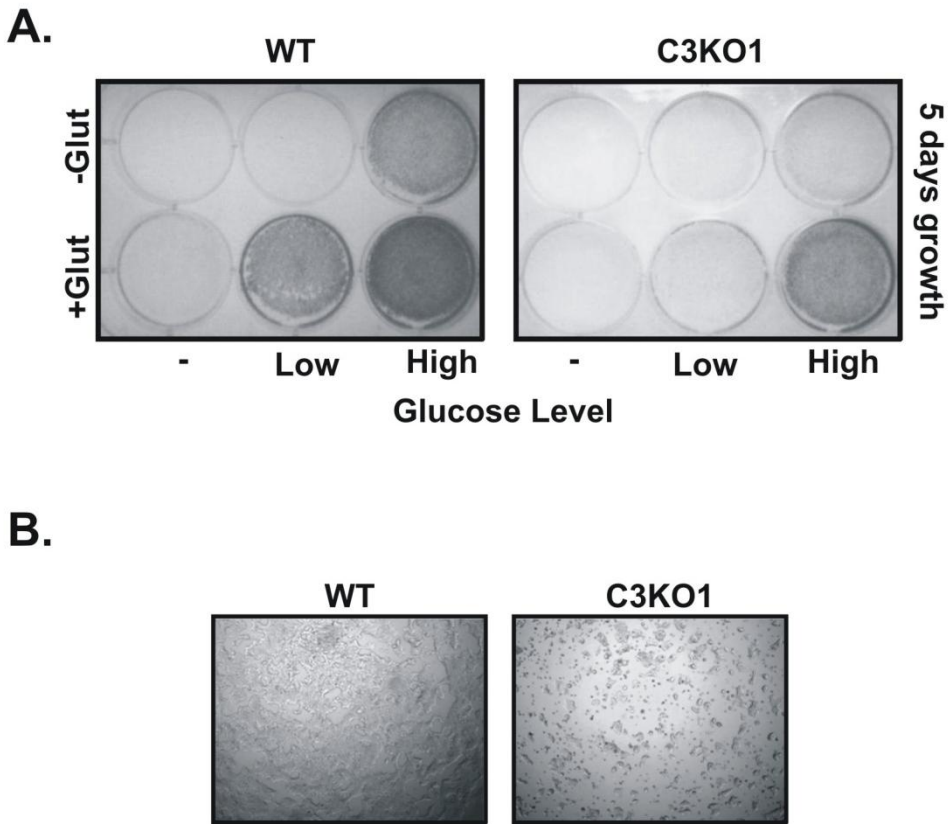

Figure 11: Caspase-3 knockout cells have impaired glucose/glutamine utilization.

(A) WT and C3KO cells maintained in varying levels of glucose +/- glutamine 5 days after seeding. Low = 5.5mM; High = 25mM. Glutamine used at 4mM. (B) Representative phase contrast images of WT and C3KO cells 3 days after seeding in high glucose + glutamine media.

2.4.7 Caspase-3 knockdown cells recapitulate growth and mitochondrial phenotypes

To ensure that the phenomenon we were witnessing was not an abnormality unique to HCT116 cells or an artifact of the knockout process we generated a short hairpin construct targeting caspase-3 for use in other cell lines. After expression of the construct and generation of stable clones, both HCT116 and RKO shCaspase-3 (shC3) cells were assayed for cell growth and mitochondrial morphology. Both HCT116 shC3 and RKO shC3 showed impaired cell proliferation as measured by cell number, CyQuant proliferation assay, and colony formation assay (Figure 12). Furthermore, RKO shC3 cells showed altered mitochondrial morphology similar to what was observed in HCT116 C3KO cells when compared to a GFP-expressing control line (Figure 13). These results confirm that altered proliferation and mitochondrial morphology as a consequence of caspase-3 loss is not unique to HCT116 cancer cells.

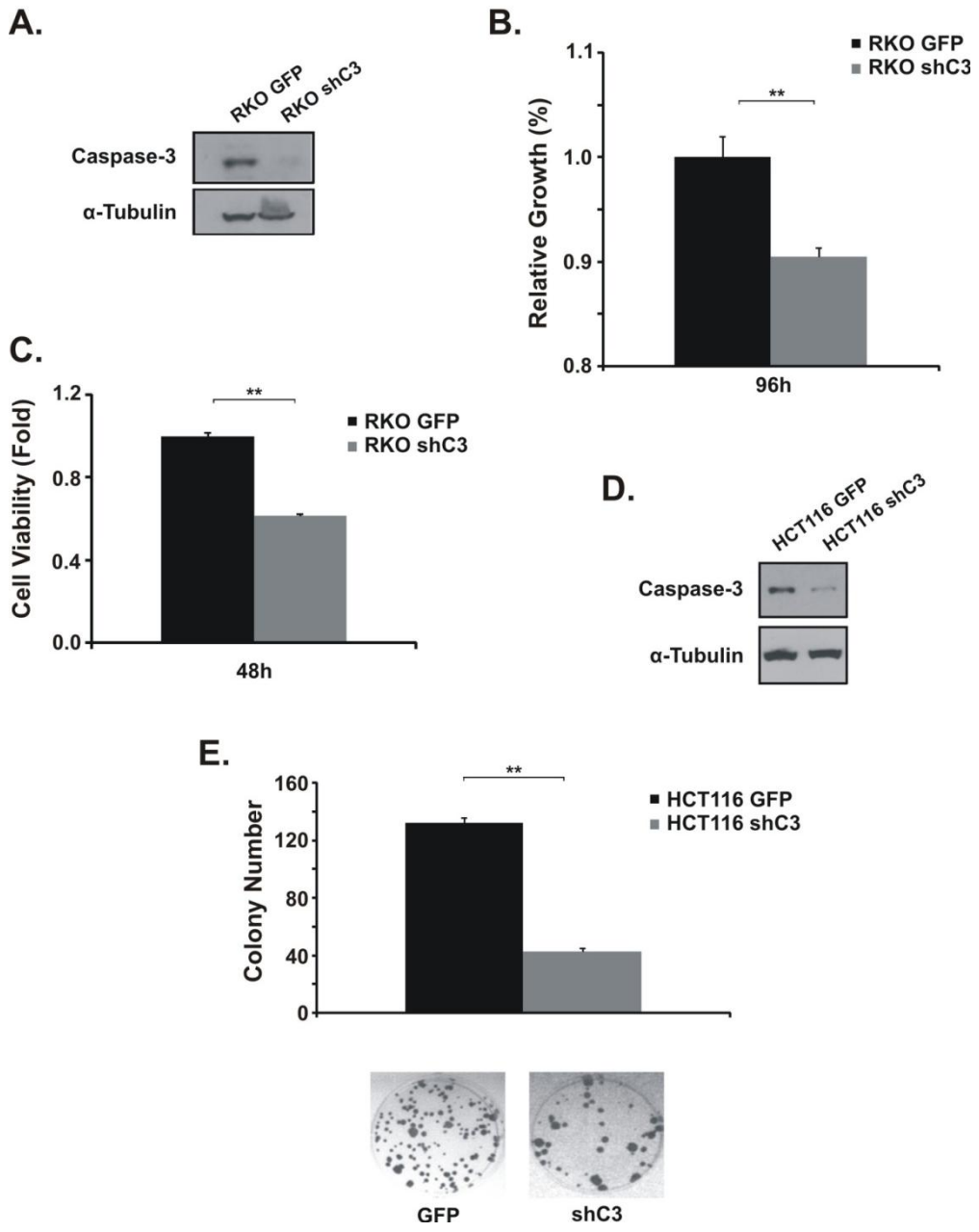

Figure 12: Caspase-3 knockdown cells recapitulate reduced proliferation phenotype.

(A) Protein expression in RKO cells expressing either a GFP control construct (GFP) or a short hairpin construct targeting caspase-3 (shC3). (B) RKO GFP and shC3 relative cell number 96hours after seeding. (C) RKO GFP and shC3 cell viability as measured by CyQuant proliferation assay. (D) Protein expression in HCT116 cells expressing either a GFP control construct (GFP) or a short hairpin construct targeting caspase-3 (shC3). (E) Colony formation in HCT116 GFP and shC3 cells.

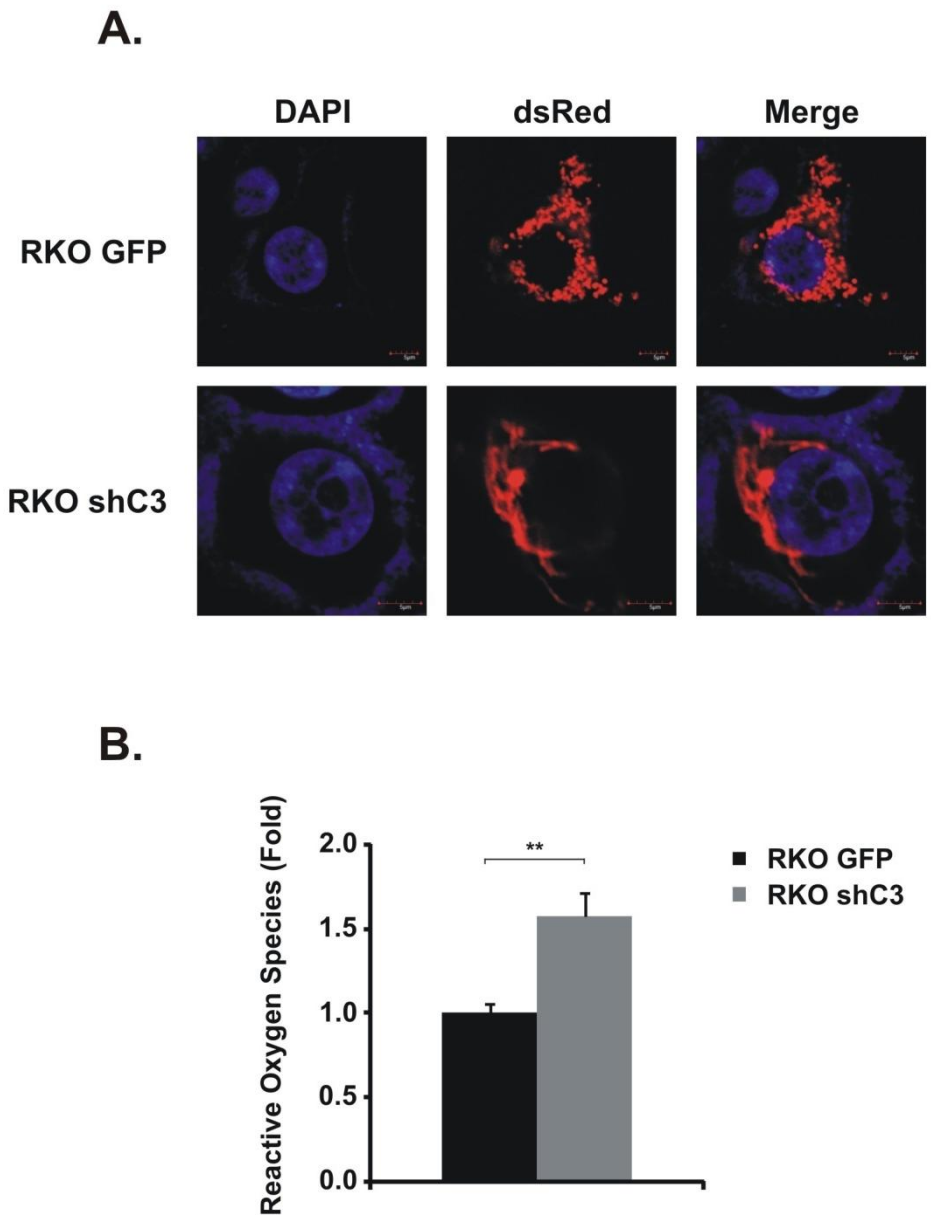

Figure 13: Caspase-3 knockdown cells recapitulate mitochondrial morphology differences.

(A) Representative images of RKO GFP and shC3 cells transfected with dsRED. (B) Mitochondrial reactive oxygen species in RKO GFP and shC3 cells.

2.4.8 Caspase-3 knockout cells show reduced viability *in vivo*

In an effort to determine if the reduced proliferation of C3KO witnessed *in vitro* had physiological relevance, we injected both WT HCT116 and C3KO cells into 7 week -old nude mice. C3KO cells showed a markedly reduced proliferation with tumor volumes less than half the size of WT (Figures 14A-B, and 15). Additionally, C3KO tumors showed less positive staining for the proliferation marker PCNA (Figure 14C-D). These data confirm that C3KO cells show reduced proliferation *in vivo*.

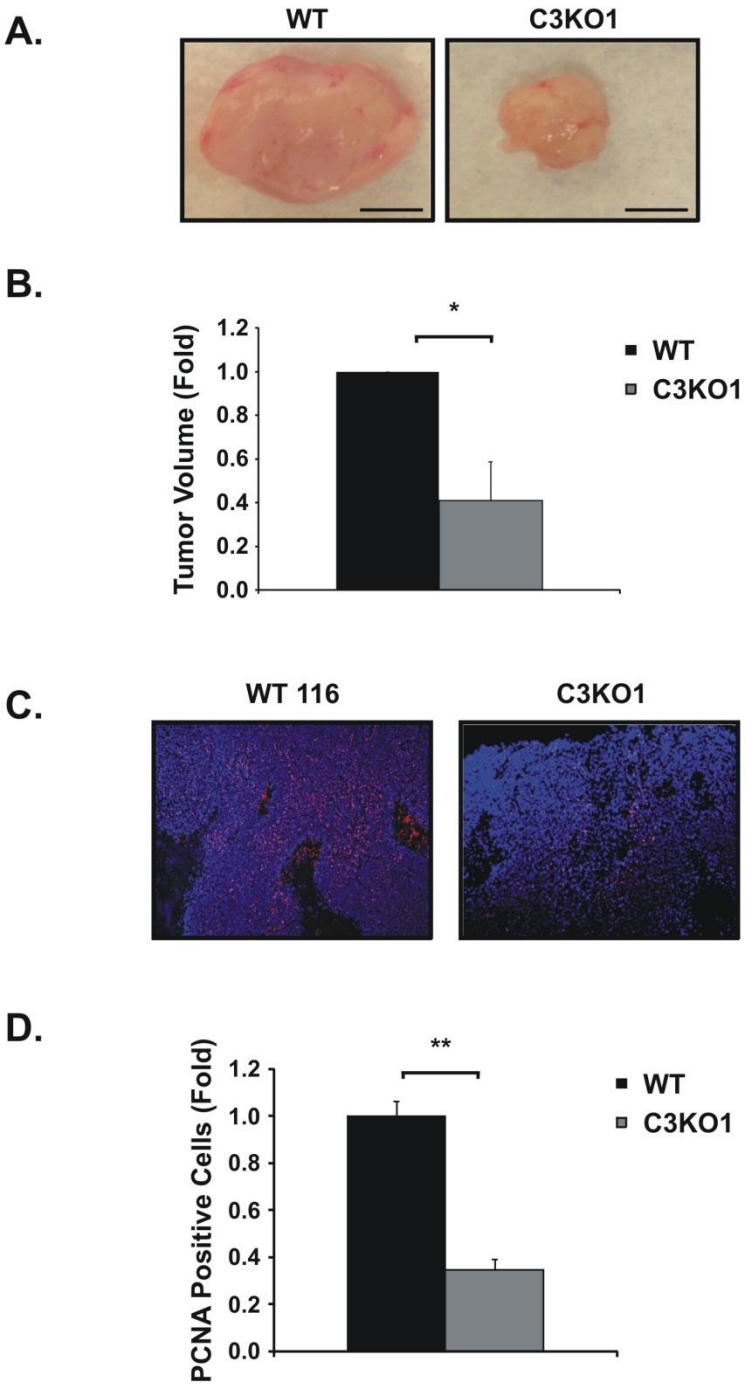

Figure 14: Caspase-3 knockout cells show reduced proliferation *in vivo*.

(A) Representative images of WT and C3KO1 xenograft tumors 21 days after injection. (B) Relative average tumor volume (mm^3). (C) PCNA -stained WT and C3KO tumor sections. (D) Relative PCNA -positive cells in WT and C3KO tumors.

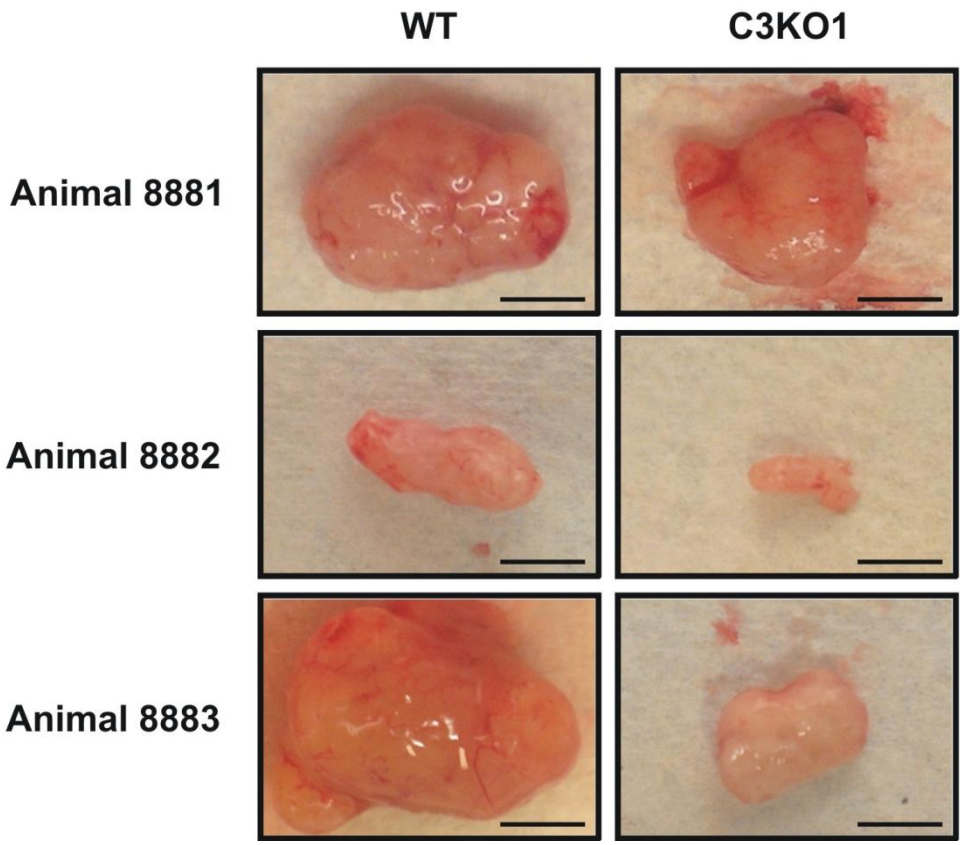

Figure 15: Caspase-3 knockout tumors are smaller than WT counterparts.

(A) Representative WT and C3KO mouse xenograft tumors.

2.5 DISCUSSION

In an effort to determine the role of caspase-3 in colorectal cancer cell maintenance and death we generated HCT116 C3KO cells. Much to our surprise, C3KO cells showed reduced survival and proliferation in the absence of treatment. Further analysis revealed altered mitochondrial morphology and decreased levels of oxidative phosphorylation. Preliminary data suggests that a reduction in the mitochondrial fusion protein MFN-2 may have a role in altering mitochondrial function, but further investigation is needed.

Historically, there has been a plethora of knowledge on the role of caspases in cell death, yet little is known about the role of caspases in metabolism. However, knowledge of caspase involvement in metabolic processes has emerged in recent years. Caspase-1-dependent production of the inflammatory cytokines IL-1 and IL-18 has been shown to be critical in the regulation of appetite, body weight, glucose homeostasis, and lipid metabolism [153]. Recent work suggests that caspase-3 might also have metabolic roles. In response to resveratrol treatment, cancer cells show a shift in hemoglobin conformation from the T to R state which results in the alteration of the cell's metabolic balance and an overall shift to intensification of the pentose phosphate pathway. This leads to higher oxygen levels and activation of caspase-3. Caspase-3, in turn, cleaves Band 3 which inhibits anion transport resulting in lower ROS levels [154, 155]. These results lend support to the reduced ROS levels seen in our experiments when caspase-3 was present.

The outer mitochondrial membrane GTPase mitofusin 2 (MFN2) was reduced in C3KO cells and might be responsible for the altered mitochondrial morphology and reduced cell survival. In MFN2 -null mouse embryonic fibroblasts, investigators found an increase in ER chaperone proteins, ER stress, and exacerbated ER stress-induced apoptosis [156]. MFN2 knockout cell models also show swollen mitochondria and a reduction in spare respiratory capacity, both of which are mimicked in our cells [157]. The amount of overlap between MFN2 knockout models and our system coupled with the reduced levels of MFN2 in C3KO cells suggests that caspase-3 might be regulating MFN2 levels. The E3-ubiquitin ligase Parkin is the best known regulator of MFN2. In response to mitochondrial depolarization PTEN induced putative kinase 1 (PINK1) is activated and translocates to the mitochondria where it phosphorylates and activates Parkin. Parkin then ubiquitinates MFN2 targeting it for proteosomal degradation [158, 159]. Perhaps caspase-3 is responsible for cleaving PINK1 or another kinase with similar function. If this were the case, restoration of caspase-3 would lead to reduced ubiquitination and degradation of MFN2. This hypothesis is also in line with the necessity of caspase-3 being catalytically active. Reconstitution of C3KO cells with C163A catalytically dead caspase-3 showed no improvement in cell growth when compared to C3KO cells expressing a GFP control (Figure 6). While our data suggest a possible connection between caspase-3 and MFN2 (Figure 16) further investigation will need to be conducted to determine if loss of MFN2 is the cause behind our phenotype or merely a consequence of it.

C3KO xenografts had reduced tumor volume and proliferation when compared to WT counterparts lending credence to the validity of our findings *in vivo*. Having determined this, it is worthwhile to further investigate targeted therapies inhibiting caspase-3 activity in CRC patients as they may prove beneficial in slowing and or reducing tumor volumes to a point where

surgical removal can more easily be performed. Caspase-3 is widely known for its role as an executioner caspase in the apoptotic response but little more. We have identified caspase-3 as a key protein in the regulation of mitochondrial morphology and cellular metabolism and proliferation. These results may prove beneficial in advancing therapies focused on exacerbating the metabolic differences between normal and cancerous cells.

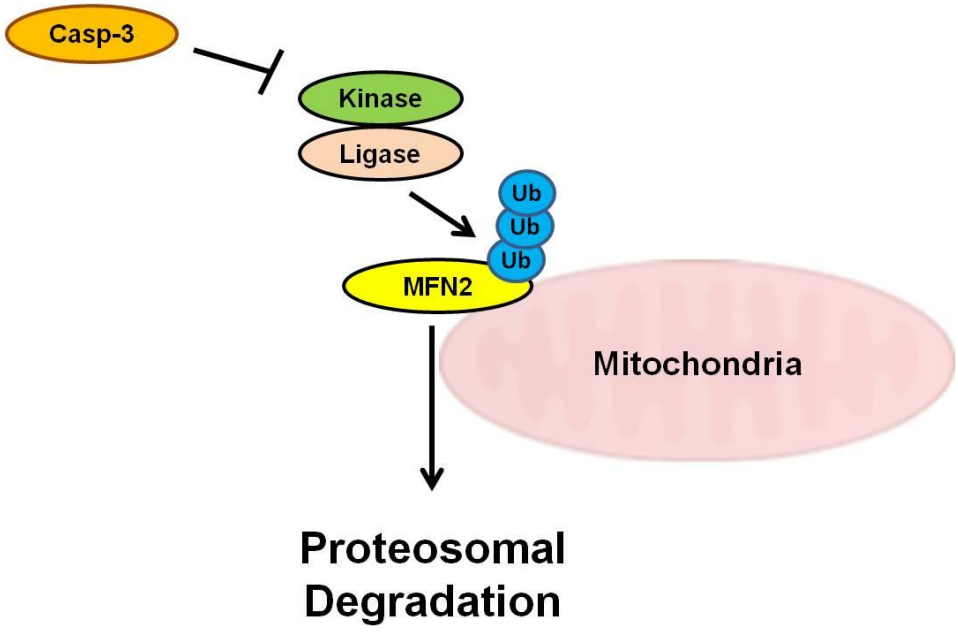

Figure 16: A model for the potential interaction between caspase-3 and MFN2

Multiple phenotypes found in C3KO cells are consistent with what is found in MFN2 knockout models. It is our hypothesis that caspase-3 may play a role in regulation of MFN2 degradation.

3.0 CASPASE-3 SUPPRESSES DNA DAMAGE-INDUCED AND RIP1-DEPENDENT NECROSIS

3.1 ABSTRACT

Caspase-3 is a cysteine protease best known to execute apoptosis. We generated caspase-3 null (C3KO) HCT 116 human colorectal cancer cells and found they were sensitized to DNA damaging agents including 5-FU, Etoposide and Camptothecin, but not to TNF-α. Compared to parental cells, C3KO cells had intact apoptosis and underwent RIP1- and ROS-dependent, but RIP3-independent, necrosis. Drug-induced necrosis was blocked by the expression of full length or catalytically deficient caspase 3 in C3KO cells. Knockdown of *Caspase 3* in HCT 116 and RKO cells also enhanced sensitivity and necrosis to DNA damaging agents. 5-FU treatment led to recruitment of the unprocessed caspase 3 to a complex containing caspase-8, FADD and RIP1 in HCT 116 cells. Genetic ablation of caspase-3 or pan caspase inhibitor z-VAD stabilized a necrotic complex containing caspase-8, RIP1 and FADD. DR5, caspase-8, and FADD were found to be required for 5-FU-induced apoptosis and necrosis in C3KO cells. Furthermore, C3KO tumors exhibited enhanced response and necrosis to 5-FU *in vivo*. These data demonstrate a novel function of caspase-3 in suppressing RIP1- and caspase-8-dependent necrosis induced by genotoxic stress, which might be exploited in cancer therapy.

3.2 BACKGROUND

Colorectal cancer is the fourth most common form of cancer in the United States and is responsible for the second largest number of cancer associated deaths [3]. Chemotherapy is a common treatment for patients with Stage III or stage IV colon cancer, and the combination of DNA damaging agents such as 5-Fluorouracil (5-FU) and irinotecan (Camptosar) is often used [3]. The 5-yr survival of patients with Stage IV or more advanced disease is only 6% even with these aggressive treatments, and new therapies are urgently needed [3]. During transformation, neoplastic cells become resistant to apoptosis as a result of genetic and epigenetic alterations, driving accumulation of additional oncogenic events, and resistance to chemotherapy and radiation [15, 160, 161]. The exploration of alternative death pathways might provide new therapeutic options.

Apoptosis is initiated by two major pathways in mammalian cells. Engaging the mitochondria-dependent intrinsic and death receptor-dependent extrinsic apoptotic pathways leads to the activation of initiator caspases-9 and -8, respectively, which in turn activate executioner caspases-3 and -7 [160, 161]. Caspase-3-dependent apoptosis in both cancer cells and the stroma was found to stimulate growth of cancer cells following radiation therapy for tumor repopulation, and higher levels of activated caspase-3 is associated with increased recurrence and shorter survival [162]. Additionally, caspase-3 is found to play nonapoptotic roles such as regulation of brain development and stem cell differentiation [82, 84, 86]. All of these functions are dependent upon its enzymatic activity, while little is known about non-enzymatic functions of caspase-3.

Necrosis has long been viewed as an unregulated form of cell demise that promotes inflammation and tissue damage. However, emerging evidence indicates that some forms of necrosis are programmed, and proceed through an orderly process that is initiated at the cell

surface upon activation of the extended TNF-α receptor family, and propagates through the receptor-interacting serine threonine kinases, RIP1 and RIP3 [163-166]. Blocking apoptosis genetically by *caspase 8* ablation or using pan-caspase inhibitor z-VAD is often required to induce programmed necrosis in a context- and cell type-dependent manner. In mice, caspase-8 suppresses RIP3-dependent necrosis during development [167, 168], and intestinal necrosis associated with inflammation involving the production of TNF-α [154, 155]. In cancer cells, TNF-α-induced necrosis has recently been investigated at the molecular level, and MLKL and PGAM5 were found to mediate events downstream of RIP1/RIP3 through the mitochondria [96, 97]. In most of these studies, necrosis is induced by a combination of TNFα, the pan caspase inhibitor z-VAD, and sometimes further enhanced by SMAC mimetics that deplete both ring-containing E3 ubiquitin ligases cIAP1 and cIAP2. Limited evidence suggests that necrotic cell death can occur independent of either RIP1, RIP3 [169, 170] or both [171]. In contrast, little is known about DNA damage-induced necrosis despite its potential significance in cancer therapy.

In the current study, we report a novel function of caspase-3, independent of its enzymatic function, in suppressing necrosis triggered by genotoxic stress in colon cancer cells. In an attempt to establish an apoptosis-resistant cancer cell model, we generated *caspase-3* null (C3KO) HCT116 colon cancer cells. Unexpectedly, *caspase-3* KO cells showed normal apoptotic response, but were significantly more sensitive to DNA damaging agents, but not to TNFα, compared to their wild-type counterparts. Elevated cell death induced by 5-FU and other DNA damaging agents in these cells was attributable to RIP1 and reactive oxygen species (ROS)-dependent necrosis, and a complex containing caspase-8/RIP1/FADD. This form of necrosis is RIP3-independent and requires death receptor DR5, caspase 8, and the adaptor protein FADD.

3.3 MATERIALS AND METHODS

3.3.1 Cell culture and drug treatment

Human colorectal cancer cell lines, including HCT116, HT29 and RKO and embryonic kidney 293T cells were obtained from the American Type Culture Collection (Manassas, VA, USA). RKO, HT29, HCT116 and derivative cell lines were cultured in McCoy's 5A modified media (Life Technologies) at 37ºC/5% CO_2. 293T cells were maintained in DMEM (Life Technologies) media at 37ºC/5% CO_2. All media was supplemented with 10% FBS and 1% Penicillin-Streptomycin solution (Sigma). Unless otherwise noted all drugs were reconstituted in 1% dimethyl sulfoxide (DMSO) and used as follows: 50 µg/ml 5-fluorouracil (5-FU), 100 µM Etoposide (Etop), 750 nM Camptothecin (CPT), 15 µM Necrostatin-1 (Nec-1) (Sigma) and 20 µM Z-VAD-FMK (z-VAD) (BaChem).

3.3.2 Targeting *Caspase-3* in HCT116 cells

Gene targeting vectors were constructed by using the recombinant adeno-associated virus (rAAV) system as previously described [147]. Briefly, two homologous arms (1.334 kb and 1.411 kb, respectively) flanking exons 5 and 7 of *caspase-3*, along with a neomycin-resistant gene cassette (*Neo*), were inserted between two Not I sites in the AAV shuttle vector pAAV-MCS (Stratagene, La Jolla, CA). Packaging of rAAV was performed by using the AAV Helper-Free System (Stratagene) according to the manufacturer's instructions.

HCT116 cells containing two copies of WT *Casapse-3* were infected with the rAAV and selected by G418 (0.5 mg/ml, Mediatech, Manassas, VA) for 3 weeks. Drug-resistant clones were pooled and screened by PCR for targeting events. Prior to targeting the second allele, the *Neo* cassette, which is flanked by Lox P sites, was excised from several heterozygous clones by infection with an adenovirus expressing Cre recombinase (Ad-Cre) [147]. Single clones were screened by PCR for *Neo* excision, and positive clone for independent heterozygotes was infected again with the same *caspase-3*-targeting construct. After the second round, *Neo* was again excised by Ad-Cre infection, and gene targeting in caspase-3 KO cells was verified by PCR and western blotting. All primer sequences used are listed in Table 3. *FADD* KO HCT116 cells were generated in Yu lab using a similar approach [153].

3.3.3 Reverse transcriptase polymerase chain reaction (RT-PCR)

Total RNA was isolated from cells using the RNAgents Total RNA Isolation System (Promega, Madison, Wisconsin, USA) according to the manufacturer's instructions. First strand cDNA was synthesized using Superscript Reverse Transcriptase (Invitrogen) according to the manufacturer's instructions. PCR was performed on a Thermo Scientific Hybaid MultiBlock MBS 0.2S Thermal Cycler using gene specific primers. Primers used are listed in Table 3. PCR products were analyzed by agarose gel electrophoresis.

Table 3: Sequences used in experiments

Target		Sequence
Caspase-3	Right Arm Forward 1	5’-CTGGGAAGATAGCAGGGTTTGTGT-3'
	Right Arm Reverse 1	5’-TTTGTGAGCATGGAAACAATACATGT-3'
	Left Arm Forward 1	5’-AGAACTGGACTGTGGCATTGAG-3’
	Left Arm Reverse 1	5'-GCTTGTCGGCATACTGTTTCAG-3’
Neomycin	Forward 1	5’-TCTTGACGAGTTCTTCTGAG-3’
	Reverse 1	5’-TTGTGCCCAGTCATAGCCG-3'
GAPDH	Forward 1	5’-TGCACCACCAACTGCTTAGC-3’
	Reverse 1	5’-GGCATGGACTGTGGTCATGAG-3’
RIP1	Forward 1	5’-GGCGTCATCATAGAGGAAGG-3’
	Reverse 1	5’-TGTGTATCACGCCTTTTCCA-3’
RIP2	Forward 1	5’-GGAATTATCTCTGAACATACCTG-3’
	Reverse 1	5’-CCTGGACAGAAGGGCATCTAGC-3'
RIP3	Forward 1	5’-TGCTGGAGGAGAAGTTGAGTTGC-3’
	Reverse 1	5’-CTGTTGCACACTGCTTCGTACAC-3’
Control	siRNA	5'-AACGUACGCGGAAUACUUCGA-3'
Caspase-8	siRNA	5’-AAGAGTCTGTGCCCAAATCAA-3’
DR5	siRNA	5'-AAGACCCUUGUGCUCGUUGUC-3'
Control	shRNA	5'-CCGCAGGTATGCACGCGT-3'
RIP1	shRNA	5’-TAAGCTGAAAGAACATGACCT-3’
Caspase-3	shRNA1	5'-GCGAATCAATGGACTCTGGAA-3'
	shRNA2	5'-CCTGAGATGGGTTTATGTATA-3'
	shRNA3	5'-CCGAAAGGTGGCAACAGAATT-3'
	shRNA4	5'-CTAAAGGTGGTGAGGCAATAA-3'
	shRNA5	5'-GTGGAATTGATGCGTGATGTT-3'
RIP3	Expression plasmid F	5’-TTCAAGCTTGATGTCGTGCGTCAAGTTATGGCC-3’
RIP3	Expression plasmid R	5’-CGTTGAGCTGAGTTGCCAGCTGGTCTAAAAGAGTATC-3’
RIP3-K50A	Expression plasmid F	5’-GATGTGGCGGTCGCAATCGTAAACTCG-3’
RIP3-K50A	Expression plasmid R	5’-CGAGTTTACGATTGCGACCGCCACATC-3’

3.3.4 Transfection

Full-length human caspase-3 (Addgene # 11813) and catalytically dead human C163A caspase-3 (Addgene# 11814) were obtained from Addgene (Cambridge, MA). RIP1 lacking the entire kinase domain rendering it dominant negative was a generous gift from Dr. Junying Yuan at Harvard University. All plasmids were transfected with Lipofectamine 2000 (Invitrogen) according to the manufacturer's instructions. Stable clones were maintained in McCoy's 5A supplemented with 0.4 mg/ml G418 (Gibco).

Small-interfering RNA (siRNA) duplexes were obtained from Qiagen (Venlo, Netherlands) and include: caspase-8, DR5 and control scrambled siRNA (Table 3). siRNA duplexes were transfected with Lipofectamine 2000 according to the manufacturer's instructions with minor modifications. Briefly, 400 pmols of siRNA duplexes were transfected into cells in 12-well plates for 4 hours, followed by incubation in medium containing 5% FBS for 20 hours, and then drug treatment in complete media containing 10% FBS.

The HA-tagged full length RIP3 expression vector was constructed by cloning RT-PCR products into the pcDNA3.1-N-HA vector (Invitrogen). Variants of this vector including the K50A point mutation rendering RIP3 catalytically dead were constructed similarly. Sequences used are listed in table 3.

3.3.5 Caspase-3 and RIP1 Knockdown

Lentiviral particles were generated by co-transfection of 4 plasmids [Control plasmid (pLK01.GFP-puro) or the CASP3 specific shRNA plasmids pLK01.CASP3-sh1 through 5

(Sigma), together with pMD2.g (VSVG), pVSV-REV and pMDLg/pRRE] into 293-FT cells using FuGene 6 Transfection reagent (Table 3). The collection and isolation of lentiviral particles, and lentiviral transduction and screening of most effective CASP3 shRNA was carried out as described previously [148]. The CASP3-specific shRNA (shRNA2, table 3) was used in HCT116, RKO and FADD KO cells. In brief, cells were plated and allowed to grow until 40% confluent. Cell media was replaced with a 1:1 dilution of lentivirus containing CASP3-shRNA2 and McCoy's 5A media supplemented with 8μg/ml polybrene (Millipore). Cells were then incubated at 32°C/5% CO_2 for 16 hours. Cell media was removed and replaced with fresh McCoy's 5A and cells were incubated for 8 hours at 37°C/5% CO_2. This process was repeated a second time before putting the cells permanently at 37°C/5% CO_2 under puromycin (2 μg/ml) selection, and single clones were isolated by limiting dilution. Knockdown of *CASP3* was determined by quantitative RT-PCR using an Applied Biosystems StepOnePlus system using the Applied Biosystems Taqman® Gene Expression Cells-to-CT kit [148], and validated by western blotting.

RIP1 knockdown lines were generated in a slightly different manner. In brief, 293T cells were plated in 12 well format and allowed to grow to 90% confluence, and transfected with 4 plasmids with Lipofectamine 2000 (Invitrogen), including pLK shRIP1 (Open Biosystems), pMD2.G (0.5 μg), pMDLg-pRRE (0.5 μg) and pRSV-Rev (0.5 μg) according to the manufacturer's instructions. Sequence data is provided in Table 3. Forty-eight hours after transfection, the viral supernatant was harvested with a syringe and needle. Supernatant was then passed through a 0.45μm filter and mixed 4:1 with McCoy's 5A containing 8 μg/ml polybrene. Virus/media mixture was then added to HCT116 caspase-3 KO cells for 48 hours. Cells were

permanently maintained at 37°C/5% CO_2 under puromycin (2 µg/ml) selection, and single clones were isolated by limiting dilution.

3.3.6 Cell viability

Cells were plated at 20-30% confluence 24 hours prior to treatment. Unless noted otherwise, cells were treated for 48 hours. Cell viability was assayed using Cell-Titer 96 Aqueous One Solution Cell Proliferation Assay and Cell-Titer-GLO Luminescent Viability Assay (Promega) according to manufacturer's recommendations. In some experiments, treated cells were washed 3 times with HBSS and stained with crystal violet dye (Sigma) for 10 minutes, followed by 3 more rinses with HBSS. All experiments were repeated for at least 3 times.

3.3.7 Mitochondrial outer membrane potential

Cells were plated at 20-30% confluence 24 hours prior to treatment. Following treatment, cells were assayed for mitochondrial outer membrane potential by MitoTracker Red CMXRos according to manufacturer's recommendations as previously described [172].

3.3.8 Propidium iodide and annexin V staining

Cells were plated at 20-30% confluence 24 hours prior to treatment. Following 48 hours treatment, cells were trypsinized and spun down at 3,000 RPM. Cells were then washed in cold PBS and reconstituted in 100µl of Annexin-binding buffer (10mM HEPES, 140 mM NaCl, 2.5 mM $CaCl_2$, adjusted to pH=7.4) containing 2 µl of Annexin V-Alexa Fluor 488 and 2 µl 50 µg/ml propidium iodide (Invitrogen). Cells were then allowed to incubate in the dark at room temperature for 15 minutes before being diluted with 300 µl Annexin-binding buffer. FL1 and FL2 emission was measured on a C6 flow cytometer (Accuri Cytometers). At minimum, 30,000 events per sample were measured and all experiments were performed in triplicate

3.3.9 Detection of reactive oxygen species

Cells were plated at 20-30% confluence 24 hours before treatment and then treated for 24 hours. Following treatment, cell media was removed and replaced with fresh media containing 2 µM mitoSox reagents (Life Technologies). Cells were then incubated for 20 minutes at 37ºC/5% CO_2. Following incubation cells were harvested washed once in cold phosphate-buffered saline (PBS) and then reconstituted in cold 1% BSA PBS. Following excitation at 518 nm, 580 nm emission was measured on a C6 flow cytometer (Accuri Cytometers). At minimum, 30,000 events per sample were measured and all conditions were performed in triplicate.

3.3.10 Immunoblotting

Cells were harvested in RIPA buffer (50 mM Tris pH 7.4, 150 mM NaCl, 1% Triton-X-100, 0.1% SDS, 1% Deoxycholate, 1 mM EDTA) supplemented with protease inhibitor cocktail (Roche Applied Sciences). Cells were rotated for one hour at 4ºC and then centrifuged at 13,000 RPM for 30 minutes. Protein concentration was determined by the Bradford assay and 40 µg per well was loaded in 10% bis-tris gels (Life Technologies). Gels were run for 40 minutes at 180v in MOPS buffer (Life Technologies). Protein was then transferred to PVDF membranes using a TransBlot SD semi-dry transfer cell (Biorad). Membranes were blocked for nonspecific binding with 5% nonfat milk in TBS-T for one hour at room temperature and then incubated in primary antibody overnight at 4ºC. Primary antibodies were used at a 1:1000 dilution and include HMGB1 (ab18256), DR5 (ab8416) (Abcam); FADD (F36620), RIP1 (610458), Ubiquitin (550944) (BD Transduction Laboratories); Caspase-7 (9492), Caspase-8 (9746), Caspase-9 (9502), p-p53 (9284) (Cell Signaling); RIP3 (IMG-5846A) (Imgenex); γ-H2AX (07-164) (Millipore); α-Tubulin (CP06), Noxa (OP180), (Oncogene Science); PUMA (3795) [173], cIAP1 (AF8181) (R&D); HA (sc-805) (Santa Cruz); Flag (F3165), β-Actin (A5441) (Sigma) and Caspase-3 (AAP103E) (Stressgen). Following primary membranes were washed with TBS-T and incubated in appropriate HRP-conjugated secondary for 1 hour at room temperature. Secondary antibodies used include goat-anti-rabbit (31462), goat-anti-mouse (31432) and mouse-anti-goat (31400) (Pierce). Presence of antibody binding was detected using Western Lighting - Plus ECL (Perkin Elmer) according to manufactures specifications. Membranes were then exposed on blue X-ray film (Phenix Research Products) [149].

3.3.11 Transmission electron microscopy

Cells grown on tissue culture plasticware were fixed in 2.5% gluaraldehyde in 100 mM PBS (8 gm/l NaCl, 0.2 gm/l KCl, 1.15 gm/l $Na_2HPO_4 \cdot 7H_2O$, 0.2 gm/l KH_2PO_4, pH 7.4) overnight at 4^{o}C. Monolayers were then washed in PBS three times then post-fixed in aqueous 1% osmium tetroxide, 1% Fe_6CN_3 for 1 hr. Cells were washed 3 times in PBS then dehydrated through a 30-100% ethanol series then several changes of Polybed 812 embedding resin (Polysciences, Warrington, PA). Cultures were embedded in by inverting Polybed 812-filled BEEM capsules on top of the cells. Blocks were cured overnight at 37^{o}C, and then cured for two days at 65^{o}C. Monolayers were pulled off the coverslips and re-embedded for cross section. Ultrathin cross sections (60 nm) of the cells were obtained on a Riechart Ultracut E microtome, post-stained in 4% uranyl acetate for 10 min and 1% lead citrate for 7 min. Sections were viewed on a JEOL JEM 1011 transmission electron microscope (JEOL, Peobody MA) at 80 KV. Images were taken using a side-mount AMT 2k digital camera (Advanced Microscopy Techniques, Danvers, MA) [150].

3.3.12 Immunoprecipitation

The protocol was modified from [174]. In brief, following harvesting of cells, 5 mg of protein reconstituted in 1 ml of RIPA per condition was used in conjunction with the Invitrogen Protein A and G Dynabead® immunoprecipitation system according to manufacturer's recommendations. Antibodies used include RIP1 (610458) (BD Transduction); Caspase-3 (sc-

7148) and Caspase-8 (sc-6136) (Santa Cruz). Resulting precipitates were processed in the same manner as other immunoblots noted above [174].

3.3.13 Xenograft studies

All animal experiments were approved by the University of Pittsburgh Institutional Animal Care and Use Committee. Female 5–6 week-old Nu/Nu mice (Charles River, Wilmington, MA) were housed in a sterile environment with micro isolator cages and allowed access to water and chow *ad libitum*. Mice were injected subcutaneously in both flanks with 4×10^6 WT or *caspase-3*-KO HCT116 cells. After implantation, tumors were allowed to grow 7 days before treatment was initiated. Mice were randomized into two groups (n = 9 per group) receiving either vehicle (PBS) or 5-FU (50 mg/kg/d) every other day for 14 days. Detailed methods on tumor measurements, harvests and histological analysis are as described [175, 176].

3.3.14 Tissue preparation and analysis of histology and Immunohistochemistry (IHC)

Following sacrifice of mice, tumors were dissected and fixed in 10% formalin for histological analysis as described previously [175, 176]. Five-micron (5 μm) sections were used for staining. Histological analysis was performed by hematoxylin and eosin (H&E) staining. Cell death was analyzed by TUNEL staining with the ApopTag Fluorescein In Situ Apoptosis Detection Kit (Chemicon International, Temecula, CA) according to the manufacturer's instructions.

Activated caspase-3 IHC was performed as described [177]. In brief, tissue sections (5µm) were deparafinized, rehydrated through graded ethanol and treated with 3% hydrogen peroxide. Antigen retrieval was performed by boiling the sections for 10 minutes in 0.1 M citrate buffer (pH 6.0) with 1 mM EDTA. Non-specific antibody binding was blocked using 20% goat serum at room temperature for 30 minutes. Sections were incubated overnight at 4◦C in a humidified chamber with 1:100 diluted rabbit-anti-caspase-3 (cleaved, Asp 175) (9661; Cell Signaling Technologies, Beverly, MA). Sections were then incubated for 1 h at room temperature with biotinylated goat-anti-rabbit secondary antibodies (#31822; Pierce) and developed with an ABC kit and DAB (Vector Laboratories, Burlingame, CA).

3.3.15 Statistical Analysis

Statistical analyses were carried out using GraphPad Prism IV software. P values were calculated by the student's t-test and were considered significant if $p < 0.05$. The means ± standard error (s.e.m.) is displayed in the figures.

3.4 RESULTS

3.4.1 *Caspase-3* knockout cells are more sensitive to DNA damaging agents

To model apoptosis resistance, we generated several *caspase-3* KO (C3KO) HCT116 human colon cancer cell lines using the recombinant adeno-associated virus (rAAV) mediated gene

targeting (Figure 17A). This line was chosen because of its well-characterized responses to a wide range of anti-cancer agents and prior successes in gene targeting. Deletion of exon 5-7 of *Caspase-3* gene was verified by polymerase chain reaction (PCR) (Figure 17B), and complete loss of protein expression was confirmed by western blot (Figure 17C). Unexpectedly, C3KO cells were found to be significantly more sensitive to common chemotherapeutics and DNA damaging agents including 5-flurouracil (5-FU), Camptothecin (CPT) and Etoposide (Etop) using MTS assays and 3 independent knockout lines (Figure 17D and data not shown).

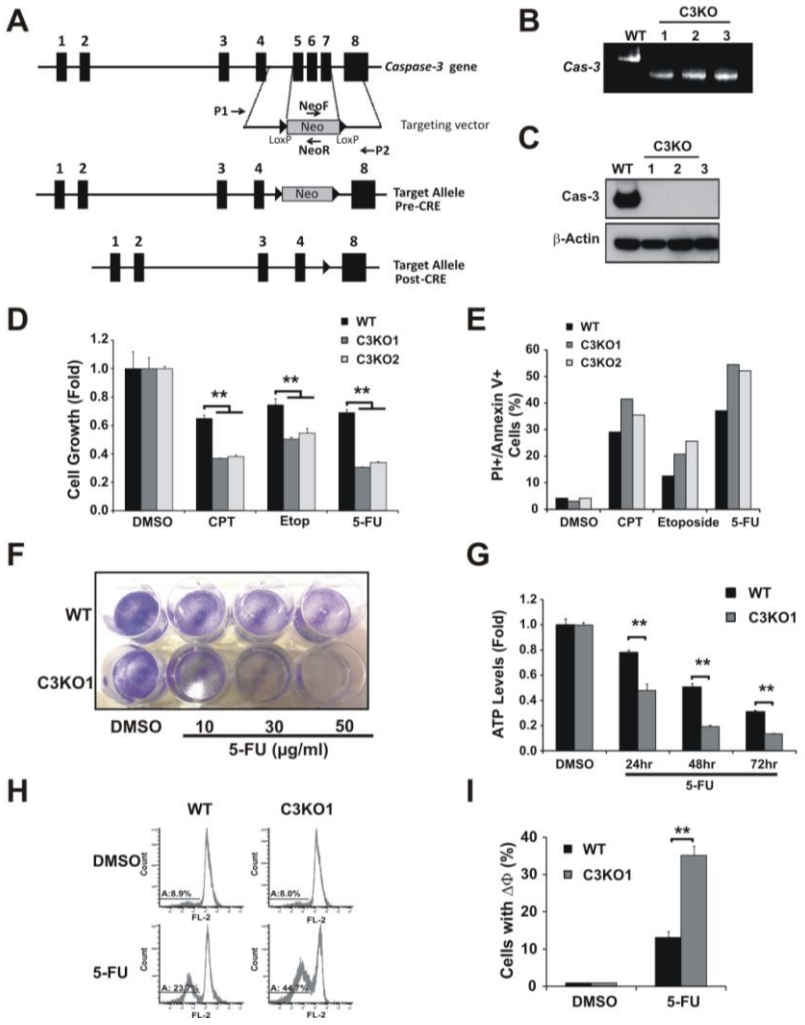

Figure 17: Caspase-3 knockout cells are more sensitive to DNA damaging agents.

(A) Schematic representation of *caspase-3* genomic locus and the targeting constructs and strategy. NeoF, NeoR, P1 and P2 are PCR primers (sequences in Table 3) for identifying knockout clones. (B) PCR analysis with primers P1 and P2 showing both full length (WT) and targeted *caspase-3* allele (C3KO). (C) Protein expression of caspase-3 in HCT116 WT and 3 independent C3KO clones. (D) Formazan production by HCT116 WT and C3KO cells treated with Camptothecin (500 nM), Etoposide (50 μM) or 5-FU (50 μg/ml) for 48h. (E) Quantification of PI+/Annexin V+ cells for cells treated as in A. (F) Adherent cells 48h after 5-FU (50 μg/ml) treatment stained by crystal violet. (G) Cellular ATP levels following 5-FU (50 μg/ml) treatment at the indicated times. Values were normalized to the DMSO treated cells. (H) Mitochondrial out membrane potential following 48h treatment with 5-FU (20 μg/ml). (I) Quantification of cells in (H) with decreased mitochondrial out membrane potential. **p<.01

Flow cytometry analysis showed highly elevated cell death in C3KO cells evidenced by the propidium iodide (PI) +/Annexin V+ population (Figure 17E). Reduction of adherent cells, cellular ATP levels and mitochondrial outer membrane potential further validated increased sensitivity of C3KO cells to 5-FU (Figure 17F-I). However, the fraction of Annexin V+, or apoptotic cells was nearly identical in WT and C3KO cells (Figure 18A). This is consistent with largely intact activation of caspase-7, -9, but not caspase-8, C3KO cells (Figure 18B). Markers of DNA damage response were also indistinguishable in WT and C3KO cells, including γ-H2AX, phosphorylated p53 (S15), induction of p53 targets PUMA, Noxa and p21, and depletion of cIAP1 (Figure 18C). These findings demonstrate that caspase-3 is dispensable for DNA-damage induced apoptosis, but suppresses non-apoptotic cell death.

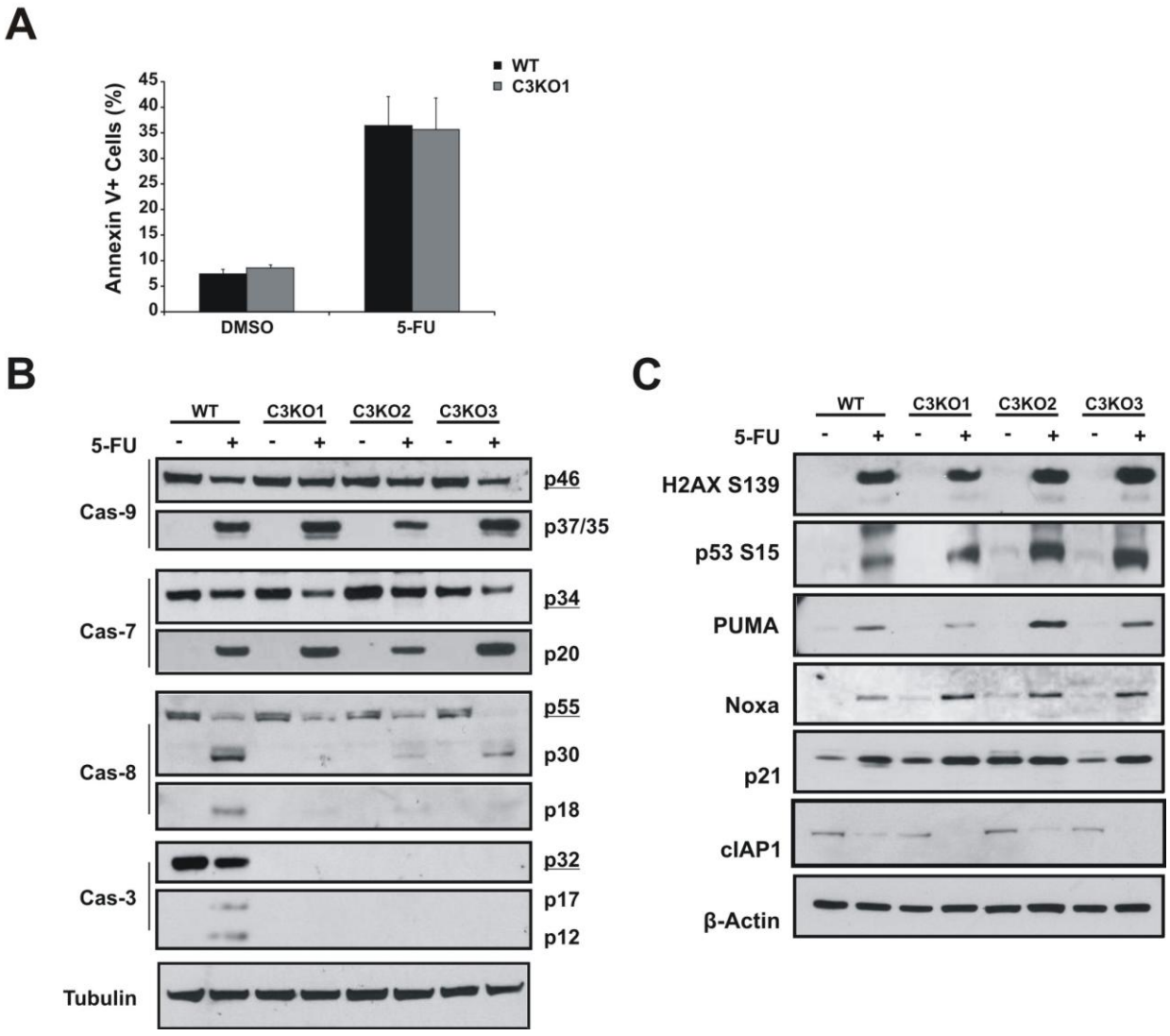

Figure 18: Apoptosis is not compromised in caspase-3 KO cells.

HCT 116 and C3KO cells were treated with 5-FU (50 μg/ml). (A) Fractions of Annexin V+ cells 48 h after treatment. (B) Western blots of the indicated caspases 24h after 5-FU treatment. The full length proteins were underlined. (C) Western blots of the indicated DNA damage response associated proteins 24h after 5-FU treatment.

3.4.2 DNA damage induces necrosis in *caspase*-3 KO cells

Significantly increased PI+ populations in C3KO cells suggested activation of non-apoptotic cell death after 5-FU treatment (Figure 19A). The release of nuclear protein HMGB1 into the culture media is a marker for necrosis [178], and was readily detected in 5-FU treated C3KO cells, but not in WT cells (Figure 19B). The pan caspase inhibitor z-VAD-FMK (z-VAD) had no affect on the PI+/Annexin V- populations, while significantly reduced the Annexin V+ apoptotic populations in both WT and C3KO cells (Figure 19C). Transmission electron microscopy revealed classical morphologic signs of necrosis in C3KO cells, such as complete leakage of nuclear content and membrane disintegration (Figure 19D). Characteristic signs of apoptosis such as condensed and fragmented nuclei were found in both WT and C3KO cells (Figure 19D). Stable expression of the full length caspase-3 (FLC3) or a catalytically dead mutant (C163A) [179] in C3KO cells specifically reduced PI+/Annexin V- cells and HMGB1 release to the levels found in WT cells (Figures 19E-G and 20B-D). C3KO cells also showed a significant increase in PI+/Annexin V- populations and HMGB1 release after CPT or Etoposide treatment (Figure 19H-I). These findings demonstrate that caspase-3 suppresses DNA damage-induced necrosis independent of its enzymatic activity.

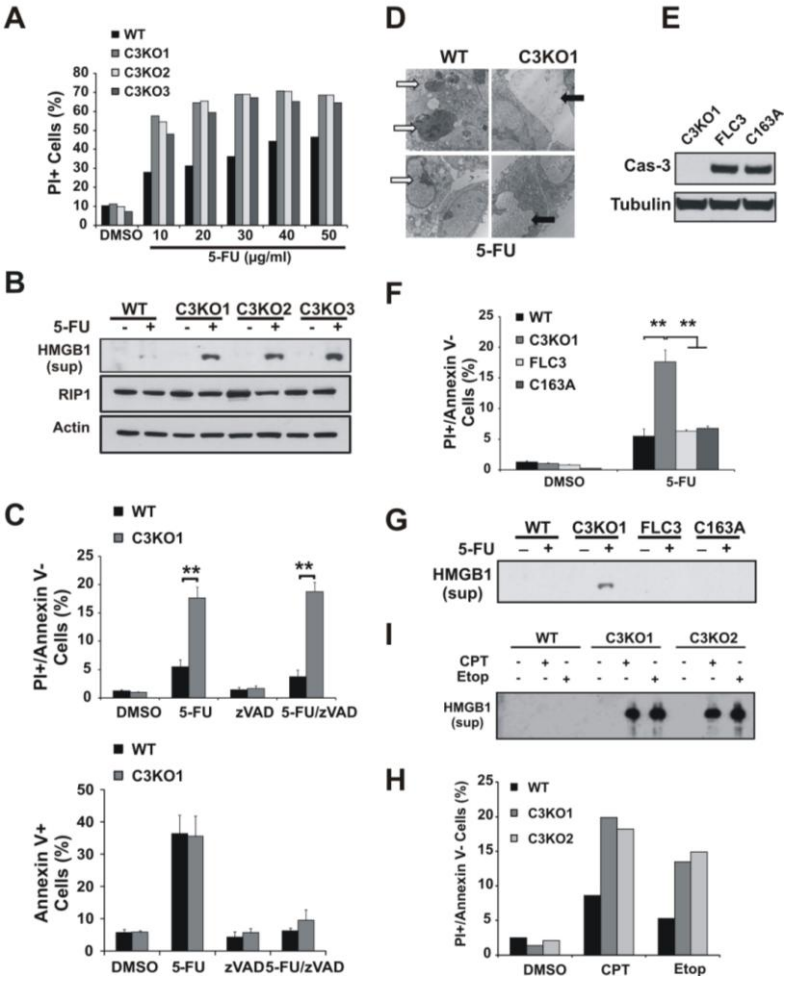

Figure 19: Induction of necrosis in 5-FU treated caspase-3 KO cells.

(A) Fractions of PI+ (dying) cells in HCT116 WT and C3KO cells treated with 5-FU (50 μg/ml) for 48h. (B) The levels of HMGB1 released into culture medium and RIP1 48h post 5-FU (50 μg/ml) treatment. (C) Fractions of PI+/Annexin V- (top) or Annexin V+ (bottom) cells 48h after 5-FU (50μg/ml) treatment with or without z-VAD (20 μM). (D) Representative images of transmission electron microscopy of cells 24h after 5-FU (50 μg/ml) treatment. White arrows denote apoptotic cells, black arrows denote necrotic cells. (E) Reconstitution of either full length caspase-3 (FLC3) or catalytically dead mutant (C163A) in C3KO cells confirmed by western blotting. (F) Fractions of PI+/Annexin V- in C3KO cells reconstituted with either full length caspase-3 or catalytically dead C163A mutant 48r after 5-FU (50 μg/ml) treatment. (G) The levels of HMGB1 in the medium of reconstituted C3KO cells 48h after 5-FU (50 μg/ml) treatment. **p<.01. (H) Fractions of PI+/annexin V- cells in WT and C3KO HCT116 cells 48h after CPT (500 nM) or Etoposide (50 μM) treatment. (I) The levels of HMGB1 in the medium of cells treated as in (H).

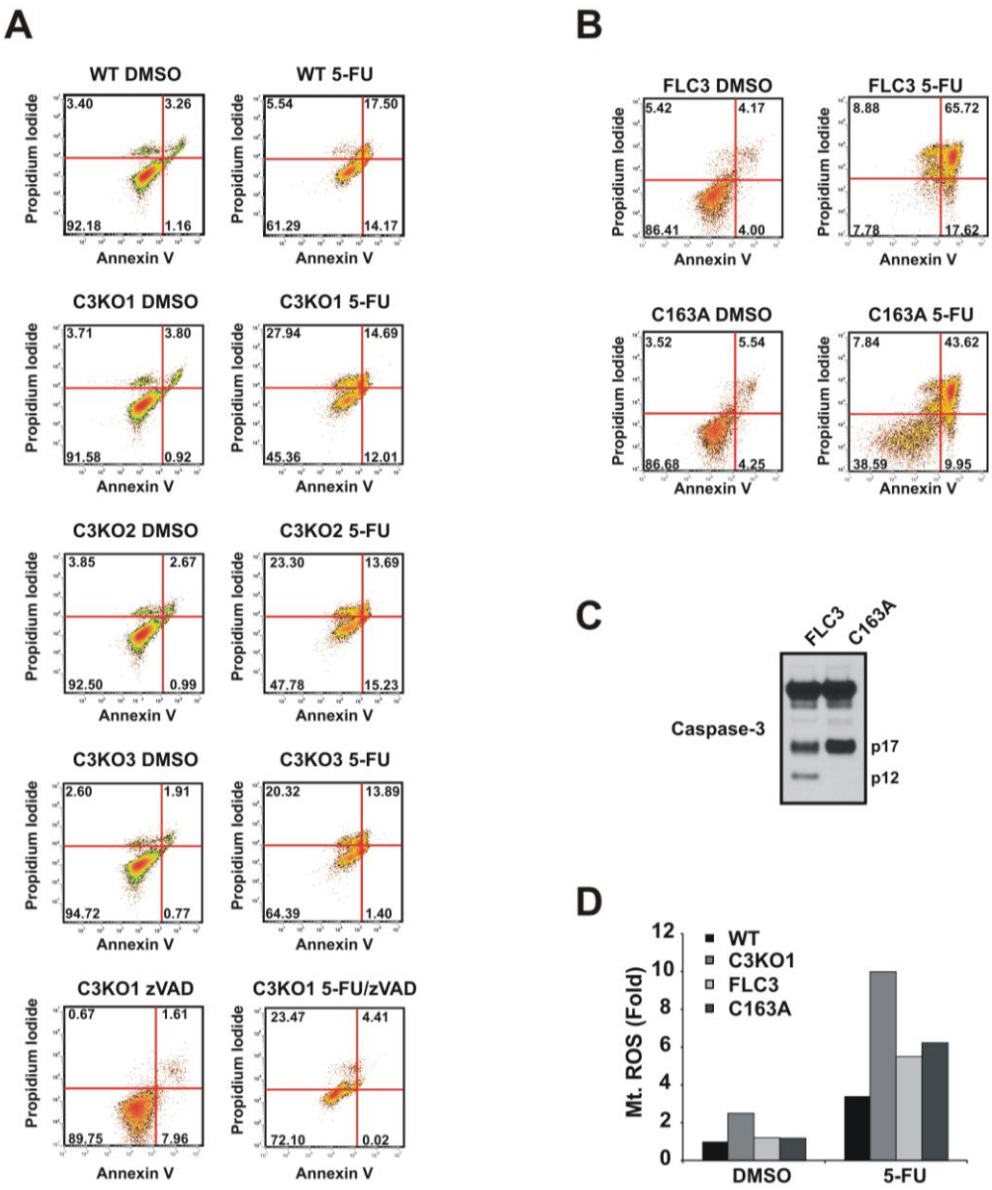

Figure 20: Induction of necrosis by DNA damage in caspase-3 KO cells.

HCT 116 and C3KO cells were treated with 5-FU (50 μg/ml) and stained by PI and annexin V, or mitoSox for cell death or ROS analyses. (A) Flow cytometry profiles of cells stained with PI and annexin V 48h after 5-FU treatment with or without z-VAD (20 μM). (B) Flow cytometry profiles for C3KO cells reconstituted with FLC3 or C163A mutant stained with PI and annexin V 48h after 5-FU treatment. (C) Caspase-3 activation in FLC3 and C163A reconstituted C3KO1 cells 24h after 5-FU (50 μg/ml) treatment was determined by western blotting. (D) Production of reactive oxygen species in C3KO cells 24h after 5-FU treatment.

3.4.3 Necrosis in *caspase-3* KO cells is RIP1-and ROS-dependent but RIP3-independent

We then investigated potential roles of receptor-interacting serine/threonine-protein kinase (RIPs) in 5-FU-induced necrosis. The expression of *RIP 1* and *RIP2* but not *RIP3* mRNA was detected by RT-PCR analysis in HCT 116 or C3KO cells (Figure 21A). RIP1, but not RIP3, protein was detected in HCT 116 and C3KO cells (Figures 19B and 21B). Exogenous expression of WT RIP3 or a kinase dead mutant (RIP3, K50A) did not increase necrosis in either WT or C3KO cells (Figures 21C-E). A highly potent, specific small molecule inhibitor of RIP1, Necrostatin-1 (Nec-1), or expression of either a short-hairpin RNA (shRNA) against RIP1 or kinase domain deleted (DN) RIP1 significantly reduced the PI+/Annexin V- population and HMGB1 release in 5-FU treated C3KO cells (Figures 22A-C). RIP1 KD, or RIP1 DN did not significantly reduce caspase-7 or-9 activation or apoptosis in C3KO cells (Figure 22C). Co-treatment of cyclohexamide and TNFα led to increased apoptosis but not necrosis in both WT and C3KO cells (Figure 23), consistent with a requirement of RIP3 for TNFα-induced necrosis.

Necrosis can occur in both a reactive oxygen species (ROS) -dependent and independent manner [97]. A significant increase in ROS production was detected in C3KO cells over WT cells 24 hours after 5-FU treatment (Figure 22D). Treatment with ROS scavenger glutathione (GSH) reduced 5-FU induced necrosis as measured by PI+/Annexin V- cells and HMGB1 release (Figures 22E-F and 24A), while *RIP1* knockdown did not affect ROS production in either WT or C3KO cells (Figure 24B). These data strongly suggest that increased sensitivity to 5-FU in C3KO cells is driven by RIP1- and ROS-dependent necrosis, and ROS likely acts upstream of RIP1.

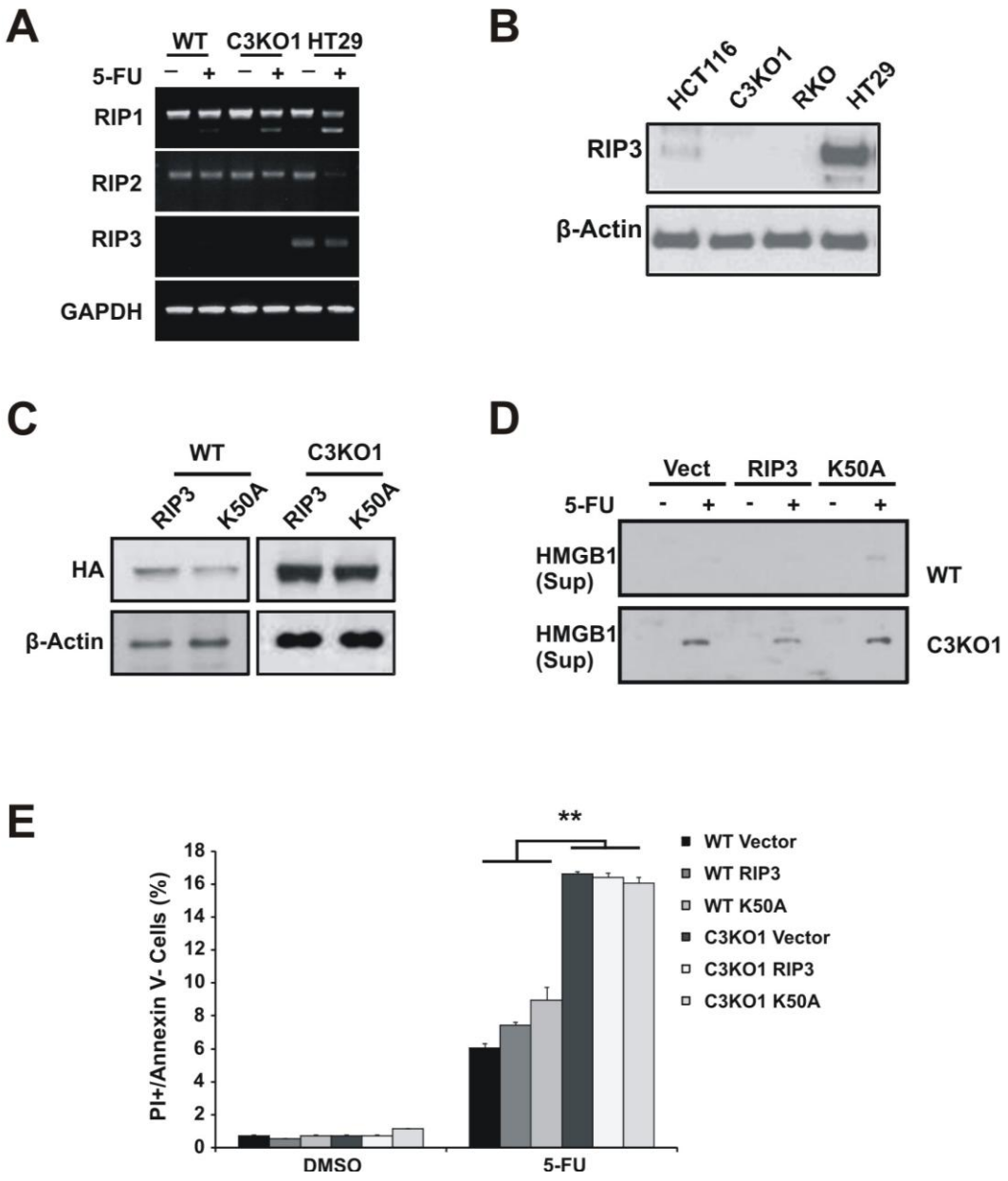

Figure 21: Caspase-3 KO cells die by RIP3-independent necrosis.

(A) *RIP1, 2 and 3 levels* were analyzed by RT-PCR in the indicated cells before or after 48h 5-FU (50μg/ml) treatment. (B) RIP3 protein levels analyzed by western blotting in the indicated colon cancer cells. (C) Expression of the full length RIP3 or catalytically dead mutant (K50A) analyzed in HCT116 WT or C3KO cells after transient transfection. (D) The levels of HMGB1 in the medium of cells transfected expression FL or K50A RIP3 48h after 5-FU (50 μg/ml) treatment. (E) Fractions of PI+/Annexin V- cells treated as in (D). **p<.01

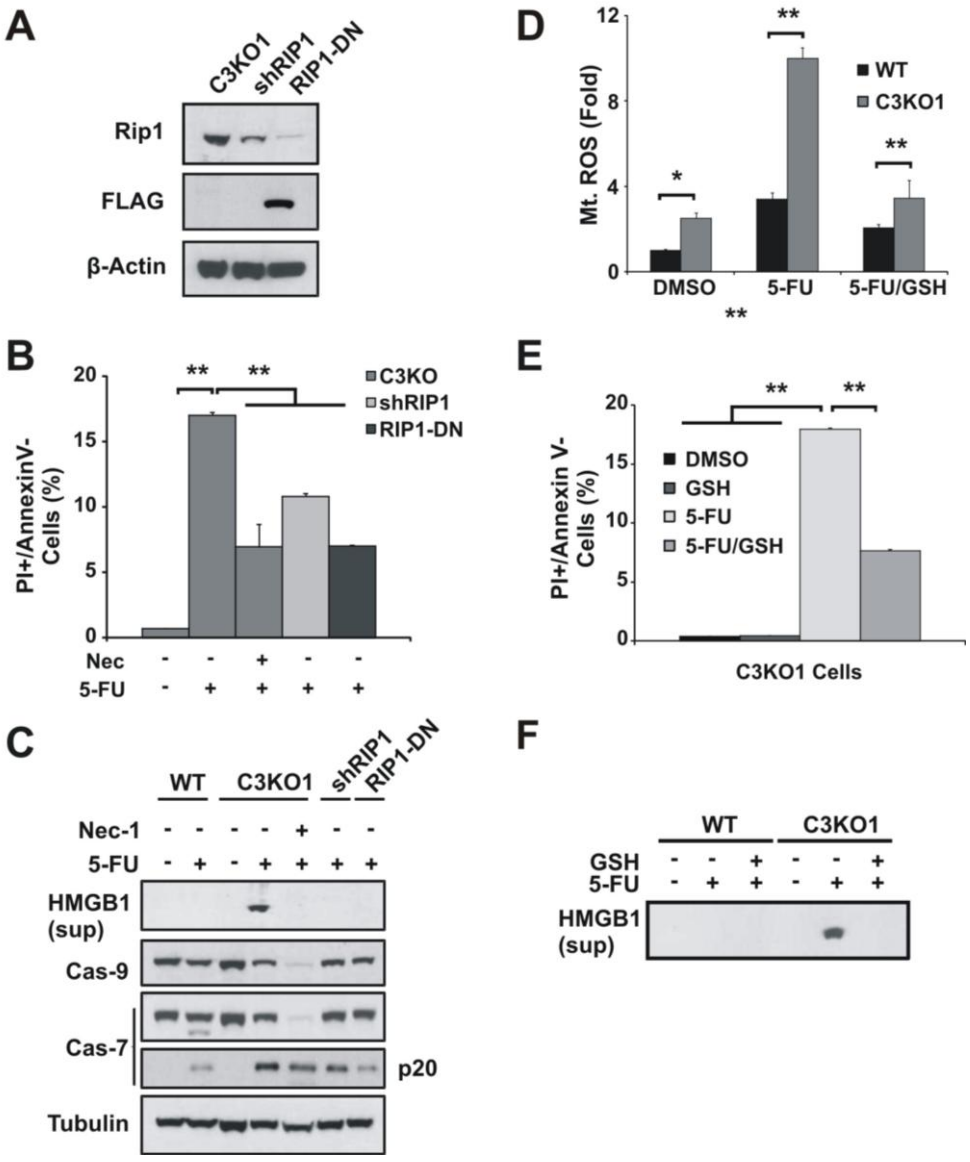

Figure 22: Caspase-3 KO cells die by RIP1 and ROS dependent necrosis.

(A) Stable expression of shRIP1 or dominant negative RIP1 (RIP1-DN) in HCT116 C3KO cells was confirmed by western blotting. (B) Fractions of PI+/Annexin- cells 48h after 5-FU (50 μg/ml) treatment with or without necrostatin-1 (15 μM). (C) The levels of HMGB1release (medium) and caspase-7 and-9 from indicated cells 48h after 5-FU (50 μg/ml) treatment. (D) Production of reactive oxygen species measured by mitoSox (Mt. ROS) in the indicated cells 24h after 5-FU (50 μg/ml) treatment with or without GSH (10 μM) treatment. (E) Fractions of PI+/Annexin V- C3KO cells at 48h after 5-FU (50 μg/ml) treatment with or without GSH (10 μM). (F) The levels of HMGB1 in the medium of the cells treated as in E. **p<.01.

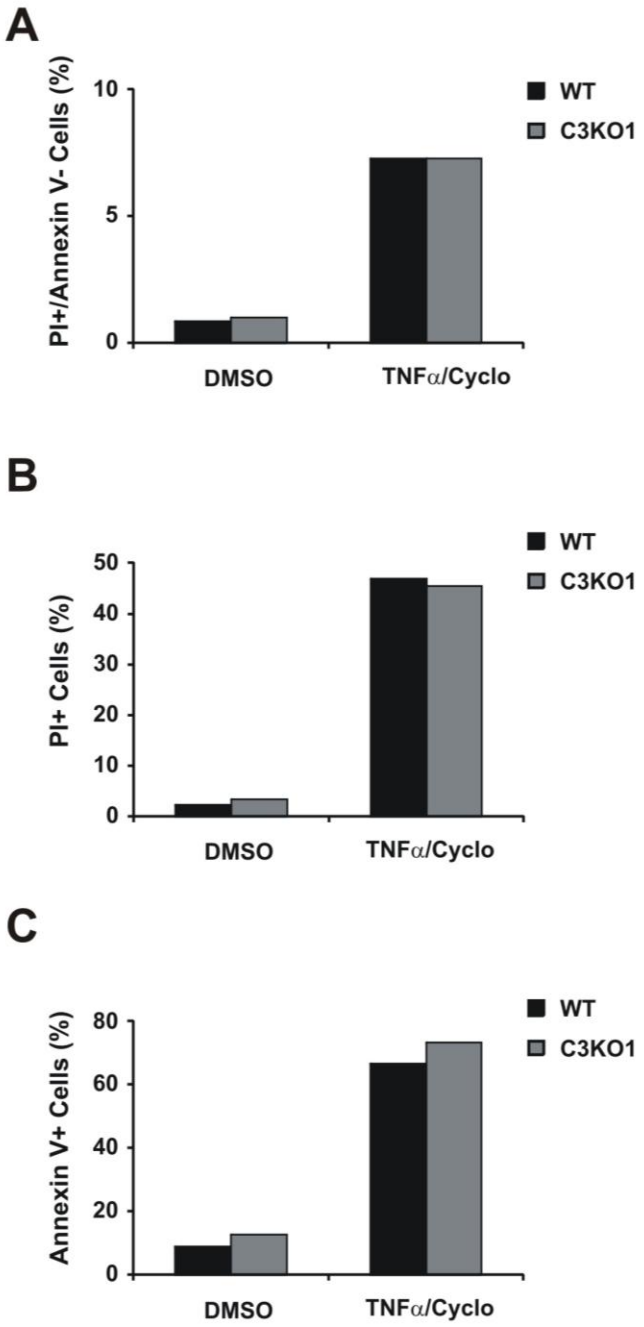

Figure 23: Caspase-3 KO does not affect apoptosis or necrosis after TNFα treatment.

HCT 116 and C3KO cells were treated with TNFα (10 ng) and cyclohexamide (5 μM) for 48h, and analyzed by flow cytometry following PI and annexin V staining. (A) Fractions of PI+/Annexin V- cells. (B) Fractions of PI+ cells. (C) Fractions of Annexin V+ cells.

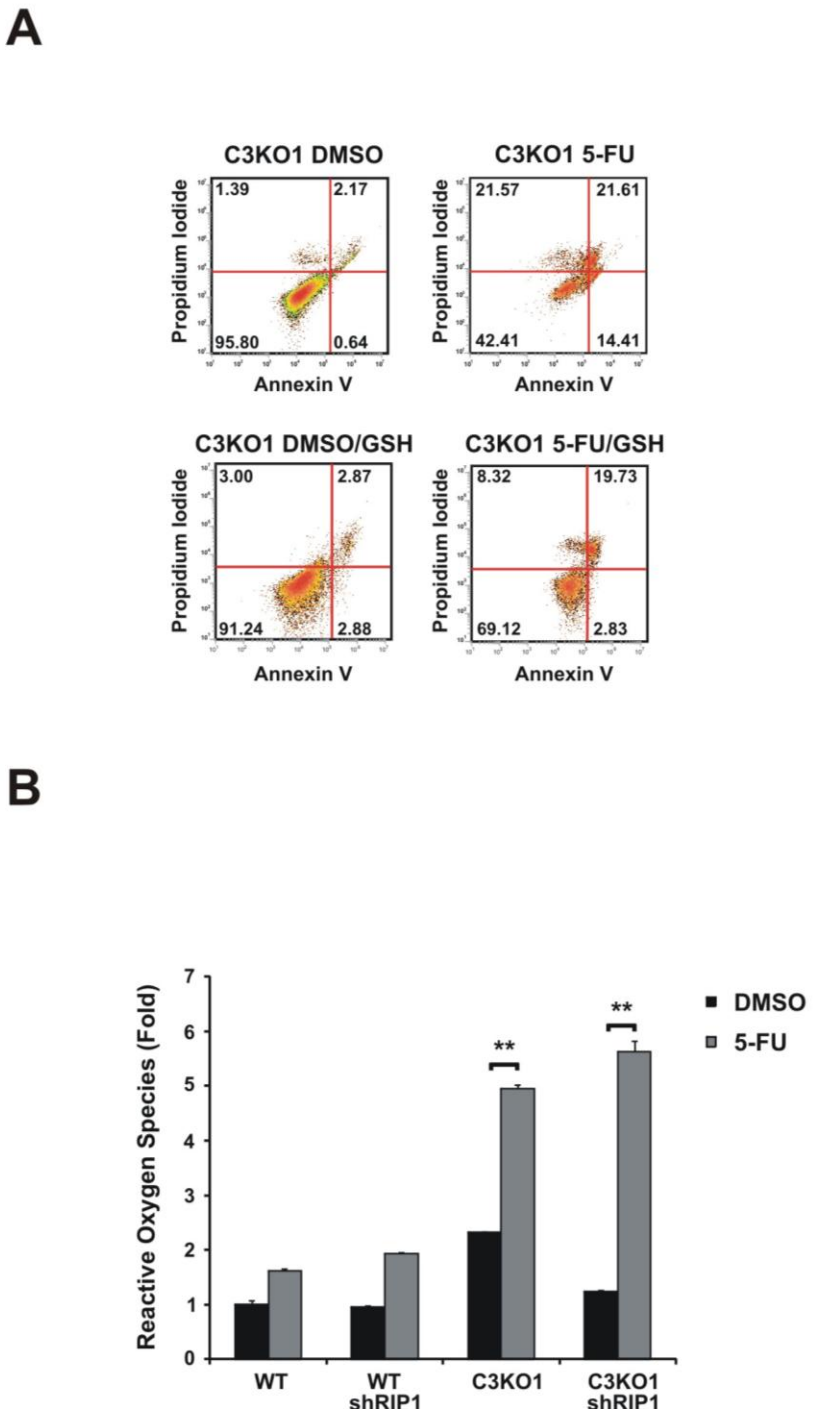

Figure 24: Caspase-3 KO cells die by ROS dependent necrosis.

(A) Flow cytometry profiles for C3KO cells stained with PI and annexin V following 48h treatment with DMSO, 5-FU (50 µg/ml), GSH (10 µM) or combination of 5-FU and GSH. (B) Reactive oxygen species generation in and C3KO cells expressing a short hairpin construct against RIP1 or scrambled control treated for 24h with 5-FU (50 µg/ml). **p<.01

3.4.4 *Caspase-3* knockdown promotes DNA-damage induced necrosis in colon cancer cells

We generated stable HCT116 and RKO *caspase-3* knockdown (KD) cell lines using shRNA. 5-FU treatment induced necrosis in *caspase-3* KD HCT116 and RKO cells as evident by increased PI+/Annexin V- populations, ROS production and HMGB1 release, as well as a steep drop in cellular ATP levels (Figures. 25A-F, 26 and 27A). The increased PI+/Annexin V- population was significantly reduced by Nec-1 but unaffected by z-VAD in *caspase-3* KD RKO cells (Figure 25G). CPT or Etoposide treatment led to necrosis in *caspase-3* KD HCT116 and RKO but not in control cells (Figure 25H-I). These results demonstrate that loss of caspase-3 leads to enhanced sensitivity of colon cancer cells to DNA damaging agents via induction of necrosis, and caspase-3 is dispensable for DNA-damage induced apoptosis.

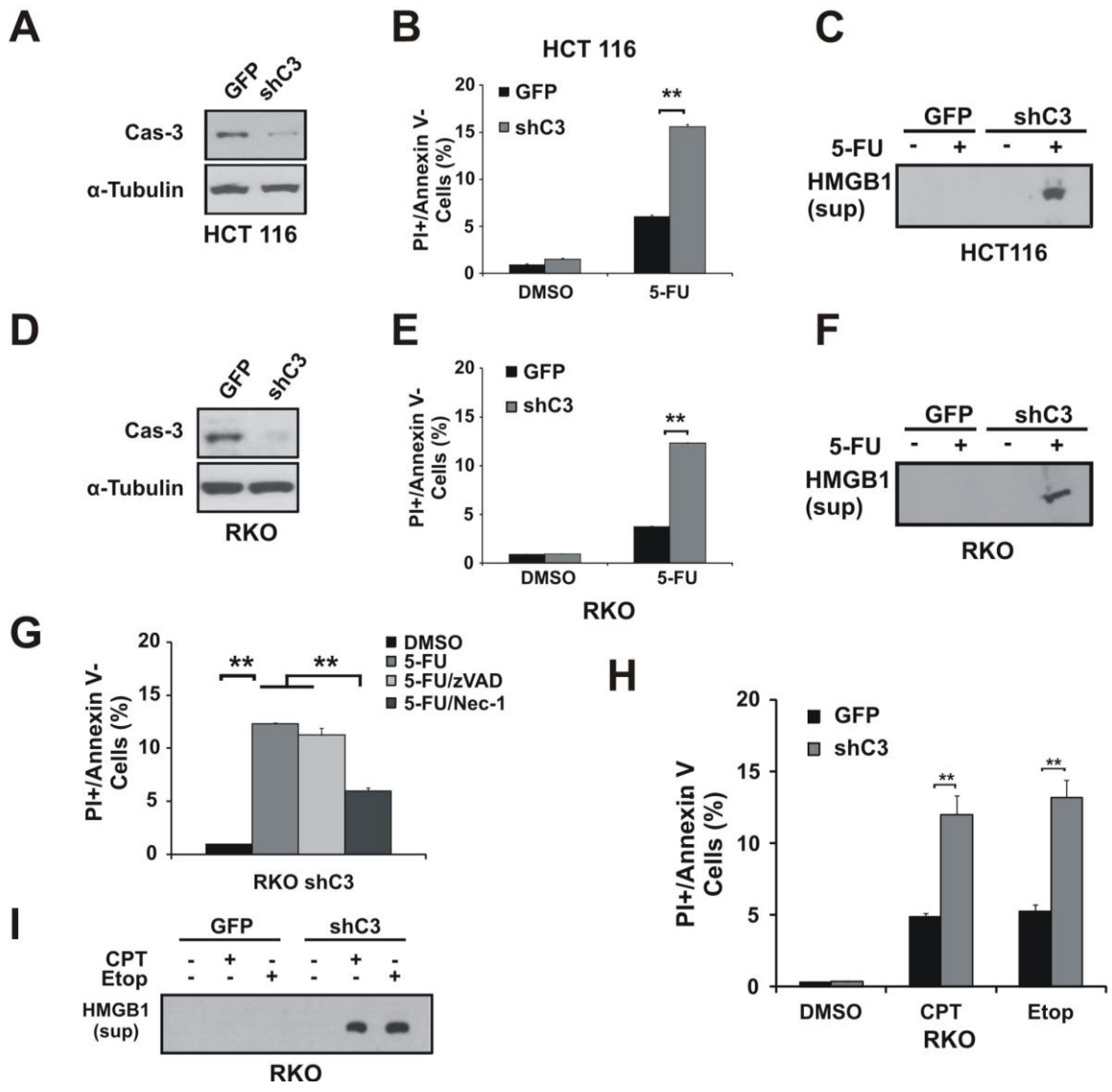

Figure 25: Caspase-3 KD increased necrosis in response to DNA damage.

(A) Stable *caspase-3* knockdown in HCT 116 cells was confirmed by western blotting. (B) Fractions of PI+/Annexin V- cells 48h after 5-FU (50 μg/ml) treatment. (C) The levels of HMGB1 in the medium from the indicated cells treated as in B. (D) Stable *caspase-3* knockdown in RKO cells was confirmed by western blotting. (E) Fractions of PI+/Annexin V- cells 48h after 5-FU (50 μg/ml) treatment. (F) The levels of HMGB1 in the medium from the indicated cells treated as in E. (G) Fractions of PI+/Annexin V- cells 48h after 5-FU (50 μg/ml) treatment, with or without pan caspase inhibitor z-VAD (20 μM) or necrostatin-1 (Nec-1, 15 μM). (G) Fractions of PI+/Annexin V- RKO cells 48h after CPT (500 nM) or Etoposide (50 μM) treatment. (H) The levels of HMGB1 in the medium from the indicated RKO cells treated as in H. **p<.01.

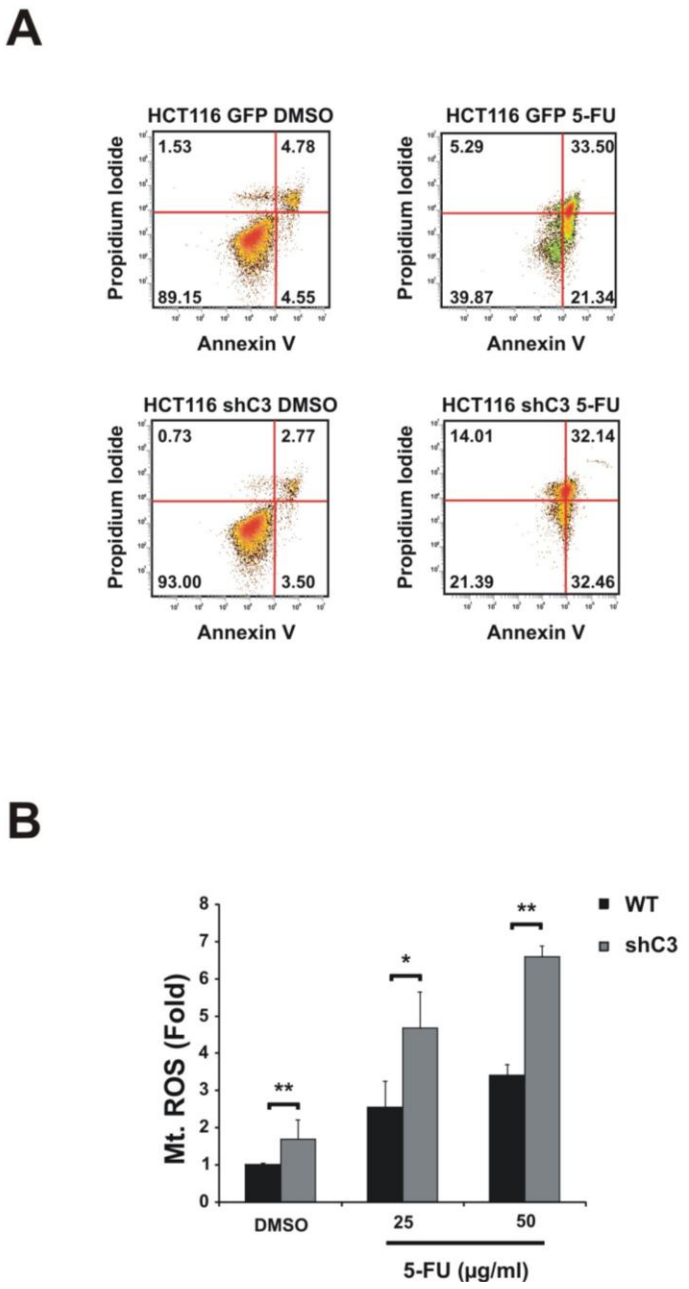

Figure 26: HCT116 caspase-3 knockdown cells show increased necrosis following 5-FU treatment.

(A) Flow cytometry output for HCT116 GFP and caspase-3 KD cells stained for PI and Annexin V following 48hr 5-FU (50µg/ml) treatment. (B) Reactive oxygen species generation in stable HCT116 GFP and caspase-3 KD cells treated for 24hr with 5-FU (50 µg/ml). *p<.05, **p<.01

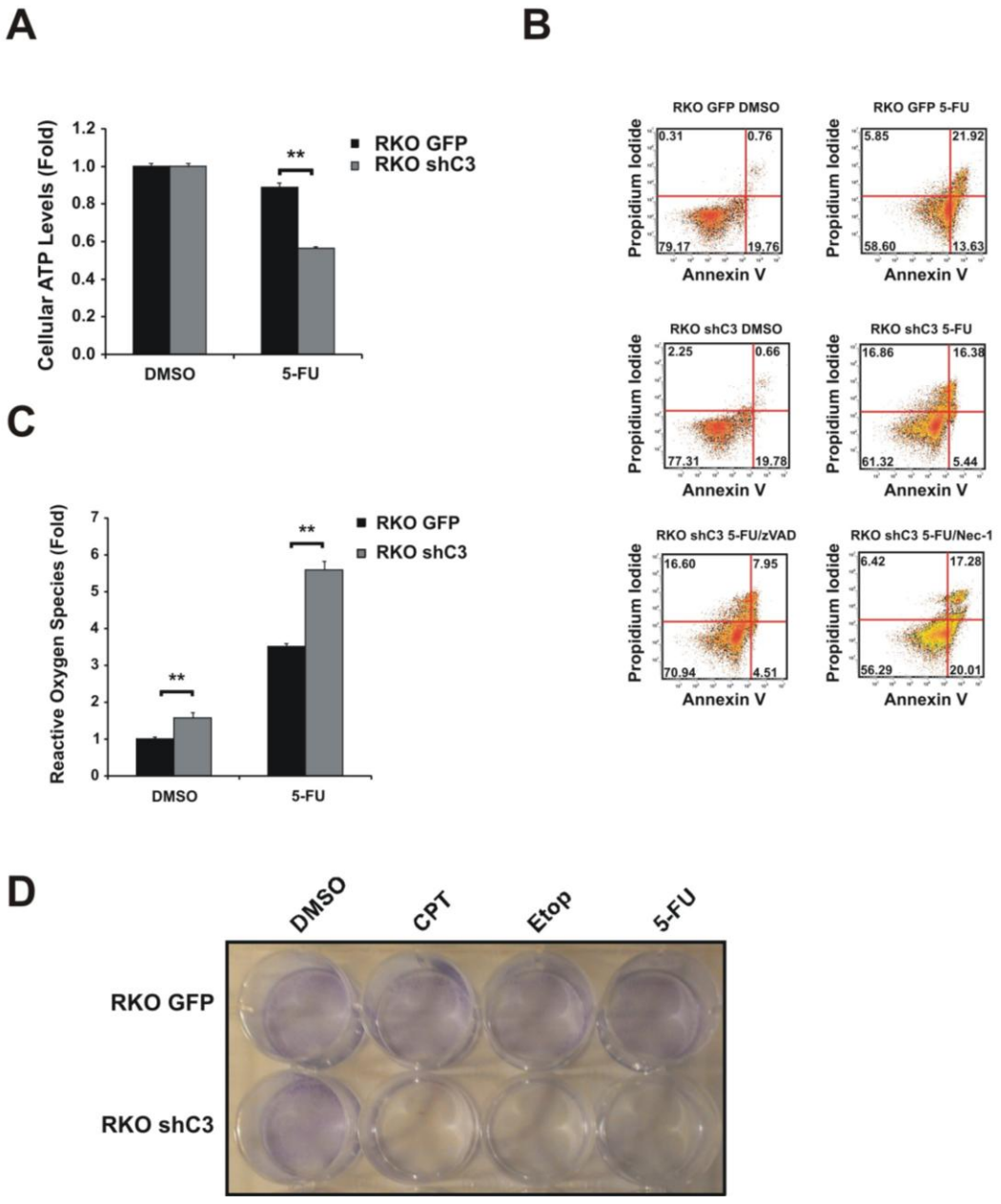

Figure 27: RKO caspase-3 knockdown cells show increased necrosis after DNA damage.

(A) Cellular ATP levels of RKO GFP and caspase-3 KD cells treated with 5-FU (50 µg/ml) for 48hr. (B) Flow cytometry output for RKO GFP and caspase-3 KD cells following 48h treatment with 5-FU (50 µg/ml), z-VAD (20 µM) and/or Nec-1 (15 µM). (C) Reactive oxygen species generation in stable RKO GFP and caspase-3 KD cells treated for 24hr with 5-FU. **p<.01 (D) Crystal violet staining of adherent cells 48h after CPT (500 nM) or Etoposide (50 µM) treatment.

3.4.5 Loss of caspase-3 stabilizes a necrotic complex and RIP1 ubiquitylation

To better understand how caspase-3 suppresses necrosis, we used immunoprecipitation (IP) experiments to examine potential cell death complexes involving RIP1 and caspase-8 in WT and C3KO cells after 5-FU treatment. Caspase-8 pull-down revealed a low level of existing caspase-8/RIP1/FADD complex in unstressed WT cells, while 5-FU treatment recruited unprocessed caspase-3 to this complex (Figure 28A). Interestingly, RIP1 was not found with caspase-8/FADD in unstressed C3KO cells, and much higher levels of caspase-8/RIP1/FADD complex were found in 5-FU treated C3KO (Figure 28A). Reciprocal caspase-3 pull-down confirmed caspase-3 recruitment to the complex after 5-FU treatment in WT cells, and the full length, but not process caspase-3 preferentially binds to caspase-8 (Figure 28B). The catalytically dead mutant C163A was found to effectively bind to this complex after 5-FU treatment in reconstituted C3KO cells (Figure 28C). These findings suggest that caspase-3 recruitment to the caspase-8/RIP1/FADD complex facilitates caspase-8 activation and perhaps apoptosis in WT cells.

z-VAD blocked 5-FU-induced apoptosis and caspase-8 processing, but not necrosis, in C3KO cells (Figure 19C). We reasoned that the necrotic complex might be stabilized upon z-VAD treatment if apoptosis competes away or cleaves components shared by apoptosis and necrosis. The caspase-8/RIP1/FADD complex and polyubiquitylated RIP was drastically enhanced in WT cells co-treated with z-VAD and 5-FU, and to a much greater levels in C3KO cells (Figure 28D). Interestingly, z-VAD treatment completely prevented binding of caspase-3 to this complex, in WT cells (Figure 28E). Higher levels of RIP1 ubiquitylation were found in unstressed C3KO cells (Figure 28F). These results suggest *caspase-3* ablation or inhibition by z-

VAD stabilizes the caspase-8/RIP1/FADD complex and caspase-3 acts as negative regulator of RIP1 polyubiquitylation and DNA damage-induced necrosis.

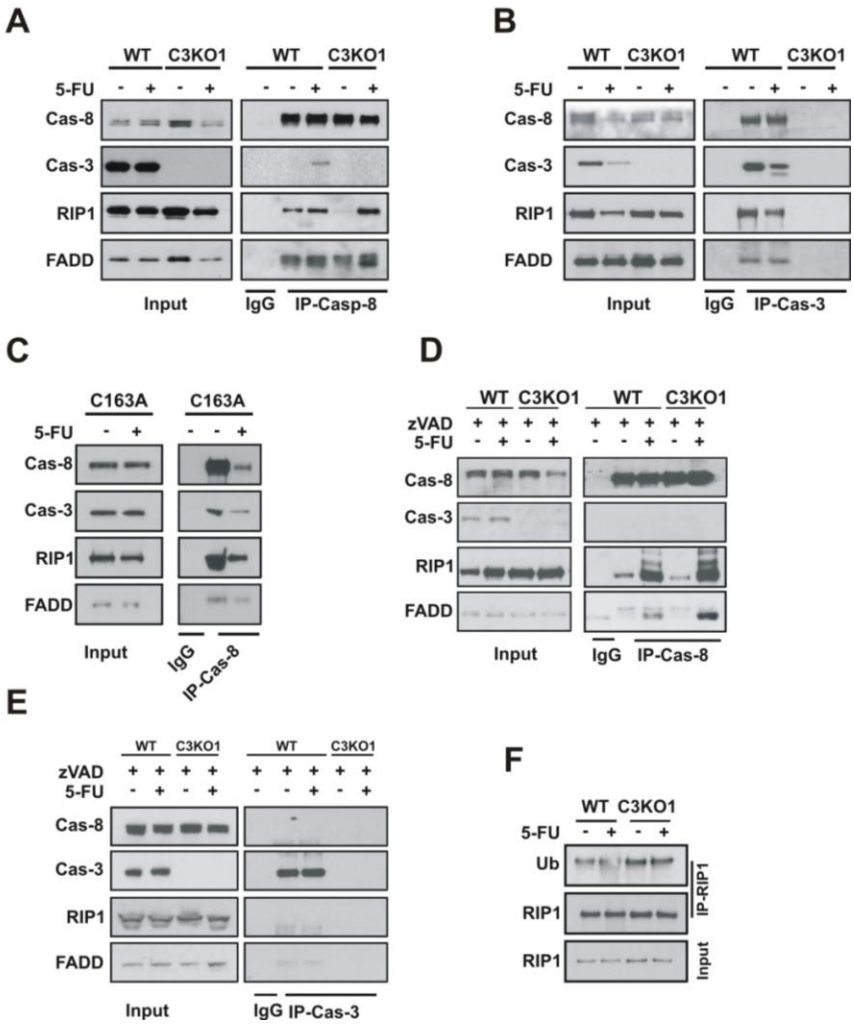

Figure 28: Loss of Caspase 3 or z-VAD treatment stabilizes the necrotic complex and RIP ubiquitination.

(A) Analysis of caspase-8 interacting proteins followed by caspase-8 immunoprecipitation in HCT116 WT and C3KO cells 24h with or without 5-FU (50 µg/ml) treatment. Input = whole cell lysate. (B) Analysis of caspase-3 interacting proteins followed by caspase-3 IP in cells treated as in (A). (C) Analysis of caspase-8 interacting proteins in C3KO cells reconstituted with C163A mutant treated as in A. (D) Analysis of caspase-8 interacting proteins in cells treated as in (A) in the presence of z-VAD (20 µM). (E) Analysis of caspase-3 interacting proteins in cells treated as in (A) in the presence of z-VAD (20 µM). (F) Analysis of RIP ubiquitylation following RIP1 IP in HCT116 WT and C3KO cells treated as in A.

3.4.6 DR5, Caspase-8 and FADD are required for both apoptotic and necrotic cell death induced by 5-FU in *caspase-3* KO cells

The above findings suggest removal of caspase-3 switches the apoptotic complex to a necrotic one, which likely requires full length caspase-8 (pro-caspase), RIP1 and FADD, for execution and lies downstream of death receptor activation. Knock down of either *DR5* or *caspase-8* using siRNA significantly blocked 5-FU-induced necrosis in C3KO cells measured by increases in the PI+/Annexin V- population and HMGB1 release (Figure 29A-C). We further generated *caspase-3* KD/*FADD* KO HCT116 cells [153] (Figure 29D), and found *FADD*KO completely blocked 5-FU-induced necrosis in C3KD cells (Figure 29E-F). Knockdown of *DR5*, *caspase-8* or *FADD* KO also blocked apoptosis (Annexin+/PI-), and total cell death (Figure 30). A better protection from 5-FU-induced cell death by *FADD* KO compared to DR5 or caspase-8 KD was likely due to complete elimination of the target. These results demonstrate the requirement for DR5, caspase-8 and FADD in 5-FU induced cell death, and a selective anti-necrosis role of caspase-3.

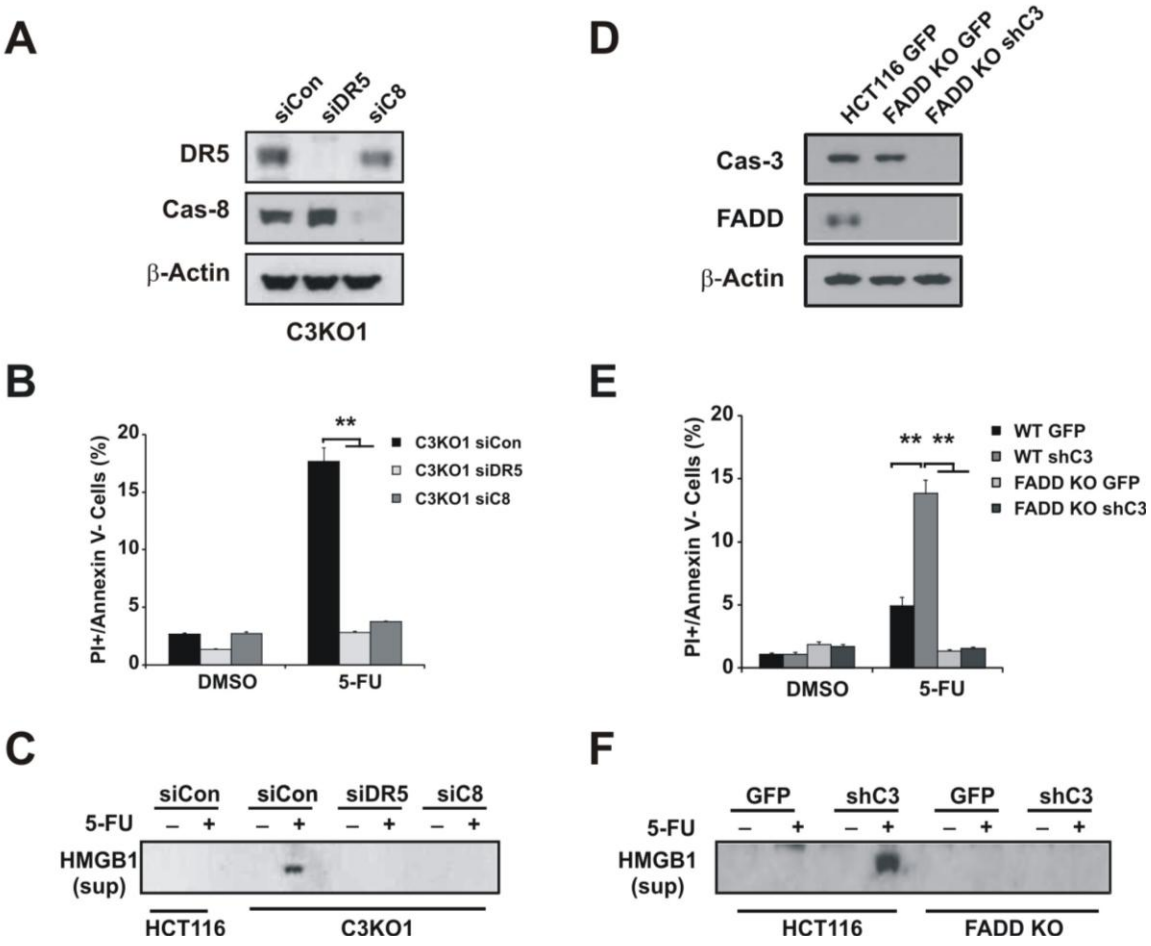

Figure 29: Death receptor 5, caspase-8 and FADD are required for 5-FU induced cell death.

(A) Knockdown of *DR5* or *caspase-8* in C3KO cells by siRNA confirmed by western blotting. (B) Fractions of PI+/annexin V- cells 48h after 5-FU (50 µg/ml) treatment. (C) The levels of HMGB1 in the medium in cells treated as in (B). (D) Stable knockdown of *caspase*-3 by shRNA in FADD KO cells confirmed by western blotting. (E) Fractions of PI+/annexin V- *FADD* KO cells 48h after 5-FU treatment. (F) The levels of HMGB1 in the medium from *FADD* KO cells treated as in (E). **p<.01

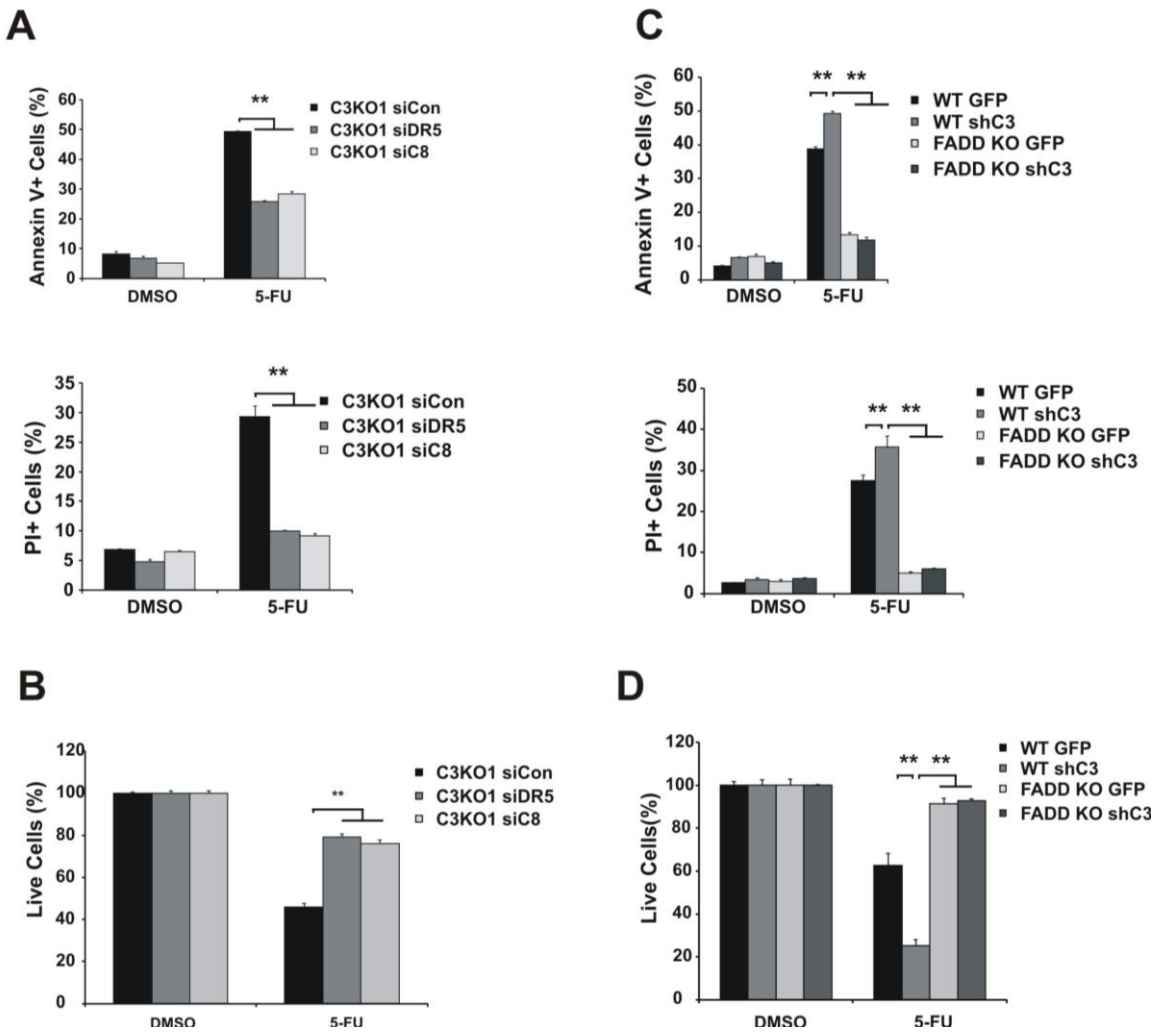

Figure 30: DR5, caspase-8, and FADD are required for 5-FU induced cell death.

(A-B), C3KO cells with DR5, Caspase-8 siRNA. (A) Quantification of dead (Annexin V+ or PI+) populations in C3KO cells transiently transfected with siRNA against DR5, caspase-8 or a scrambled control following 48h treatment with 5-FU (50 µg/ml). (B) Quantification of live (PI-/Annex V-) populations in C3KO cells transiently transfected with siRNA against DR5, caspase-8 or a scrambled control following treatment as in A. **p<.01. (C-D), C3KD with or without *FADD* KO. (C) Quantification of dead (Annexin V+ or PI+) populations in HCT116 *FADD* KO cells with stable expression of a caspase-3 KD construct or GFP control following 48h treatment with 5-FU (50 µg/ml). (D) Quantification of live (PI-/Annex V-) populations in HCT116 FADD KO cells with stable expression of a caspase-3 KD construct or GFP control following treatment as in A. **p<.01

3.4.7 *Caspase-3* KO tumors show increased response and necrosis to 5-FU *in vivo*

Next we determined the role of *caspase-3* in the therapeutic responses to 5-FU in mouse xenograft experiments. Equal numbers of WT and C3KO cells were implanted subcutaneously on the flanks of seven-week old female nude mice. Mice with established tumors were treated with either 50 mg/kg 5-FU or vehicle every other day for 14 days. C3KO tumors showed a significantly greater response to 5-FU compared to WT tumors (Figure 31A-C). Tumors were harvested at the end of the treatment, and analyzed for histopathology and markers of cell death. C3KO tumors exhibited significantly more necrosis with areas of complete loss of cellularity and more TUNEL positive cells, compared to WT tumors in the same host (Figures 31D-F and 32). These results strongly indicate that loss of *caspase-3* enhances tumor responses to 5-FU via induction of necrosis *in vivo*.

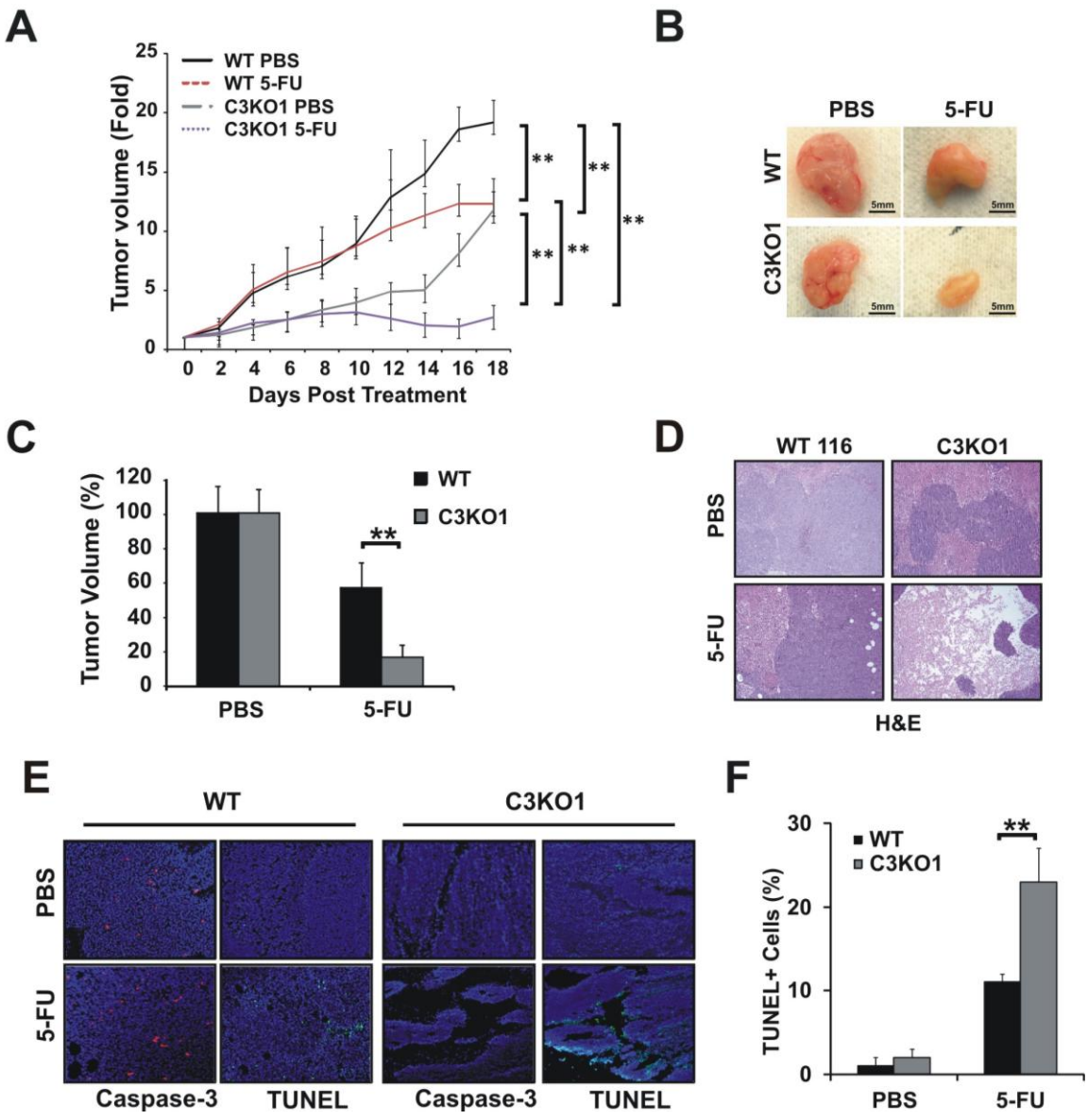

Figure 31: Caspase-3 KO cells show increased response and necrosis to 5-FU in vivo.

(A) The relative growth of tumors compare to the volume before the first 5-FU treatment (day 0, 1). The average tumor volume is about 50 mm^3. 5-FU (50 mg/kg) was given intraperitoneally (I.P) every other day for 14 days. (B) Representative HCT116 WT and C3KO tumors after the last treatment. (C) Relative volume of HCT116 WT and C3KO tumors after the last treatment. (D) H&E staining of tumors with indicated genotype after the last treatment. (E) Staining of active caspase-3 and TUNEL in the tumors after the last treatment. (F) Quantization of TUNEL positive cells in HCT116 WT and C3KO xenograft tumors with the indicated treatment. Three tumors were randomly chosen in each group. **p<.01

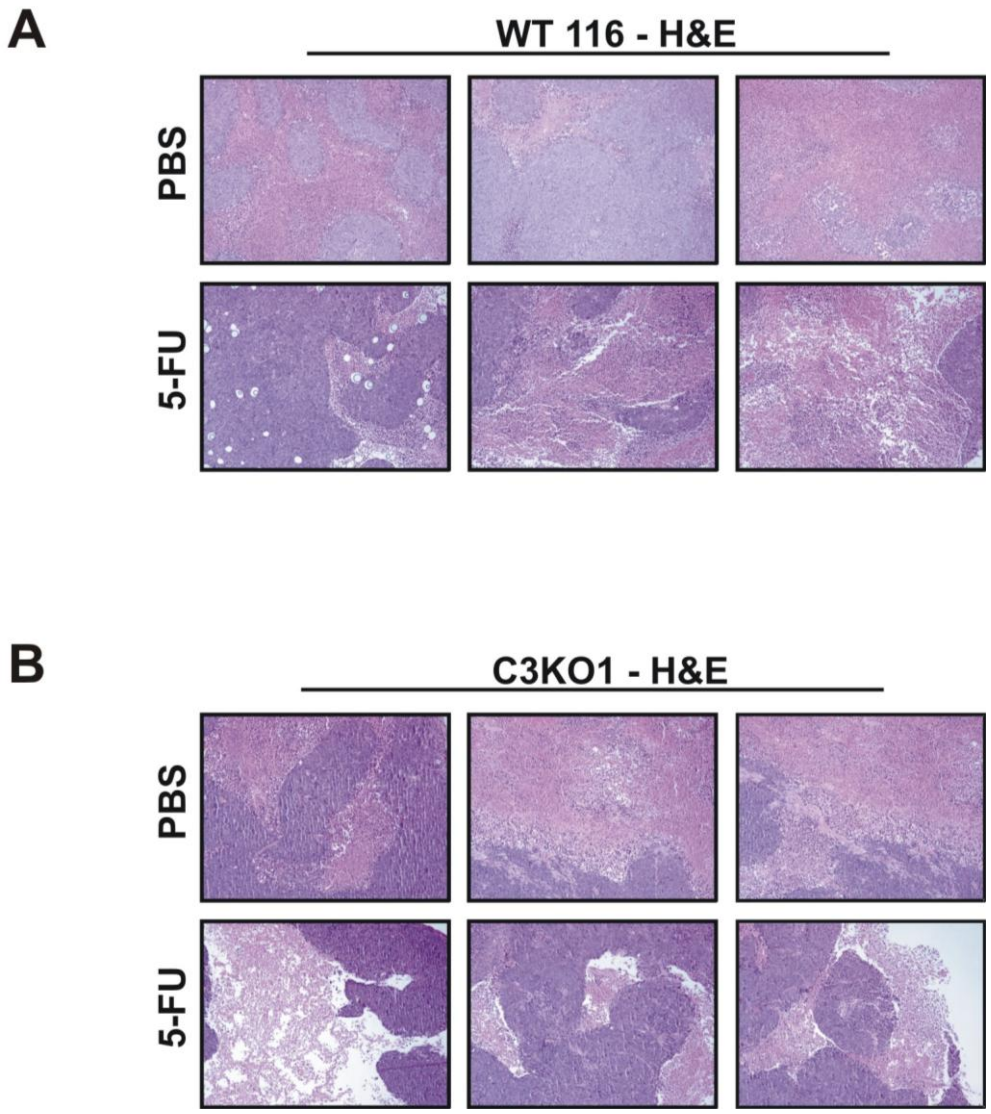

Figure 32: Caspase-3 KO cells show enhanced responses to 5-FU in vivo.

Tumor bearing mice were treated as in Figure 8A. (A) H&E staining of HCT116 WT tumors at the last treatment. (A) H&E staining of C3KO tumors at the last treatment.

3.5 DISCUSSION

Most cancer therapies promote apoptosis, but an inherent difficulty with this approach is that oncogenic alterations often render cancer cells resistant [15, 160, 161]. Therefore, activation of alternative cell death pathways is worth exploring. Molecular mechanisms of programmed necrosis have been under intensive investigation, and the best understood is TNFα-induced necrosis through both RIP1 and RIP3. In contrast, very little is known about DNA damage-induced necrosis [99 , 180]. Our work demonstrates that targeting caspase-3 promotes RIP1- and ROS-dependent necrosis in cancer cells in response to genotoxic stress, independent of RIP3. RIP3 is expressed in many normal tissues [99] but not in most colon cancer cells or in lung cancer cell lines [103], which might explain why cancer cells generally do not undergo necrosis in response to TNFα even in the presence of z-VAD. *Caspase-3* KO mice have limited abnormality in apoptosis, but were recently found to be more sensitive to DNA damaging agents such as UV-B and doxorubicin with a necrosis-like cell death [181], consistent with an anti-necrotic function of caspase-3. Therefore, a better mechanistic understanding of RIP3-independent necrotic cell death triggered by DNA damage could bear important fruits for cancer therapy

To our knowledge this is the first report indicating caspase-3 as an inhibitor of caspase-8 and RIP1-dependent necrosis induced by DNA damage yet completely dispensable for apoptosis, and represents another example of competition between apoptosis and necrosis. Caspase-3 recruitment to the caspase-8/RIP1/FADD/caspase-3 complex switches on apoptosis to block necrosis (Figure 33). RIP1 activity is highly regulated by K377 ubiquitylation with a Lysine-63 linkage leading to its activation and a Lysine-48 linkage leading to proteasome-mediated

degradation [182]. Since *RIP1* knockdown does not affect apoptosis, one interesting possibility is that enhanced RIP1

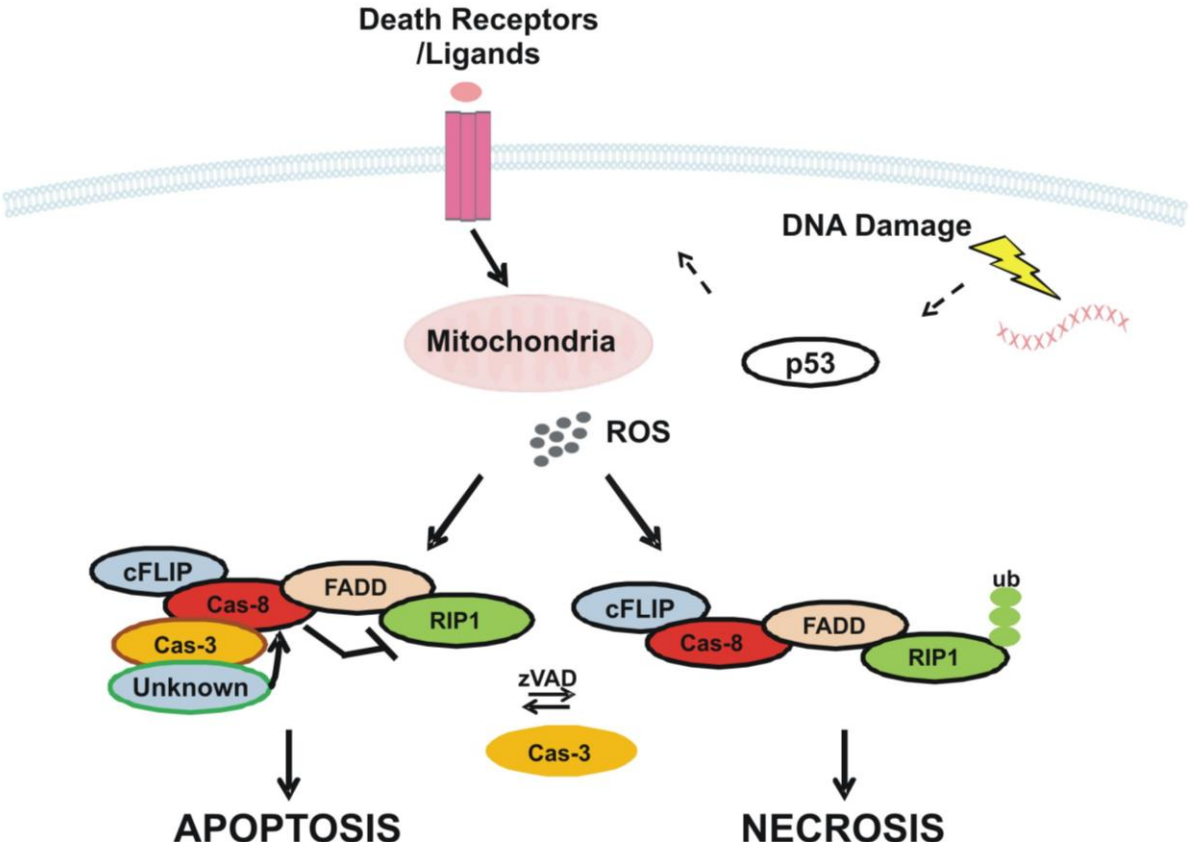

Figure 33: A model for caspase-3-mediated suppression of DNA-damage induced necrosis.

The extrinsic pathway and ROS can mediate both apoptosis and necrosis in response to genotoxic stress via distinct death promoting complexes. Loss of caspase 3 shifts the equilibrium to necrotic complex containing caspase-8/RIP1/FADD which might involve polyubiquitylation of RIP1. The apoptotic complex containing caspase-3, but not the necrosis complex is sensitive to z-VAD. Increased expression of death receptor and ligand might enhance cell killing in p53 WT cells.

ubiquitylation, rather than deubiquitantion [182], in C3KO cells likely promotes necrosis (Figure 8). The complex described in our study might be related to the Ripoptosome [146], which contains caspase-8/RIP1,/FADD, and can initiate either apoptosis or necrosis depending on the relative levels and activation of caspases and inhibitor of apoptosis proteins (IAPs) [144, 146]. Inhibition of caspase-8 activity in the Ripoptosome by cFLIP overexpression leads to necrosis [146], while activated caspase-8 can cleave RIP1 to inhibit necrosis [168]. Our work also suggests that z-VAD functions as an allosteric inhibitor, and specifically prevents caspase-3 recruitment to the caspase-8/RIP1/FADD complex and its stabilization. This bears resemblance to Nec-1, an allosteric inhibitor of RIP1, that affects both kinase-dependent and -independent functions [183]. These findings demonstrate a complex interaction between caspases and RIP1 in regulating cell fate.

Non-overlapping functions of caspase-3 and caspase-8, or RIP1 and RIP3 are well-supported by genetic studies. *Caspase-3* knockout mice in the C57BL/6 background are fertile but have developmental abnormalities, which is a sharp contrast with the embryonic lethality upon gene ablation in *Casapse-8, FLIP* or *FADD* via RIP3-dependent necrosis. On the other hand, *RIP1* KO mice have much more profound immune and survival defects, compared to *RIP3* KO mice [99, 180]. Further investigation will be required to fully understand the manner in which caspase-3 affects caspase-8 or RIP1 activity and modulates the switch between apoptosis and necrosis. Given the important roles of these proteins, more precise genetic manipulation by knocking in enzymatic, binding or modification defective alleles in mice and human cancer cells will likely provide fundamental insights on cell fate determination.

Our findings also raise several interesting questions for further investigation. Severe DNA damage can induce caspase-8-dependent and p53-independent apoptosis via a ATM/NF-κB /RIP1 and TNF-α feed forward mechanism in cancer cells [132]. In our model, apoptosis was largely

unaffected by the absence of RIP1 or caspase-3 in response to several DNA damaging agents, suggesting the intact apoptosis is likely mediated by the ATM/NF-κB/RIP1 arm and perhaps additional apoptotic complexes such PIDDSome (PIDD/Caspase-2) [93, 184]. In p53 WT cells, induction of DR5, DR4 and TRAIL (data not shown) might enhance 5-FU-induced cell death (Figure 33), as *p53* KO HCT 116 cells are partially resistant [185]. In addition, ROS production appears upstream of RIP1, suggesting some necrotic components might be redox sensitive. The downstream events of RIP1 in DNA damage-induced necrosis, and the importance of RIP1 kinase and inflammation remain completely unexplored. Even though RIP3 is not required for DNA-damage induced necrosis, a role of MLK or PGAM5 [96, 97] has not been excluded.

Is summary, we have shown that targeting caspase-3 leads to an enhanced response to DNA damaging agents through induction of necrosis in colon cancer cells, with unaltered apoptotic response. This necrosis requires caspase-8, RIP1, FADD and DR5 but not RIP3, and involves a caspase-8/RIP1/FADD complex. Therefore, pharmacological targeting of caspase-3 or other components in this complex may provide a novel approach to target chemotherapy resistant tumors.

4.0 FUTURE DIRECTIONS

4.1 IDENTIFY THE ROLE OF CASPASE-3 IN TUMOR METABOLISM

4.1.1 Investigate the role of caspase-3 on glycolysis and oxidative phosphorylation

Cancer cells generally exhibit altered metabolic pathways, including increased aerobic glycolysis for ATP generation and macromolecule formation, which support high rates of proliferation. In some instances, this is due to mitochondrial respiration injury and hypoxia, frequently leading to therapeutic resistance [186]. We witnessed a significant increase in sensitivity to both glucose and glutamine deprivation in C3KO cells not seen in WT cells (Figure 11), suggesting alteration of glycolytic and glytaminolytic pathways. While glucose and glutamine addiction in cancer cells is not uncommon, seeing increased dependence in C3KO cells brings about many questions [47]. Increased glucose dependence could be the result of reduced ability of glucose to enter glycolysis or dysfunctional glycolysis such that glucose enters the cycle but is never fully processed into pyruvate. As a result of reduced end product, starving cells would be more dependent upon high glucose levels. Alternatively, increased glucose dependence could be a result of the exact opposite; glycolysis is upregulated rather than deficient. Increased glycolysis rates would require an increase in raw materials such as glucose. Increased glutamine dependence suggests an increase in glutaminolysis, an alternative energy pathway often seen in

tumor cells [187-189]. Inhibition of glycolysis by use of 2-Deoxy-D-glucose, a glucose molecule which has the 2-hydroxyl group replaced by hydrogen causing it to act as a dominant negative molecule in glycolysis, would aid in determining whether glycolysis is being increased or decreased in C3KO cells. Furthermore, use of this molecule would help identify the level to which alternative energy sources (i.e. glutamine) could compensate for lost glucose. A better understanding of the alterations in glucose and glutamine metabolism will help delineate the role of caspase-3 in metabolism.

In addition to altered glucose and glutamine dependence we witnessed significant changes in oxidative phosphorylation in C3KO cells. Namely, C3KO cells showed reduced ability to perform oxidative phosphorylation as shown by decreased maximum respiration and spare respiratory capacity (Figure 9). Extensive studies will need to be performed to identify the defective complex(es) leading to reduced respiration. One potential player is the mitochondria fusion protein mitofusin 2. Levels of MFN2 were significantly reduced in C3KO cells (Figure 10). Studies are currently underway to determine if reconstitution of MFN2 restores mitochondrial morphology/function to WT levels. Identifying caspase-3 as having a role in cancer cell proliferation and metabolism is exciting in that it provides an opportunity to slow tumor growth. *In vivo* studies suggest that if an inhibitor of caspase-3 were successfully generated it could reduce tumor size by more than half (Figure 14). There is potential for using a caspase-3 inhibitor with conventional chemotherapy to reduce tumor volume to a point where surgical intervention becomes a viable option. Identifying the role caspase-3 has on mitochondria morphology and cellular metabolism could have an incredible impact on development of next generation therapies.

4.1.2 Identify the effects of caspase-3 loss on cell survival and proliferation in other cancers.

In chapter two we highlighted the consequence of caspase-3 loss on cell survival and proliferation in HCT116 colon cancer cells (Figures 5, 6 and 7). We were able to replicate these results in other colon cancer cell lines but have not expanded beyond that (Figures 12 and 13). One of the first steps in identifying if the phenomenon we see is relevant to cancer as a whole or simply CRC is repeating experiments in other cancer cell models. A logical first step in this direction would be using MCF 7 breast cancer cells as they harbor a deletion mutation resulting in loss of exon 3 and as a result do not express caspase-3 [190, 191]. If reconstitution of caspase-3 in MCF 7 leads to an increase in cell survival and proliferation it would warrant investigating additional models.

4.2 FURTHER DELINEATE THE ROLE OF CASPASE-3 IN NECROSIS

4.2.1 Identify all components of cell death complex

Having identified a role for caspase-3 in necrosis following treatment of HCT116 cells with DNA damaging agents, we investigated potential cell death protein complexes involved (Figures 19-21 and 28). We were able to positively identify caspase-8, FADD and RIP1 as binding partners with caspase-3 following treatment in WT cells (Figure 28). The same complex minus caspase-3 formed in C3KO cells following treatment. While our data suggest that the same

complex is involved in both apoptosis and necrosis, and the pathway initiated is dependent upon the presence of caspase-3, we have yet to definitively confirm this. We attempted to address this question through FADD knockout experiments and demonstrated nearly complete loss of cell death in these cells (Figures 29 and 30). However, an inherent difficulty in answering this question is the fact that caspase-8 and FADD are required proteins for many cell death complexes including the DISC, Necrosome and Ripoptosome (Figure 4). Another approach for identifying the role of cell death complexes present in our study would be immunoprecipitation of the complex followed by mass spectrometry to identify other proteins present. While this method is valid, it is time and cost intensive. A third option that we are currently undertaking is gel filtration chromatography. This technique allows for identification of protein complexes as proteins bound to one another will elute from the column in the same fraction. Discovery of additional proteins bound to caspase-3, caspase-8, FADD and RIP1 following drug treatment in both C3KO and WT HCT116 cells will allow us to further categorize the protein complex we are dealing with and determine the consequences of manipulating it.

4.2.2 Verify binding locations and partners of caspase-3

Since we have demonstrated that caspase-3 is a critical part of pro-death protein complexes, the next logical step would be to identify caspase-3 binding partners and their specific binding domains. Using C3KO cells reconstituted with caspase-3 expression constructs containing point mutations in potential binding domains coupled with immunoprecipitation of potential binding partners and immunoblotting, should allow us to identify putative caspase-3 binding partners. Verification of these interacting proteins will help us further understand how caspase-3 is dictating activation of certain cell death pathways.

4.2.3 Establish how posttranslational modification of RIP1 affects cell death

The literature surrounding RIP1 and its plethora of roles in cell biology has been expanding exponentially in recent years. RIP1 has been shown to have roles in cell proliferation, inflammation, immune response and cell death [130, 192]. This ability to function in numerous processes is due to RIP1's ability to undergo various posttranslational modifications. For instance, phosphorylation via RIP3 or autophosphorylation leads to increased necrosis. Alternatively, ubiquitination can lead to inflammation, cell proliferation, or proteosomal degradation. Our data suggests that RIP ubiquitination is increased in 5-FU treated C3KO cells indicating either activation of the inflammatory response or RIP1 is being marked for degradation (Figure 28). However, we have yet to verify if it is K63 or K48-linked ubiquitination. K63-linked ubiquitin would suggest that the NF-κB response is activated and inflammation may be occurring. This would be detrimental for patient therapy. Conversely, K48-linked ubiquitin would suggest that RIP1 has been marked for degradation by the proteasome. While degradation of RIP1 does not imply cell death will cease as we witnessed cell death in RIP1 KD cells (Figure 22), it does suggest the involvement of a RIP1-independent cell death complex. Classification of RIP1's ubiquitination/phosphorylation status will give us a better understanding of additional pathways/cell responses unique to C3KO cells.

4.2.4 Identify potential cell death pathway components

Following identification of the cell death complex involved in 5-FU induced C3KO cell death, we looked to further characterize the death response by knocking out potential downstream signaling molecules. Both transient knockdown of DR5 and caspase-8, in addition to knockout

of FADD, resulted in reduced apoptosis and necrosis (Figures 29 and 30). However, stable knockdown of RIP1 did not result in reduced cell death (Figure 22). While these data provide a foundation for understanding the signaling pathways involved in C3KO cell death, there is still much to be uncovered. The necessity of DR5 and caspase-8 suggests that the extrinsic apoptotic response is activated in response to 5-FU, but this will need to be confirmed through knockout of other known extrinsic pathway proteins. Furthermore, experiments will need to be conducted to determine activation of known DR5 downstream pathways including the JNK, p38 and NF-κB pathways, among others. Identification of pathway activation and the proteins involved in 5-FU mediated C3KO cell death will provide better understanding of the consequences of caspase-3 loss in cancer cells.

4.2.5 Establish if p53 is required for cell death in C3KO cells

It is well established that p53 is one of the most commonly mutated genes in cancer[27]. Mutated p53 can result in a diminished or absent DNA damage response and reduced cell death [185]. While p53 is commonly mutated in CRC, the model we used for our experiments, HCT116 contains two wild-type alleles [30]. Additionally, the cell line we verified work in, RKO also contains WT p53. In light of this, the question of whether or not p53 is required for the 5-FU response we see needs to be answered. Literature outlining the role of the PIDDosome in response to 5-FU in HCT116 suggests that in the absence of p53, 5-FU does not induce cell death [93, 94]. In support of this, our results show that p53 and a number of its downstream targets are induced in response to 5-FU treatment in both WT and C3KO cells. While it is our hypothesis that the cell death we witnessed is p53-dependent, further experimentation in p53 KO HCT116 and RKO colon cancer cells will need to be completed.

4.2.6 Expand on chemotherapeutics and cell models used

While our data show conclusively that loss of caspase-3 leads to increased sensitivity to 5-FU through activation of necrosis in HCT116 cells, it fails to show this phenomenon is relevant to cancer models beyond CRC. Further experimentation in additional cancer models would elucidate the potential broad range of our findings. Moreover, treatment of C3KO cells with additional classes of drugs beyond DNA-damaging agents will help identify the role of caspase-3 in other cell death responses.

Identifying caspase-3 as a key mediator in the decision for a cell to die by apoptosis or necrosis following DNA damage is an exciting finding that could potentially have extensive applications in future therapeutics. Additional future studies will help determine if our findings are able to be applied strictly to CRC or more globally to cancer as a whole. Regardless of the outcome, our data show caspase-3 to be a critical regulator of cell survival, proliferation and death pathway activation, warranting further investigation and consideration for future therapeutics.

APPENDIX A

ABBREVIATIONS

Table 4: In-text abbreviations

Abbreviation	Full Name
5-FU	5-fluorouracil
A20	TNFAIP3 Interacting Protein 2
AAV	Adeno-associated virus
AIF	Apoptosis-inducing factor
AKT	V-Akt murine thymoma viral oncogene homolog 1
APAF-1	apoptotic peptidase activating factor 1
APC	Adenomatous polyposis coli
ATP	Adenosine triphosphate
Bad	BCL2-associated agonist of cell death
Bak	BCL2-antagonist/killer 1
Bax	BCL2-associated X protein
Bcl-2	B-cell CLL/lymphoma *2*
Bcl-xl	BCL2-associated agonist of cell death
BH3	Bcl-2 homology domain 3
Bid	BH3 interacting domain death agonist
Bik	BCL2-interacting killer
Bim	BCL2-like 11
BIR	Baculovirus Interacting Repeat
Bmf	Bcl2 modifying factor
BMPR1A	Bone morphogenetic protein receptor, type IA
Bok	BCL2-related ovarian killer
BSA	Bovine serum albumin
C163A	Catalytically dead C163A mutated caspase-3 expression construct
C3	Caspase-3

Table 4 continued

C3KO	Caspase-3 knockout cells
CARD	Caspase recruitment domain
CASP3	Caspase-3
c-FLIP	CASP8 and FADD-like apoptosis regulator
cIAP1	Cellular inhibitor of apoptosis 1
cIAP2	Cellular inhibitor of apoptosis 2
CPT	Camptothecin
CRC	Colorectal cancer
CYLD	Cylindromatosis
DIABLO	IAP-binding mitochondrial protein
DISC	Death-inducing signaling complex
DR5	Death receptor 5
EGFR	Epithelial growth factor receptor
EMT	Epithelial-mesenchymal transition
EndoG	Endonuclease G
EPCAM	Epithelial cell adhesion molecule
ERK	Extracellular-signal-regulated kinase
Etop	Etoposide
FADD	Fas (TNFRSF6)-associated via death domain
FAP	Familial adenomatous polyposis
FAS	TNF receptor superfamily, member 6
FAS-L	FAS ligand
FDA	Food and Drug Administration
FH	Fumurate hydratase
FLC3	Full length caspase-3 expression construct
Foxo3a	Forkhead box O3, a
GADD45	Growth arrest and DNA-damage-inducible protein
GFP	Green fluorescent protein
GIST	Gastrointestinal stromal tumors
GLUD1	Glutamate dehydrogenase 1
GLUL	Glutamate-ammonia ligase
GTP	Guanosine triphosphate
H2AX	H2A histone family, member X
HBSS	Hank's buffered salt solution
HMGB1	High mobility group box 1
HRP	Horse radish peroxidase
Htra2	HtrA serine peptidase 2
IAP	Inhibitor of apoptosis protein
IDH1	Isocitrate dehydrogenase I
IGF-BP3	Insulin-like growth factor binding protein 3

Table 4 continued

JNK	c-Jun N-terminal kinase
JPS	Juvenile polyposis syndrome
KIT	v-*kit* Hardy-Zuckerman 4 feline sarcoma viral oncogene homolog
KRAS	v-Ki-ras2 Kirsten rat sarcoma viral oncogene homolog
LC3	microtubule-associated protein 1 light chain 3 gamma
MAP2K4	MAPK kinase 4
MAP3K5	Mitogen-activated protein kinase kinase kinase 5
MAPK	Mitogen-activated protein kinase 1
Mcl-1	Myeloid cell leukemia sequence 1 (BCL2-related)
MFN2	Mitofusin 2
MLH1	MutL homolog 1, colon cancer, nonpolyposis type 2 (E. coli)
MLKL	Mixed lineage kinase domain-like
MOMP	Mitochondrial outer membrane potential
MSH2	MutS homolog 2, colon cancer, nonpolyposis type 1 (E. coli)
MSH6	MutS homolog 6 (E. coli)
mTOR	Mechanistic target of rapamycin
MYC	v-*myc* myelocytomatosis viral oncogene homolog (avian)
MYH	Myosin, heavy chain 1, skeletal muscle, adult
NADH	Nicotinamide adenine dinucleotide
Nec-1	Necrostatin-1
NEMO	NF-kappa-B essential modulator
Neo	Neomycin
NF-κB	Nuclear factor of kappa light polypeptide gene enhancer in B-cells
Noxa	Phorbol-12-myristate-13-acetate-induced protein 1
NSAID	Nonsteroidal anti-inflammatory drug
omi	HtrA serine peptidase 2
p21	Cyclin-dependent kinase inhibitor 1
p38	Mitogen-activated protein kinase 14
p53	Tumor protein *p53*
p65	Nuclear factor of kappa light polypeptide gene enhancer in B-cells
PBS	Phosphate-buffered saline
PDGFRA	Platelet-derived growth factor receptor, alpha polypeptide
PGAM5	Phosphoglycerate mutase family member 5
PI	Propidium iodide
PI3K	Phosphoinositide-3-kinase
PIDD	p53-induced death domain protein
PIK3C2G	PI3K, class2, gamma polypeptide
PIK3R2	Phosphoinositide-3-kinase, regulatory subunit 2
PKM2	Pyruvate kinase muscle form 2
PMS2	Postmeiotic segregation increased 2

Table 4 continued

PRR	Pathogen recognition receptors
PTEN	Phosphatase and tensin homolog
PUMA	p53 upregulated modulator of apoptosis
PYGL	Phosphorylase glycogen liver
RAF	v-*raf*-1 murine leukemia viral oncogene
RAIDD	CASP2 and RIPK1 domain containing adaptor with death domain
RIP1	Receptor (TNFRSF)-interacting serine-threonine kinase 1
RIP2	Receptor (TNFRSF)-interacting serine-threonine kinase 2
RIP3	Receptor (TNFRSF)-interacting serine-threonine kinase 3
RIPA	Radio-Immunoprecipitation Assay Buffer
ROS	Reactive oxygen species
RYK	Tyrosine receptor kinase
SDH	Succinate dehydrogenase
sh	Small hairpin
si	Small interfering
SMAC	Secondary mitochondrial activator of cytochrome c
SMAD4	SMAD family member 4
STK11	Serine/threonine kinase 11
STK33	Serine threonine kinase 33
TAB1	TGF-beta activated kinase 1/MAP3K7 binding protein 1
TAB2	TGF-beta activated kinase 2/MAP3K7 binding protein 2
TAK1	Nuclear receptor subfamily 2 group C member 2
tBid	Truncated bid
TBST	Tris-buffered saline/Tween 20
TCA	Tricarboxylic acid cycle
TGFBR1	Transforming growth factor beta receptor 1
TGFβ	Transforming growth factor, beta
TNFR	Tumor necrosis factor receptor
TNF-α	Tumor necrosis factor, alpha
TOR	Target of rapamycin
TP53	Tumor protein p53
TRADD	TNFRSF1A-associated via death domain
TRAF2	THF receptor associated factor 2
TRAIL1	TNF-related apoptosis-inducing ligand receptor 1
TRAIL2	TNF-related apoptosis-inducing ligand receptor 2
TSP1	Spermatogenic leucine zipper 1
TUNEL	Terminal deoxynucleotidyl transferase dUTP nick end labeling
VEGF	Vascular endothelial growth factor
WNT	Wingless-type MMTV integration site family
XIAP	X-linked inhibitor of apoptosis

Table 4 continued

zVAD	Z-VAD-FMK

APPENDIX B

CONTRIBUTIONS OF KIT AND ABL1 TO THE THERAPEUTIC RESPONSE OF GIST CELLS TO IMATINIB MESYLATE (GLEEVEC®)

B.1 ABSTRACT

Gastrointestinal stromal tumors (GISTs) are the most common mesenchymal tumors of the gastrointestinal tract. Most GISTs are caused by activating mutations in the *KIT* receptor tyrosine kinase gene allowing for their effective treatment with the small molecule kinase inhibitor imatinib mesylate (IM). IM is an inhibitor of KIT as well as ABL1, a kinase that is constitutively activated in chronic myeloid leukemia (CML). This study was designed to determine whether GISTs express both KIT and ABL1 and their respective contributions to the therapeutic response of GISTs to IM. Having shown through IHC that GISTs express both KIT and ABL1, we aimed to dissect the contributions of each to GIST cell proliferation/survival through siRNA-mediated knockdown. As expected, siRNA-mediated knockdown of KIT led to reduced cell proliferation and increased apoptosis in GIST882 cells; while siABL1 showed little

effect. Knocking down KIT and ABL1 simultaneously led to a reduced apoptotic response when compared to siKIT alone. To determine the cause of apoptosis attenuation in KIT-and ABL1-deficient cells, cell lysates were made after siRNA transfection and analyzed for signaling mediators and regulators of cell cycle and apoptosis by immunoblotting. Knockdown of KIT led to inhibition of downstream signaling as well as cell cycle arrest and apoptosis. These effects were not present after siABL1. Unexpectedly, ABL1 knockdown led to a substantial increase in activated and total AKT. To dissect the pathway leading to increased AKT activation after siABL1, we examined upstream signaling regulators of AKT and found increased PDK1 phosphorylation.

In conclusion, we have shown ABL1 to be expressed in a GIST tissue microarray. Whereas knockdown of KIT showed expected results with respect to cellular proliferation and apoptosis, combined knockdown of KIT and ABL1 attenuated the apoptotic response seen by siKIT. Immunoblot analysis of whole cell lysates following ABL1 knockdown showed increased levels of activated and total AKT. We hypothesize these levels are a result of elevated active and total PDK1 levels.

B.2 BACKGROUND

B.2.1 Gastrointestinal stromal tumors (GIST) are the most common mesenchymal tumor of the gastrointestinal (GI) tract.

In the past GISTs were viewed as a highly treatment-refractory sarcoma with fewer than 10% of patients responding to conventional radio- and chemotherapy [193, 194]. Until the introduction

of targeted small kinase inhibitors, the only treatment option for non-responsive tumors was surgery [195]. GISTs arise from the bowel wall in the GI tract with the stomach and small intestine being the most frequently affected areas [196].

B.2.2 GISTs arise from interstitial cells of Cajal (ICCs)

Until the 1990's GISTs were often misdiagnosed as leimyosarcomas [197]. At this time investigators noticed similarities between GISTs and interstitial cells of Cajal (ICCs). ICCs are cells located in the muscularis propria around the myenteric plexus throughout the GI tract, serving as pacemakers for peristaltic contraction [198-201]. Differentiation and proliferation of ICCs are critically dependent on expression of the KIT receptor tyrosine kinase (RTK) [199]. Hypothesizing that GISTs arise from the KIT-dependent ICC lineage and that oncogenic KIT mutations were known to be found in various human tumors [202-204] Hirota et al. investigated whether KIT activating mutations might be significant in GIST pathogenesis. They demonstrated high KIT expression in GISTs and found genomic mutations in *KIT* exon 11. *KIT* genomic mutations were found to be associated with constitutive activation of the KIT kinase function *in vitro* [198]. These findings have been confirmed in several subsequent studies encompassing hundreds of GISTs, and it is now known that *KIT* genomic mutations are key events in GIST pathogenesis (Figure 34) [205-211].

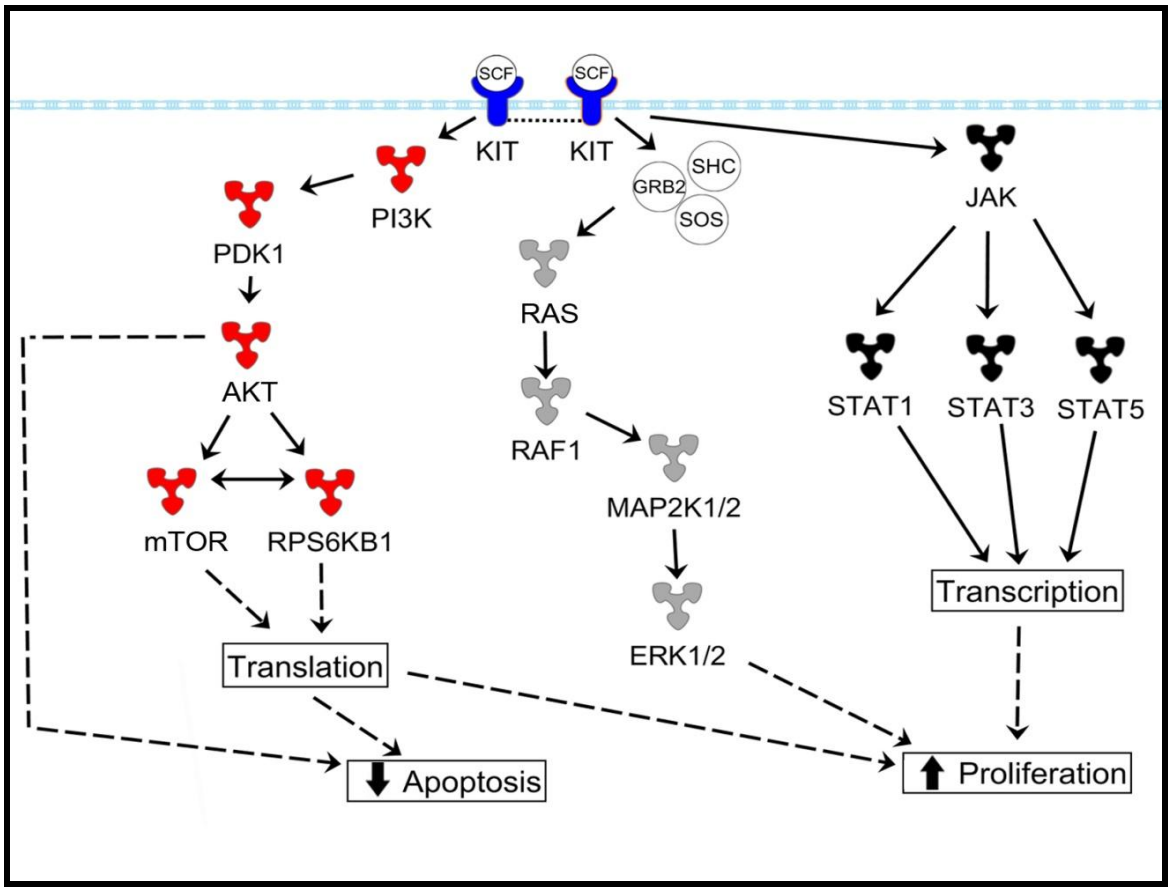

Figure 34: Physiologic KIT signal transduction.

KIT activation in non-neoplastic cells is triggered by binding of the dimeric KIT ligand stem cell factor (SCF) leading to homodimerization of two KIT molecules. This is accompanied by structural changes in the receptor resulting in activation of the KIT kinase domain. Activated KIT then cross phosphorylates tyrosine residues in the associated homodimer partner, leading to additional KIT structural alterations, and further activation of the receptors. Phosphorylated tyrosine residues on KIT serve as binding sites for various cell signaling proteins. These proteins include members of the RAS/RAF/MAPK and the PI3K/AKT pathways, which are regulated by binding of GRB2 and PI3-K to the phosphorylated forms of KIT tyrosine residues Y703 and Y721, respectively. Furthermore, the signal transducer and activator of transcription (STAT) family of proteins, namely STAT1, STAT3 and STAT5 have been implicated in KIT signaling. Ultimately, the phosphorylated KIT receptor stimulates intracellular signaling pathways controlling cell proliferation, adhesion, apoptosis, survival and differentiation. Importantly, downstream signaling mediated by oncogenically activated KIT in GISTs differs from physiologic KIT signaling.

B.2.3 Structure and Function of KIT

KIT is a member of the type III receptor tyrosine kinase family [212]. KIT is composed of an extracellular ligand-binding domain containing five immunoglobulin-like repeats, a transmembrane domain, a juxtamembrane domain, and a cytoplasmic kinase domain (Figure 35) [213, 214]. KIT is physiologically expressed in hematological stem cells, mast cells, melanocytes, germ cells and ICC [199, 215-218]. KIT has known roles in cellular survival, proliferation and migration. Stem cell factor (SCF) is the endogenous ligand for KIT and binding induces receptor dimerization and trans-phosphorylation resulting in full activation [219-223]. Oncogenic KIT is constitutively active without ligand stimulation and activates both pro-survival and anti-apoptotic pathways (Figure 34) [224, 225].

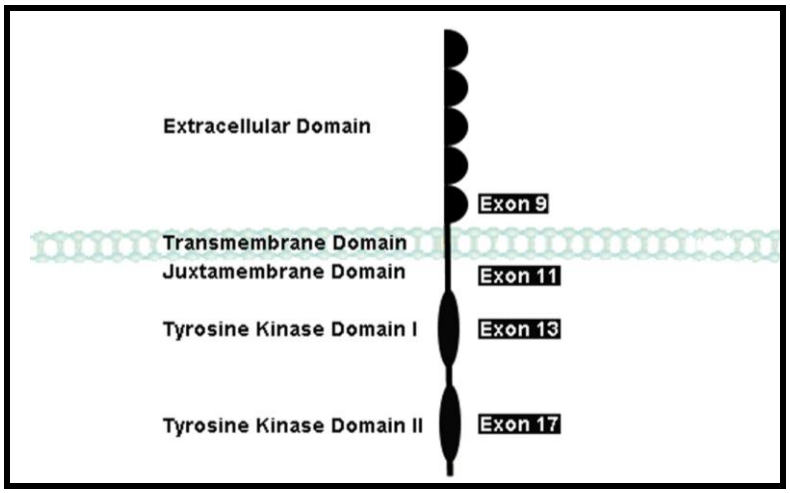

Figure 35: Structure of the receptor tyrosine kinase (RTK) KIT

KIT is the cellular homolog of the Hardy-Zuckerman 4 feline sarcoma virus oncogene v-KIT. It belongs to the type III family of RTKs. These RTKs are characterized by five extracellular IgG-like loops and a split kinase domain where the ATP-binding and the phosphotransferase regions are separated by a short polypeptide kinase insert. The KIT ligand, stem cell factor (SCF), binds to the extracellular region and leads to receptor dimerization. The juxtamembrane domain is important for negative regulation of activation and has autoinhibitory function. Mutations within KIT most commonly affect exon 11. Additionally mutations have been found in exons 9, 13 and 17.

B.2.4 KIT mutations in GISTs

Activating mutations of *KIT* are present in up to 85% of GISTs with the most frequent mutations being detected in *KIT* exon 11 affecting the juxtamembrane region of the protein [226]. The exon 11 mutations are heterogeneous, including deletions of various sizes, insertions, and point mutations. In wild-type KIT the juxtamembrane domain forms an alpha helix structure that provides an auto-inhibitory function. Loss of this interaction due to mutation leads to constitutive kinase signaling [227]. Approximately 15% of GISTs have mutations in *KIT* exon 9. Mutations in this exon commonly involve duplication of the alanine and tyrosine at position 504 [208]. Additionally there are mutations involving *KIT* exons 13 and 17, corresponding to the ATP-binding and phosphotransferase domains of the tyrosine kinase region, respectively [207, 208, 210].

Despite the fact that *KIT* mutations in GISTs are found in different parts of the gene therefore affecting various domains of the protein, all of them lead to constitutive, ligand-independent activation of KIT [209]. Up to 20% of GISTs do not contain *KIT* mutations [228]; of this subset 30% harbor mutation in platelet-derived growth factor receptor alpha (*PDGFRA*). *PDGFRA* mutations are found predominately in exons 12 and 18 which correspond to exons 11 and 17 of KIT, respectively [229]. Similar to *KIT* mutations, *PDGFRA* mutations lead to constitutive, ligand-independent kinase activation. Furthermore, *KIT* and *PDGFRA* mutations appeared to be alternative and mutually exclusive oncogenic events [229].

B.2.5 The small molecule kinase inhibitor, imatinib mesylate

Imatinib mesylate (Gleevec; IM) is a small molecule kinase inhibitor that was originally FDA-approved to target the BCR-ABL fusion oncoprotein that is generated by the t(9;22) Philadelphia chromosome in chronic myeloid leukemia (CML) [230]. Imatinib is a competitive inhibitor of ATP and blocks kinase enzymatic activity. It should be noted that due to conformational changes upon activation, imatinib is only able to bind kinases in their inactive form [231]. Because imatinib is not entirely specific in its binding, it not only inhibits phosphorylation of the ABL kinase but also of the KIT and PDGFR kinases [232].

Imatinib is the first-line therapy for patients with metastatic or inoperable GISTs [233-235]. It has been shown that up to 85% of patients benefit from imatinib therapy [234]. Upon initial treatment patients not responding to imatinib are regarded as having primary resistance. These patients often have exon 9 mutations or no known mutation in *KIT* (wild-type). Within 2 years of treatment greater than 50% of patients develop resistance mostly due to secondary mutations in the *KIT* kinase. Secondary mutations in the *KIT* kinase involve either the ATP binding pocket of the kinase domain (exons 13, 14) or the kinase activation loop (exons 17, 18). Secondary kinase mutations occur more frequently in GISTs with exon 11 primary mutations. The underlying mechanism for imatinib resistance varies between secondary mutations. Mutations in the ATP binding pocket inhibit the binding of imatinib. A common ATP binding pocket mutation is the T670I "gatekeeper" mutation. Homologous mutations are found in *BCR-ABL* as well as *PDGRFA* [236]. Secondary mutations involving the activation loop of KIT aid in stabilizing the kinase in its active conformation. This is detrimental for imatinib as it is unable to recognize the active conformation of kinases [226]. In addition to secondary mutations, GISTs have been shown to develop imatinib resistance through genomic amplification of *KIT* and/or

becoming hemi- and/or homozygous for the primary *KIT* mutation by deleting the remaining wild-type *KIT* allele [237, 238].

If a patient progresses while on imatinib therapy, first response is to increase drug dose as tolerated. In a phase III trial, 33% of patients showed improved imatinib response when the dose was increased from 400 mg to 800 mg. It is thought that increased dosage is capable of counteracting decreased binding affinity associated with ATP bonding pocket mutations. If a patient fails to respond to increased imatinib dosage, sunitinib is the second line of therapy. Sunitinib (Sutent®, Pfizer) is a small molecule kinase inhibitor that inhibits KIT, PDGFRA, VEGF and FLT3. Similarly to imatinib, sunitinib cannot inhibit activated KIT and therefore is ineffective against activation loop mutations. Furthermore, sunitinib resistance is frequent and generally occurs within six months [226]. For a patient unresponsive to sunitinib, there are no therapeutic options beyond surgical removal of tumors.

B.2.6 Function and inhibition of ABL

The cause behind chronic myeloid leukemia (CML), BCR-ABL is the target protein imatinib-mesylate was originally developed for. Fusion of the breakpoint cluster region (BCR) on chromosome 9 with ABL on chromosome 22 results in the t(9;22) Philadelphia chromosome fusion protein BCR-ABL. In BCR-ABL, full length wild-type ABL is retained with exception to a small N-terminal region upstream of the SH3 domain. Fusion of ABL with BCR disrupts auto-inhibitory interactions in ABL and results in a constitutively active kinase [239]. ABL is a ubiquitously expressed kinase that localizes to the cell nucleus, plasma membrane and actin cytoskeleton [240-242]. Two isoforms (1a, 1b) of ABL originate from alternate splicing of a single gene. ABL 1b differs from 1a in that it contains a myristoyl fatty acid moiety binding

region at the N-terminus and it is more highly expressed. This myristoyl group has been shown to interact with the catalytic domain in an auto-inhibiting fashion [243, 244]. The amino-terminus of ABL is highly similar in structure to the SRC family kinases (SFK) (Figure 36) [245]. ABL has multiple sites of activation including Y245 and Y412 (Figure 36). ABL has been shown to play a role in signaling pathways activated by growth factors, oxidative stress, ionizing radiation and integrin stimulation [246]. Activation of nuclear ABL in response to DNA double strand breaks induces apoptosis, while activation of the cytoplasmic/membrane pool promotes proliferation and migration [247]. ABL has been shown to be involved in the development of multiple normal tissues as well as several malignancies [241, 248, 249]. While BCR-ABL has been shown to have properties similar to oncogenic KIT, the non-translocated wild-type ABL has vastly different functions. Since ABL is a ubiquitously expressed kinase, we hypothesize it is likely expressed in GIST. Because imatinib inhibits both KIT and ABL, we aim to dissect the relative contributions of KIT and ABL inhibition in imatinib-induced apoptosis (Figure 37). We hypothesize that imatinib-induced inhibition of ABL may play a role in GIST cell apoptosis.

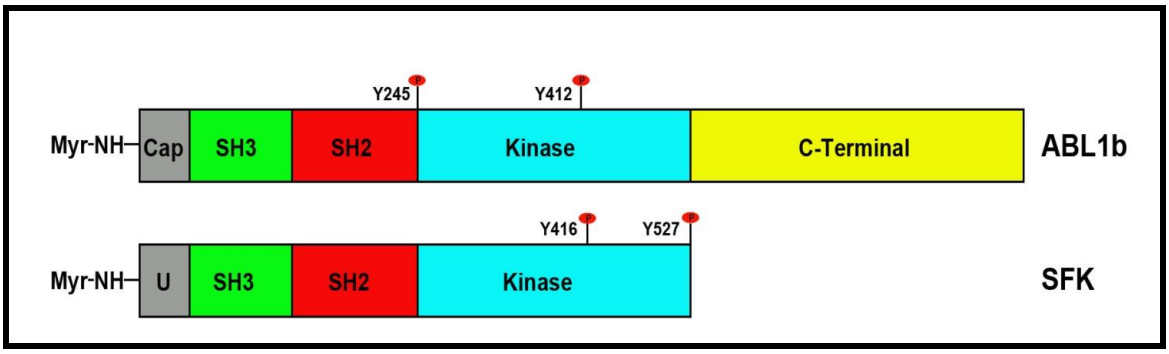

Figure 36: ABL and SFK structure.

ABL1b and SRC family kinases (SFK) both contain SH2, SH3 and Kinase domains. Additionally both are myristoylated at the N-terminus. ABL1b differs from SFKs in its C-terminal tail. Phosphorylation sites are indicated in red. U. Unique region

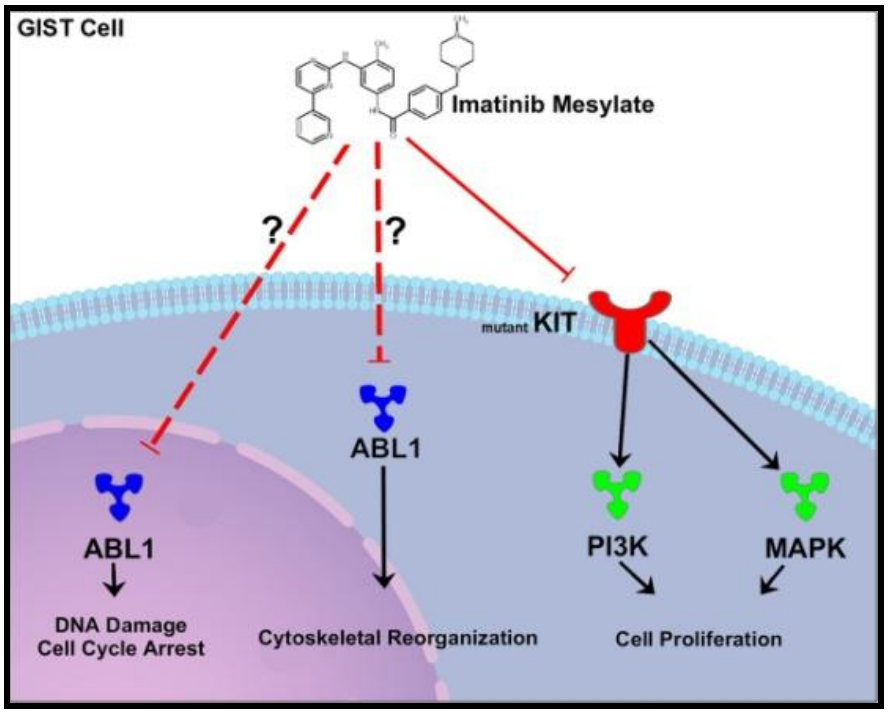

Figure 37: Imatinib inhibits both KIT and ABL

GISTs are caused by activating mutations in the KIT gene. Activated KIT leads to increased proliferation through PI3K and MAPK signaling. KIT activity is inhibited by imatinib mesylate (IM), however IM is known to inhibit both KIT and ABL. ABL is a ubiquitously expressed protein involved in the DNA damage response within the nucleus and cytoskeleton reorganization within the cytoplasm. Little is known about the contributions of KIT and ABL inhibition to the therapeutic response of GIST to IM.

B.2.7 Significance

Although 85% of patients benefit from the small kinase inhibitor, imatinib mesylate initially, more than 50% will develop drug resistance within two years of treatment. In addition to drug resistance there is a substantial amount of residual tumor mass following imatinib therapy. Imatinib mesylate has been shown to inhibit ABL as well as KIT. Better understanding of imatinib's mode of action and the relative contribution of KIT and ABL inhibition in imatinib-treated GISTs will help to develop novel and better treatment strategies.

B.3 MATERIALS AND METHODS

B.3.1 Cell culture

The imatinib-sensitive human GIST cell line GIST882 (kindly provided by Jonathan A. Fletcher, Brigham and Women's Hospital, Harvard Medical School, Boston, MA, USA) were derived from untreated metastatic GISTs and maintained in RPMI1640 (supplemented with 15% fetal bovine serum, FBS; 1% L-glutamine, 50 U/ml penicillin, 50 µg/ml streptomycin, 0.5 µg/ml amphotericin B). GIST882 cells carry a homozygous mutation in KIT exon 13 (K642E) (39). Imatinib-sensitive GIST-T1 cells (a generous gift of Dr. Takahiro Taguchi, Kochi Medical School, Kochi, Japan) were maintained in DMEM supplemented with 10% fetal bovine serum (FBS, Mediatech, Herndon, VA), 5 ml L-Glutamine, 50 U/ml penicillin (Cambrex, Walkersville,

MD) and 50 µg/ml streptomycin (Cambrex) at 37°C/5% CO_2. Human chronic myeloid leukemia K562 cells were obtained from the American Type Culture Collection (Manassas, VA, USA) and maintained in the same manner as GIST882.

B.3.2 Immunohistochemistry

For immunohistochemistry a TMA containing 28 GIST samples (in collaboration with Dr. Shih-Fan Kuan, Department of Pathology, University of Pittsburgh School of Medicine, Pittsburgh, PA; IRB #0509050) was incubated overnight at 65°C. Slides were deparafinized in xylene, rehydrated in ethanol and washed in dH_2O. Slides were pretreated by heating to 95°C 3 times in buffer citrate (0.1M citric acid, 0.1M sodium citrate). Slides were then cooled and washed with dH_2O followed by PBS. Slides were then stained using "Histo-Plus 3rd Generation IHC Kit" (Invitrogen, Carlsbad, CA) according to manufacturer's recommendations. Rabbit polyclonal antibody against c-ABL Y412 (Cell Signaling) was used to access activation loop phosphorylation. K562 cells embedded in paraffin served as positive control for constitutive BCR-ABL activation.

B.3.3 Transient transfection

GIST882 cells were transfected with siRNA targeting a single kinase alone (Qiagen, Valencia, CA) or in combination (SMARTpool, Dharmacon) using Amaxa nucleofection technology as recommended by the manufacturer. K562 cells were maintained in RPMI-1640 as described above until 50% confluent. Media was then be removed and replaced with antibiotic free RPMI-1640 containing 3µl HiPerFect transfection reagent (Qiagen) and 5 µl siRNA diluted in 100 µl

serum free media. Cells were transfected with siRNA against KIT, ABL, a combination of KIT and ABL or a non-coding siRNA control (Dharmacon, Lafayette, CO). Cells were then grown at 37°C/5% CO_2 for 72 h before being lysed.

B.3.4 In vitro apoptosis and proliferation assays

Apoptosis and cell viability studies were performed using the Caspase-Glo and CellTiter-Glo luminescence-based assays (Promega, Madison, WI, USA) as described previously (13). For these studies, cells were plated in a 96-well flat-bottomed plate (Perkin Elmer, San Jose, CA), cultured for 24 h and then incubated for 48 h (Caspase-Glo) or 72 h (CellTiter-Glo) with the respective compounds at indicated concentrations or DMSO-only solvent control. Luminescence was measured with a BioTek Synergy 2 Luminometer (BioTek, Winooski, VT), and the data were normalized to the DMSO-only control group.

B.3.5 Immunoblot

Protein lysates of GIST monolayer cultures (24) were prepared by washing twice with PBS and then scraping cells into RIPA buffer [1% NP40, 50 mmol/L Tris-HCl (pH 8.0), 100 mmol/L sodium fluoride, 30 mmol/L sodium pyrophosphate, 2 mmol/L sodium molybdate, 5 mmol/L EDTA, and 2 mmol/L sodium orthovanadate] containing protease inhibitors (10 μg/mL aprotinin, 10 μg/mL leupeptin, and 1 μmol/L phenylmethylsulfonyl fluoride). Whole cell lysates were then incubated for one hour with shaking at 4°C and then cleared by centrifugation for 30 minutes at 14,000 rpm at 4°C. Protein concentrations were determined by the Bradford assay

(Biorad, Hercules, CA). 25 µg of protein for each sample was separated on a 4-12% Bis-Tris gel and blotted onto a nitrocellulose membrane.

. Primary antibodies used for immunoblotting include: S6K, p-S6K (T389), (Abcam); H2AX, (Bethyl); p-ABL1 (Y412), p-AKT (S473), p-AKT (T308), AKT, p-KIT (Y719), PDK1, p-PDK1 (S241), p-PI3K (Y458), PI3K, p-PTEN (S380), PTEN, (Cell Signaling); KIT, (Dako); p-KIT (Y703), PARP, (Invitrogen); ABL1, (Santa Cruz); β-Actin, (Sigma); and p-H2AX (S139), (Upstate).

B.3.6 Statistical analysis

Statistical significance was assessed using Student's t test for independent samples and the Mann-Whitney U test for not normally distributed samples (VassarStats, http://vassarstats.net). P values ≤ 0.05 were considered significant.

B.4 RESULTS

B.4.1 ABL is expressed in GIST

In an effort to determine the effects of inhibiting ABL in GIST we first tested whether ABL is expressed in GISTs by staining a tissue microarray containing 28 GISTs for ABL by immunohistochemistry. Individual cores were assessed for ABL and positive staining intensity was scored as follows: 1 (weak), 2 (medium), 3 (strong). Most GISTs (78%) were positive for ABL. The majority of positive stains were weak to medium intensity with staining found

predominately in the cytoplasm. All assessable cores were positive for KIT (Figure 38). Having shown that most GISTs in fact do express ABL as well as KIT, we aimed to dissect the relative contributions of each to GIST cell proliferation/survival through siRNA-mediated knockdown.

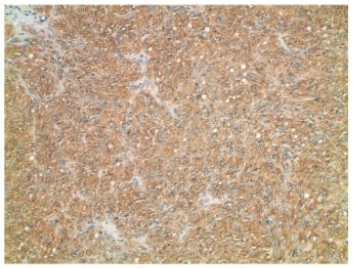

KIT (core #5)

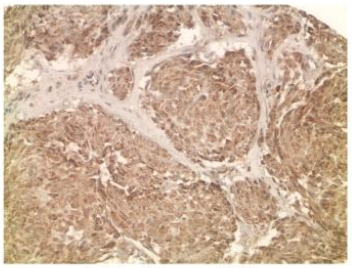

ABL (core #5)

Staining Intensity	KIT (n)	ABL1 (n)
Negative	0% (0)	14% (4)
1	29% (8)	46% (13)
2	32% (9)	25% (7)
3	36% (10)	7% (2)
Not ass.	4% (1)	7% (2)
Total	100% (28)	100% (28)

Figure 38: Most GISTs express ABL

Immunohistochemical staining of a tissue microarray containing 28 GISTs showed high levels of KIT in all assessable samples (left panel, table). Comparatively, ABL1 was present in 78% of GISTs (right panel, table). Staining intensity was scored as 1 (weak), 2 (medium) or 3 (strong). Not ass., not assessable.

B.4.2 Dual knockdown of both KIT and ABL attenuates apoptosis

To determine the relative contributions of KIT and ABL to GIST cell proliferation and survival we used the human GIST cell line GIST882 as a model (a generous gift of Dr. Jonathan Fletcher, Brigham and Women's Hospital, Harvard Medical School, Boston, MA). The GIST882 cell line was derived from an imatinib-sensitive metastatic GIST and harbors a constitutively activating homozygous *KIT* mutation in exon 13 (K642E) [250, 251]. Following siRNA transfection cells were assayed with luminescent-based assays to determine cell viability or apoptosis. As expected siRNA-mediated knockdown of KIT led to reduced cell proliferation and increased apoptosis in GIST882 cells. By contrast, siRNA against ABL showed little effect on GIST882 proliferation or apoptosis. Interestingly, knockdown of both KIT and ABL led to reduced apoptosis of GIST882 cells when compared to KIT knockdown alone (Figure 39). Proliferation was not changed when KIT and ABL were knocked down in combination compared to KIT alone (Figure 39).

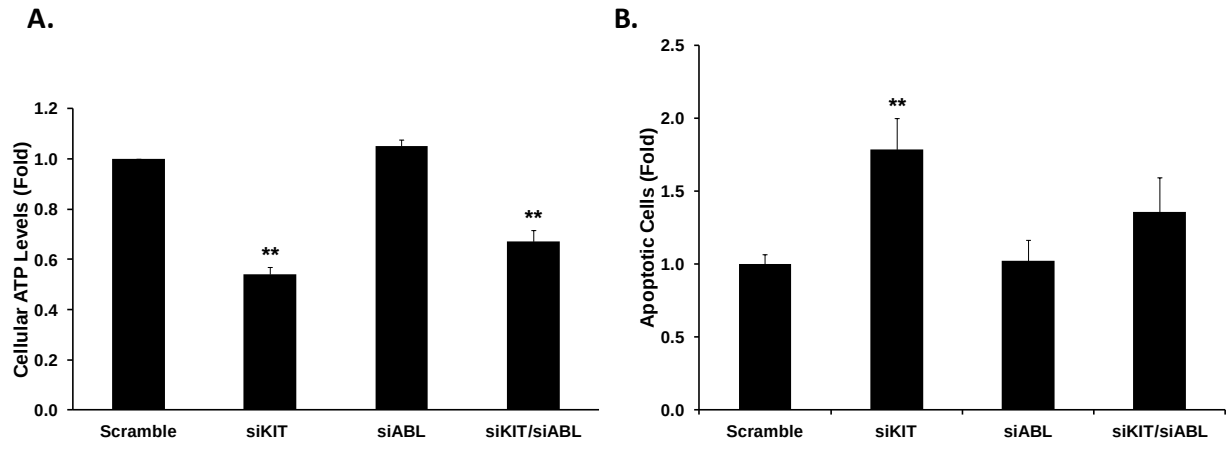

Figure 39: Effects of siRNA-mediated knockdown of KIT and ABL1 on cell viability and apoptosis in GIST882 cells.

Cells were transfected with siKIT and siABL alone or in combination (SMARTpool; Dharmacon, Lafayette, CO) using Amaxa nucleofection technology. Cellular proliferation (A) and apoptosis (B) were assessed 72 h and 48h post transfection respectively, using Cell-Titer-GLO and Caspase-GLO, respectively (Promega, Madison, WI). Cells were not treated with IM.

B.4.3 Dual knockdown of both KIT and ABL does not affect BrdU incorporation of p27 levels.

After identifying that dual knockdown of KIT and ABL led to attenuated apoptosis in GIST882 cancer cells we aimed to determine the effects of cell proliferation following single knockdown of KIT and ABL or dual knockdown of both. 48h hours after transient transfection of siRNA targeting ABL GIST882 cells showed BrdU incorporation levels on par with control (Figure 40). In contrast, BrdU incorporation was significantly reduced when either KIT or both KIT and ABL were knocked down (Figure 40). Levels of p27 following siRNA transfection showed a similar phenotype as BrdU incorporation. p27 levels were greater following dual knockdown or KIT

knockdown alone, but were largely unchanged following single knockdown of ABL (Figure 41). These data confirm that loss of cell proliferation in GIST882 cells following dual siRNA mediated knockdown of KIT and ABL is due to the loss of KIT rather than ABL.

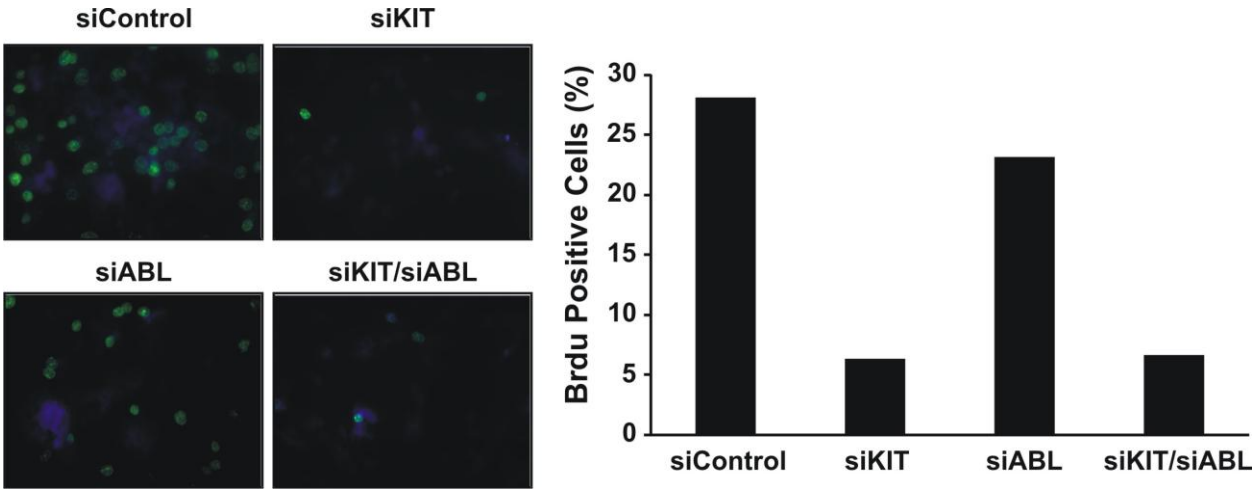

Figure 40: Effects of siRNA-mediated knockdown of KIT and ABL1 on BrdU incorporation in GIST882 cells.

Cells were transfected with siKIT and siABL alone or in combination (SMARTpool; Dharmacon, Lafayette, CO) using Amaxa nucleofection technology. BrdU incorporation was assessed 48h post transfection. Representative images and quantification shown. 300 cells per condition were counted.

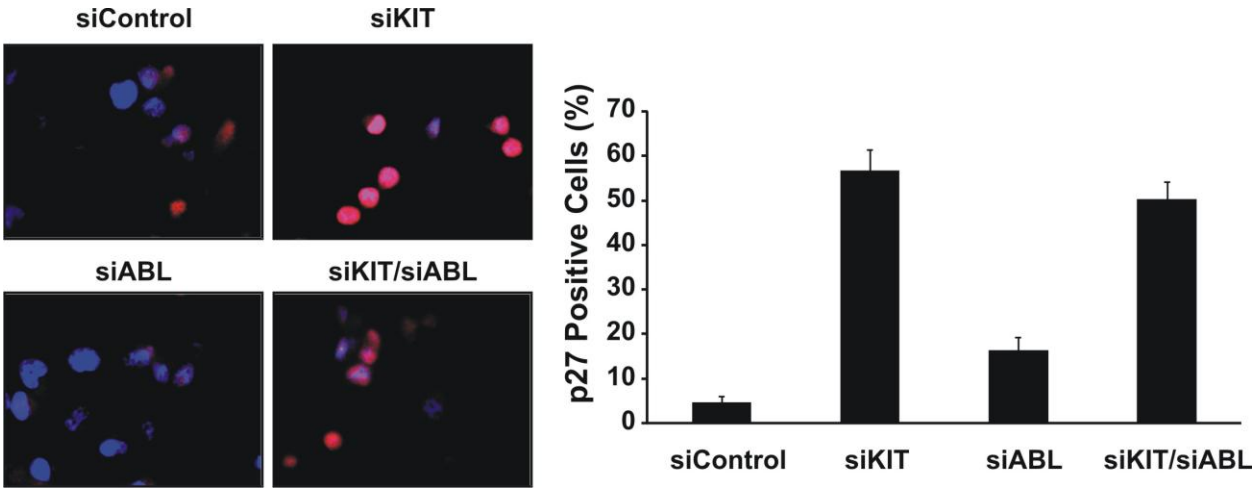

Figure 41: Effects of siRNA-mediated knockdown of KIT and ABL1 on p27 levels in GIST882 cells.

Cells were transfected with siKIT and siABL alone or in combination (SMARTpool; Dharmacon, Lafayette, CO) using Amaxa nucleofection technology. p27 levels were assessed 48h post transfection. Representative images and quantification shown. 300 cells per condition were counted.

B.4.4 ABL Knockdown leads to increased AKT activity

To determine the cause of apoptosis attenuation in KIT and ABL deficient cells, whole cell lysates were made 24, 48 and 72 h after siRNA transfection with KIT, ABL and combination of the two, then analyzed by immunoblotting for signaling mediators as well as regulators of the cell cycle and apoptosis (Figure 42). A non-coding scrambled siRNA served as negative control. KIT knockdown occurred within 24 h of transfection whereas sufficient knockdown of ABL was seen after 48 h in both single and combination experiments (Figure 42). As expected, knockdown

of KIT led to inhibition of downstream signaling (PI3K and MAPK pathways); as well as cell cycle arrest and apoptosis (data not shown). These effects were not present after knockdown of ABL. Unexpectedly, ABL knockdown led to a substantial increase in activated (AKT S473) and total AKT as well as increased S6K phosphorylation (Figure 42). To dissect the pathway leading to increased AKT activation after ABL knockdown, we analyzed the activation of signaling regulators upstream of AKT and found that PDK1 as well as PI3K phosphorylation increased (Figure 42). These effects were abolished when KIT was knocked down in combination with ABL. These findings suggest that loss of ABL modulates known survival pathways in GIST.

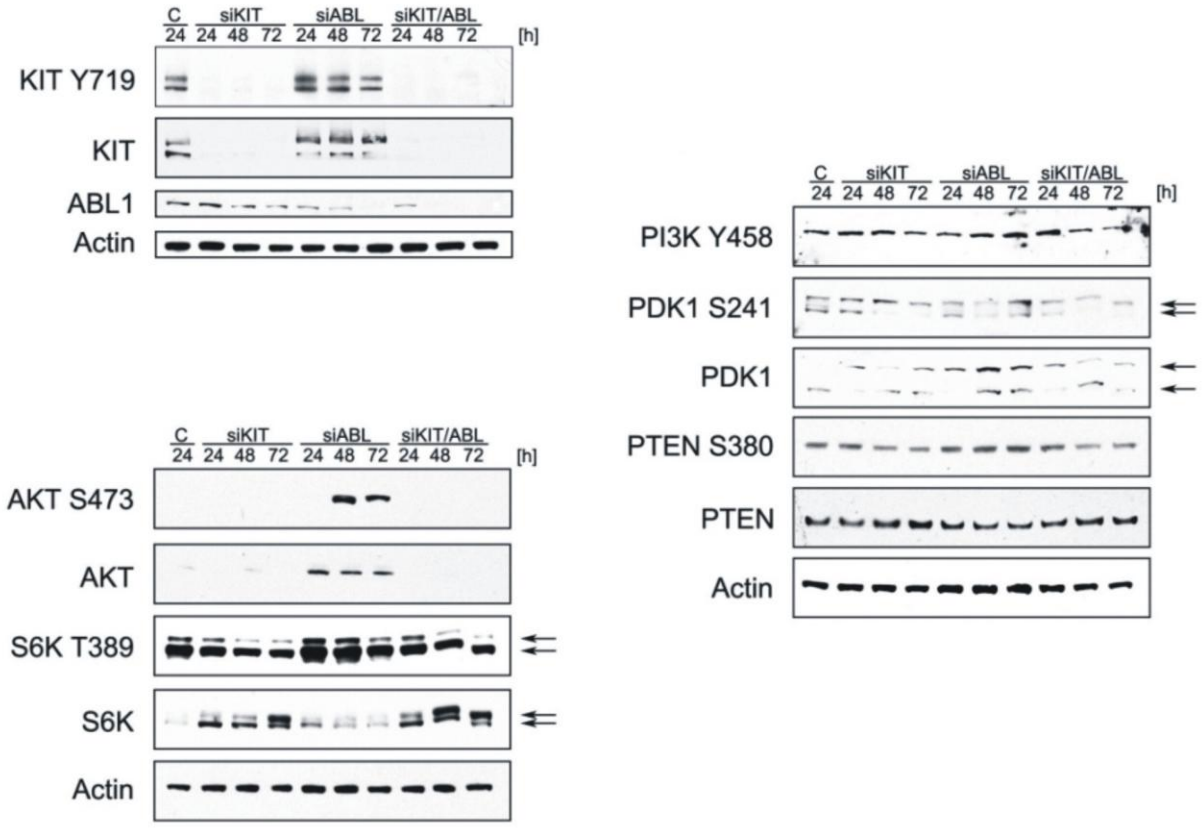

Figure 42: Effects of siRNA-mediated knockdown of KIT and ABL1 on downstream signaling as well as regulators of cell cycle and apoptosis in GIST882 cells.

Immunoblot analysis of GIST882 cells at 24, 48 and 72 h after siRNA transfection as indicated. Cells were transfected with siKIT and siABL1 alone or in combination (SMARTpool, Dharmacon) using Amaxa nucleofection technology. Whole cell lysates were run on a 4-12% polyacrylamide gel. Actin is shown to demonstrate equal loading. C, control siRNA. Greater than 80% of KIT protein was absent after 24 h. ABL protein was reduced by 50% at 48 h and 70% at 72 h post siRNA.

B.5 DISCUSSION

Imatinib mesylate was initially engineered and FDA approved for the treatment of CML by inhibition of the BCR-ABL fusion protein. However, it was soon found to be effective in other diseases including GIST. Over a decade after being approved for metastatic GIST patients, Imatinib mesylate remains the first line therapy for more than half of GIST patients with unresectable or metastatic disease [182]. While initial response rates are very promising, nearly half of patients initially responsive to therapy will become resistant to it within 24 months of initial treatment [147]. While drug resistance due to acquired secondary mutations in KIT has been extensively published there still remain patients with inherent resistance for unknown reasons. Having initially been FDA approved for another disease and protein target it is clear Imatinib mesylate has off target effects that need to be taken into account when dissecting its activity.

We have outlined a molecular consequence of chronic imatinib mesylate treatment in GIST cancer cells due to off target suppression of ABL signaling. Reduction in ABL signaling leads to increased signaling through the PI3K/AKT/mTOR proliferative pathway. This would obviously be detrimental to both imatinib sensitive and resistant patients. In the case of patients showing reduced drug efficacy imatinib might be doing more harm than good. Our findings provide further evidence for the need to develop more specific inhibitors of KIT and its downstream targets for the long term treatment of patients with unresectable GIST.

APPENDIX C

IDENTIFYING NEW THERAPEUTIC TARGETS IN GIST

C.1 ABSTRACT

Gastrointestinal stromal tumors (GISTs) are the most common mesenchymal tumors of the gastrointestinal tract. They are caused by activating mutations in the KIT or platelet-derived growth factor receptor alpha (PDGFRA) receptor tyrosine kinase genes. While most primary mutations can be effectively treated with small molecule kinase inhibitor imatinib mesylate (Gleevec®; Novartis Pharma, Basel, Switzerland); secondary mutations are resistant to such therapy. Therefore new therapeutic options are urgently needed.

The results of a small preliminary siRNA screen targeting kinases identified the SRC family kinase, LYN as having a role in GIST cell survival as measured by ATP based luminescent assay. Further investigation confirmed loss of LYN leads to decreased BrdU incorporation and increased $p27^{Kip1}$ expression. Having provided proof of principle that kinases besides KIT play a role in GIST survival, proliferation and apoptosis we expanded our approach and performed a siRNA mediated screen encompassing all known kinases in the human genome (n=709). This search was conducted with a siRNA library (Qiagen, Hilden, Germany) used in conjunction with a Cell Line 96-well Nucleofector Kit (Amaxa; Cologne, Germany). Following

kinase transient knockout proliferation and apoptosis were determined using the CellTiter-Glo and Caspase-Glo luminescent assays, respectively. All measurements were taken in triplicate and averaged. A candidate was considered a hit when its siRNA-mediated knockdown led to a ≥40% inhibition of cell proliferation when compared to control siRNA. In the primary screen we identified 65 kinases that resulted in decreased cell proliferation when targeted by siRNA. These include several members of the PI3K and MAPK pathways such as PIK3R2 (phosphoinositide-3-kinase, regulatory subunit 2), PIK3C2G (PI3K, class2, gamma polypeptide), MAP3K5 (mitogen-activated protein kinase kinase kinase 5) and MAP2K4 (MAPK kinase 4). Both pathways are known to actively regulate cell survival and cell proliferation signaling in GIST cells. Identifying members of these two pathways provides evidence of the efficacy of the screen. Identification of additional therapeutic targets in imatinib-resistant GIST may prove valuable in the development of second generation small molecule inhibitors.

C.2 BACKGROUND

C.2.1 The SRC family kinase LYN

Hypothesizing that kinases besides KIT and PDGFRA may function in GIST cell survival, proliferation and apoptosis we investigated the role of the SFK LYN in GIST. SRC Family Kinases (SFKs) are human homologs of viral oncoproteins known to be involved in multiple signaling pathways controlling an array of networks regulating viability, metabolism, proliferation, migration and differentiation within many different cell lineages [252, 253]. Each SFK is about 60kD in molecular weight and has a common structure consisting of an N-terminal

unique domain, SH2 domain, SH3 domain and a tyrosine kinase domain (Figure 36) [254]. All SFKs show similar modes of regulation. There are nine members of the SFKs that are further grouped into subfamilies: LYN related (LYN, HCK, LCK and BLK), SRC-related (SRC, YES, FYN and FGR) and FRK. SFKs are frequently deregulated in cancer, in which they have been linked to tumor development and progression. The LYN gene is localized on human chromosome 8q13 and exists in two isoforms, p53 and p56 arising from alternate splicing of exon 2 with no functional differences between isoforms currently known [255]. LYN is an important component in cytokine signaling in a variety of cells but has predominately been characterized by its role in the regulation of growth and apoptosis of hematopoietic cells. LYN is known to be involved in a positive feedback loop where it is phosphorylated by activated KIT and in turn phosphorylates KIT [225, 256]. Moreover, LYN has been shown to activate ABL [257] and play a role in imatinib-resistance in CML. Activation of LYN in CML cells results in upregulation of the anti-apoptotic protein BCL-2, and caspase-cleaved LYN has been shown to relocalize from the plasma membrane to the cytosol and protect CML cells from imatinib-induced apoptosis [258, 259]. The role of LYN in KIT signaling as well as imatinib-resistant CML led us to hypothesize that LYN may play a role in GIST cell proliferation and apoptosis.

C.2.2 Kinases as therapeutic targets

Having shown proof-of-principle that kinases besides KIT and PDGFRA have important functions in GIST cell survival, proliferation and apoptosis we broadened our approach to all kinases within the human genome. With roles in cell motility, proliferation, survival and apoptosis kinases are potential targets for future therapies. The ATP binding pocket of kinases has been shown to be easily targeted by ATP-competitive inhibitors, a large number of which

have already been FDA-approved for the treatment of various malignancies [260-262]. The prototype example of this is imatinib mesylate in treatment of GIST and CML. Furthermore, in recent years there has been development of both specific (i.e. GNF-2, GNF-5) and broad (i.e. nilotinib, sunitinib, erlotinib) small molecule kinase inhibitors. Because imatinib resistance in GIST patients is often due to secondary mutations in the *KIT* or *PDGFRA* kinases, treating these tumors with second-line therapies targeting these receptors is problematic. Identification of additional kinases involved in GIST cell proliferation and survival would allow for potentially new therapeutic targets.

There are over seven hundred identified and predicted kinases in the human genome. With such a large population of targets, high throughput screens are the preferred approach. Small-interfering RNA (siRNA) has been shown to be a powerful tool in eliciting cellular roles by targeting specific genes. Use of siRNA in a high-throughput manner will allow for efficient identification of kinases involved in GIST proliferation and apoptosis. Identification of additional kinases that regulate GIST cell survival, proliferation and apoptosis will provide new therapeutic targets for tumors unresponsive to imatinib. In support of this, recent clinical trials have shown response to broader tyrosine kinase inhibitors in patients resistant to imatinib [226]. We hypothesize that kinases besides KIT and PDGFRA play a role in GIST survival, proliferation and apoptosis.

C.2.3 Significance

Although 85% of patients benefit from the small kinase inhibitor, imatinib mesylate initially, more than 50% will develop drug resistance within two years of treatment. Imatinib-resistance in GIST patients is usually due to secondary mutations in the *KIT* or *PDGFRA* kinase. As a

result of this, additional therapies targeting KIT or PDGFRA are problematic. Since kinases are attractive "druggable" targets, identifying kinases other than KIT and PDGFRA that play a role in GIST cell proliferation and survival will open new avenues for the treatment of imatinib-resistant GIST.

C.3 MATERIALS AND METHODS

C.3.1 Cell culture

The imatinib-sensitive human GIST cell line GIST882 (kindly provided by Jonathan A. Fletcher, Brigham and Women's Hospital, Harvard Medical School, Boston, MA, USA) were derived from untreated metastatic GISTs and maintained in RPMI1640 (supplemented with 15% fetal bovine serum, FBS; 1% L-glutamine, 50 U/ml penicillin, 50 µg/ml streptomycin, 0.5 µg/ml amphotericin B). GIST882 cells carry a homozygous mutation in KIT exon 13 (K642E) (39). Imatinib-sensitive GIST-T1 cells (a generous gift of Dr. Takahiro Taguchi, Kochi Medical School, Kochi, Japan) were maintained in DMEM supplemented with 10% fetal bovine serum (FBS, Mediatech, Herndon, VA), 5 ml L-Glutamine, 50 U/ml penicillin (Cambrex, Walkersville, MD) and 50 µg/ml streptomycin (Cambrex) at 37°C/5% CO_2. Human chronic myeloid leukemia K562 cells were obtained from the American Type Culture Collection (Manassas, VA, USA) and maintained in the same manner as GIST882.

C.3.2 Transient transfection

GIST882 cells were transfected with siRNA targeting a single kinase alone (Qiagen, Valencia, CA) or in combination (SMARTpool, Dharmacon) using Amaxa nucleofection technology as recommended by the manufacturer. In vitro apoptosis and proliferation assays

Apoptosis and cell viability studies were performed using the Caspase-Glo and CellTiter-Glo luminescence-based assays (Promega, Madison, WI, USA) as described previously (13). For these studies, cells were plated in a 96-well flat-bottomed plate (Perkin Elmer, San Jose, CA), cultured for 24 h and then incubated for 48 h (Caspase-Glo) or 72 h (CellTiter-Glo) with the respective compounds at indicated concentrations or DMSO-only solvent control. Luminescence was measured with a BioTek Synergy 2 Luminometer (BioTek, Winooski, VT), and the data were normalized to the DMSO-only control group.

C.3.3 Immunoblot

Protein lysates of GIST monolayer cultures (24) were prepared by washing twice with PBS and then scraping cells into RIPA buffer [1% NP40, 50 mmol/L Tris-HCl (pH 8.0), 100 mmol/L sodium fluoride, 30 mmol/L sodium pyrophosphate, 2 mmol/L sodium molybdate, 5 mmol/L EDTA, and 2 mmol/L sodium orthovanadate] containing protease inhibitors (10 μg/mL aprotinin, 10 μg/mL leupeptin, and 1 μmol/L phenylmethylsulfonyl fluoride). Whole cell lysates were then incubated for one hour with shaking at 4°C and then cleared by centrifugation for 30 minutes at 14,000 rpm at 4°C. Protein concentrations were determined by the Bradford assay (Biorad, Hercules, CA). 25 μg of protein for each sample was separated on a 4-12% Bis-Tris gel and blotted onto a nitrocellulose membrane.

C.3.4 Statistical analysis

Statistical significance was assessed using Student's t test for independent samples and the Mann-Whitney U test for not normally distributed samples (VassarStats, http://vassarstats.net). P values ≤ 0.05 were considered significant.

C.4 RESULTS

C.4.1 LYN is involved in GIST cell cycle regulation

To test whether kinases other than KIT and PDGFRA play a role in GIST cell proliferation and survival we tested whether LYN could be involved. LYN is a SFK that is involved in KIT downstream signaling and that has been shown to be upregulated in imatinib-resistant CML [257, 263, 264]. To test whether LYN plays a role in GIST we performed siRNA-mediated knockdown of LYN followed by luminescent assays in GIST882 cells (data not shown). We then performed follow-up studies to illicit LYN's role in GIST. We have shown using siRNA-mediated studies that LYN plays a role in both GIST proliferation and cell cycle progression (Figure 43). Assaying for cell cycle arrest by staining for $p27^{Kip1}$ levels following LYN knockdown showed a significant increase in cell cycle arrest (Figure 43A-B). This trend of reduced cell proliferation was confirmed by BrdU incorporation following LYN knockdown

which showed a significant reduction in GIST882 cell proliferation similar to siRNA against KIT (Figure 43C-D). These studies provide proof of principle that kinases besides KIT play a role in GIST survival, proliferation and apoptosis.

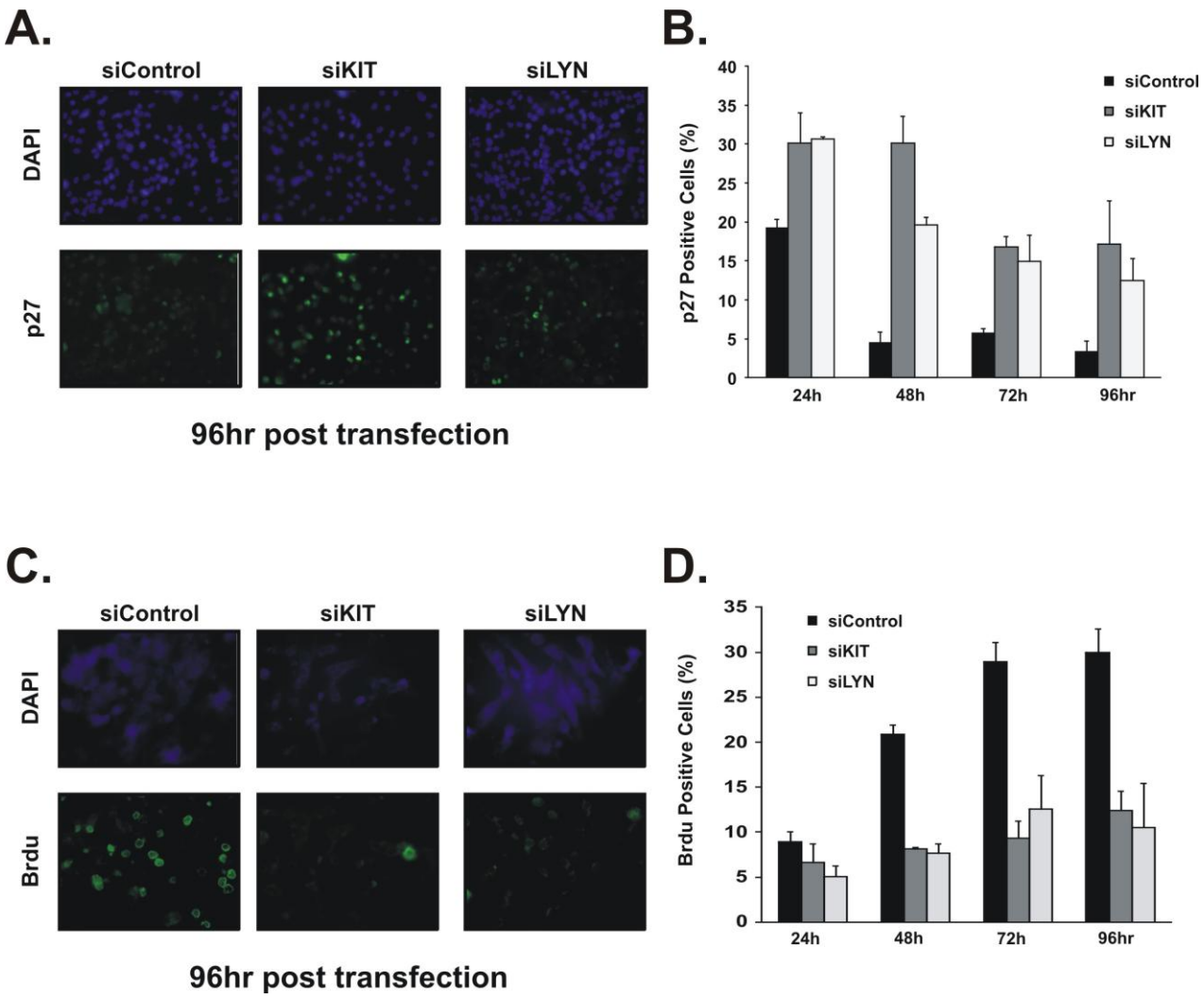

Figure 43: Effects of siRNA-mediated knockdown of KIT and LYN on $p27^{Kip1}$ levels and BrdU incorporation in GIST882 cells.

Cells were transfected with siKIT and siLYN alone (SMARTpool; Dharmacon, Lafayette, CO) using Amaxa nucleofection technology. p27 levels (A-B) and BrdU incorporation (C-D) were assessed 96h post transfection. Representative images and quantification shown. 300 cells per condition were counted.

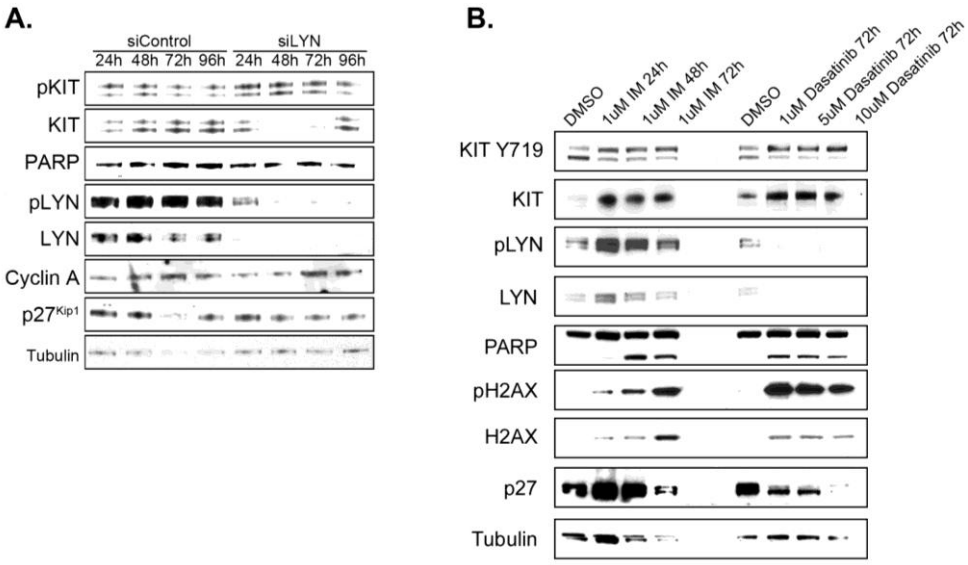

Figure 44: Inhibition of LYN induces cell death in GIST882 cells.

(A) Whole cell lysate protein levels of GIST882 cells following transient transfection of siRNA targeting KIT or LYN. (B) Whole cell lysate protein levels of GIST882 cells following treatment with an inhibitor of KIT (Imatinib) or LYN (Dasatinib). Treatment concentrations and time are indicated.

C.4.2 Inhibition of LYN leads to increased cell death in GIST882 cells

After identifying that LYN knockdown led to increased $p27^{Kip1}$ levels and decreased BrdU incorporation we aimed to determine the effects of both LYN knockdown and a LYN inhibitor (Dasatinib) on GIST882 cell survival. Transient knockdown of LYN by siRNA showed an increase in $p27^{Kip1}$ levels 72 hours following transfection indication increased levels of cell cycle arrest (Figure 44). In line with these results, inhibition of LYN by Dasatinib led to increased levels of PARP, γ-H2AX and H2AX 72 hours after treatment with dosages as low as 1 μM (Figure 44).

C.4.3 Identification of additional kinases involved in GIST survival and/or proliferation

Having shown proof-of-principle that other kinases besides KIT and PDGFRA play an important role in GIST cell survival we hypothesize that additional kinases may be involved in regulating cell viability and apoptosis in GIST. To determine this we broadened our initial screen to include all identified kinases in the human genome. A siRNA library containing 4 individual siRNA sequences (A-D) against all kinases (n=709; Qiagen) was used with Amaxa nucleofection. In our initial validation studies a 30% reduction in cell proliferation was observed following KIT knockdown when compared to a non-coding scrambled siRNA control. This figure served as the threshold for determining a "hit" kinase. In the primary screen (sequence A) we identified 65 kinases that resulted in decreased cell proliferation as determined above when targeted by siRNA

(Appendix A). These include several members of the PI3K and MAPK pathways such as PIK3R2 (phosphoinositide-3-kinase, regulatory subunit 2), PIK3C2G (PI3K, class2, gamma polypeptide), MAP3K5 (mitogen-activated protein kinase kinase kinase 5) and MAP2K4 (MAPK kinase 4). Both pathways are known to actively regulate cell survival and cell proliferation signaling in GIST cells. Identifying members of these two pathways provides credibility of the efficacy of the screen. A secondary screen (sequence B) was performed to validate initial hits. This screen narrowed the 65 hit kinases down to 37 (Table 5). Of the 37 we further investigated a smaller subset of 10 kinases. When targeted with siRNA, all ten candidate kinases decreased cell viability and increased apoptosis in GIST882 cells (Figure 45). These kinases were chosen for previous evidence showing their role in disease. Three of the ten hits we have chosen to further focus on include serine threonine kinase 33 (STK33), recently shown to play a role in KRAS dependent synthetic lethality in cancer cells [265-267], transforming growth factor beta receptor 1 (TGFBR1), shown to play a role in breast cancer and related to tyrosine receptor kinase (RYK), shown to play a role in Wnt signaling [268]. Further experiments will be performed to dissect the exact role these candidate kinase plays in GIST survival, proliferation and apoptosis.

Table 5: Hits in unbiased siRNA screen of GIST882 cells

Symbol	Description	Screen 1A	Screen 2A	Screen 2B	Screen 2A	Screen 2B
ABL1	v-abl Abelson murine leukemia viral oncogene homolog 1	0.66	1.50	0.41	0.85	0.95
ACVR1B	activin A receptor, type IB	0.62	0.33	0.82	0.84	1.28
ACVR2	activin A receptor, type II	0.63	1.14	1.28	0.97	1.40
CSNK1A1	casein kinase 1, alpha 1	0.66	1.71	1.36	0.84	1.08
CSNK1D	casein kinase 1, delta	0.65	1.53	1.25	0.79	1.26
CSNK2B	casein kinase 2, beta polypeptide	0.60	2.13	1.65	0.95	1.07
KDR	kinase insert domain receptor (a type III receptor tyrosine kinase)	0.52	2.69	2.29	1.04	1.59
KIT	v-kit Hardy-Zuckerman 4 feline sarcoma viral oncogene homolog	0.64	1.92	1.02	0.63	0.67
LYN	v-yes-1 Yamaguchi sarcoma viral related oncogene homolog	0.54	0.89	0.46	0.87	1.46
MAP3K5	mitogen-activated protein kinase kinase kinase 5	0.50	0.59	1.42	0.92	1.19
PIK3C2G	phosphoinositide-3-kinase, class 2, gamma polypeptide	0.65	1.18	1.29	0.92	1.23
PIK3R2	phosphoinositide-3-kinase, regulatory subunit 2 (p85 beta)	0.39	2.17	1.88	1.05	1.45
PRKAB2	protein kinase, AMP-activated, beta 2 non-catalytic subunit	0.27	1.89	2.06	0.79	1.50
PRKACA	protein kinase, cAMP-dependent, catalytic, alpha	0.24	2.79	1.71	0.96	1.31
PRKACB	protein kinase, cAMP-dependent, catalytic, beta	0.14	2.54	1.91	0.89	1.06
PRKAR1B	protein kinase, cAMP-dependent, regulatory, type I, beta	0.59	2.60	1.30	0.91	1.05
PRKAR2A	protein kinase, cAMP-dependent, regulatory, type II, alpha	0.51	0.54	0.71	0.61	1.43
PRKG2	protein kinase, cGMP-dependent, type II	0.59	1.03	1.13	0.88	1.40
MAP2K7	mitogen-activated protein kinase kinase 7	0.56	1.01	1.10	0.82	1.25
PTK6	PTK6 protein tyrosine kinase 6	0.57	1.69	1.56	0.84	1.77
GRK1	G protein-coupled receptor kinase 1	0.30	2.62	1.82	0.93	1.56
ROCK1	Rho-associated, coiled-coil containing protein kinase 1	0.35	2.43	2.01	0.87	1.35
ROS1	v-ros UR2 sarcoma virus oncogene homolog 1 (avian)	0.20	2.60	2.09	0.96	1.07
RPS6KB1	ribosomal protein S6 kinase, 70kDa, polypeptide 1	0.43	2.71	1.61	0.86	1.25
RYK	RYK receptor-like tyrosine kinase	0.46	0.68	0.57	0.81	1.04
MAP2K4	mitogen-activated protein kinase kinase 4	0.27	1.27	0.94	0.68	1.25

Table 5 continued

SRC	v-src sarcoma (Schmidt-Ruppin A-2) viral oncogene homolog (avian)	0.40	1.04	1.06	0.85	1.02
SRPK1	SFRS protein kinase 1	0.39	1.71	1.69	0.82	1.38
SRPK2	SFRS protein kinase 2	0.41	1.94	1.72	0.90	1.10
NEK4	NIMA (never in mitosis gene a)-related kinase 4	0.17	2.55	1.70	0.85	1.35
STK10	serine/threonine kinase 10	0.29	2.57	1.58	0.72	1.09
STK11	serine/threonine kinase 11 (Peutz-Jeghers syndrome)	0.44	2.37	1.28	0.67	0.74
TGFBR1	transforming growth factor, beta receptor I (activin A receptor type II-like kinase, 53kDa)	0.21	0.47	0.57	0.82	1.34
TGFBR2	transforming growth factor, beta receptor II (70/80kDa)	0.60	1.42	0.86	0.91	1.05
TYK2	tyrosine kinase 2	0.27	1.93	1.15	0.93	1.07
TYRO3	TYRO3 protein tyrosine kinase	0.63	1.49	1.50	0.77	1.26
IKBKG	inhibitor of kappa light polypeptide gene enhancer in B-cells, kinase gamma	0.61	1.69	1.89	0.80	1.22
PDXK	pyridoxal (pyridoxine, vitamin B6) kinase	0.37	2.16	1.67	0.80	1.15
TNK1	tyrosine kinase, non-receptor, 1	0.43	3.19	1.37	0.98	0.95
RIPK1	receptor (TNFRSF)-interacting serine-threonine kinase 1	0.27	2.60	1.55	0.75	1.08
AKAP4	A kinase (PRKA) anchor protein 4	0.21	0.59	0.90	0.85	1.41
STK19	serine/threonine kinase 19	0.57	1.17	0.80	0.94	1.10
STK29	serine/threonine kinase 29	0.09	1.92	1.40	0.93	0.91
MAP3K7IP2	mitogen-activated protein kinase kinase kinase 7 interacting protein 2	0.55	1.74	2.11	0.99	1.29
MAST2	microtubule associated serine/threonine kinase 2	0.22	2.22	1.87	0.85	1.27
EPS8L1	EPS8-like 1	0.32	1.96	1.70	0.72	1.04
ETNK2	ethanolamine kinase 2	0.56	2.84	1.45	0.92	1.17
PI4K2B	phosphatidylinositol 4-kinase type-II beta	0.23	2.25	1.50	0.98	0.97
PAK6	p21(CDKN1A)-activated kinase 6	0.32	0.42	0.75	0.64	1.40
TAOK1	TAO kinase 1	0.31	0.85	0.97	0.79	1.15
CERK	ceramide kinase	0.35	1.88	1.01	1.02	1.06
STK33	serine/threonine kinase 33	0.24	1.40	1.24	0.90	1.11
Sharpin	shank-interacting protein-like 1	0.45	1.69	1.79	0.75	1.09
BRSK1	BR serine/threonine kinase 1	0.18	1.92	1.66	0.78	1.10
NYD-SP25	protein kinase NYD-SP25	0.34	2.34	1.54	0.80	1.07
LYK5	protein kinase LYK5	0.32	1.54	1.33	0.63	0.97
LMTK3	lemur tyrosine kinase 3	0.36	0.43	0.75	0.71	1.24
DCAMKL2	doublecortin and CaM kinase-like 2	0.39	0.64	0.80	0.87	1.02
ERK8	extracellular signal-regulated kinase 8	0.60	1.25	0.79	0.92	0.87
CDKL4	cyclin-dependent kinase-like 4	0.58	0.84	1.16	0.73	1.12
SBK1	SH3-binding domain kinase 1	0.59	0.96	1.28	0.68	1.11

Table 5 continued

LOC391295	similar to spermiogenesis associated serine/threonine kinase 22D; serine/threonine kinase FKSG81; spermiogenesis associated 4	0.24	1.20	1.49	0.73	1.26
LOC391533	similar to Vascular endothelial growth factor receptor 1 precursor (VEGFR-1) (Vascular permeability factor receptor) (Tyrosine-protein kinase receptor FLT) (Flt-1) (Tyrosine-protein kinase FRT) (Fms-like tyrosine kinase 1)	0.24	1.39	1.44	0.72	0.96
LOC392265	similar to Cell division protein kinase 5 (Tau protein kinase II catalytic subunit) (TPKII catalytic subunit) (Serine/threonine-protein kinase PSSALRE)	0.58	1.16	1.11	0.59	1.07
	Below or very close to KIT control					
	Within 1 standard deviation of KIT control					
	Within 3 standard deviation of KIT control					

The 37 targets confirmed in screen 2 are listed in bold

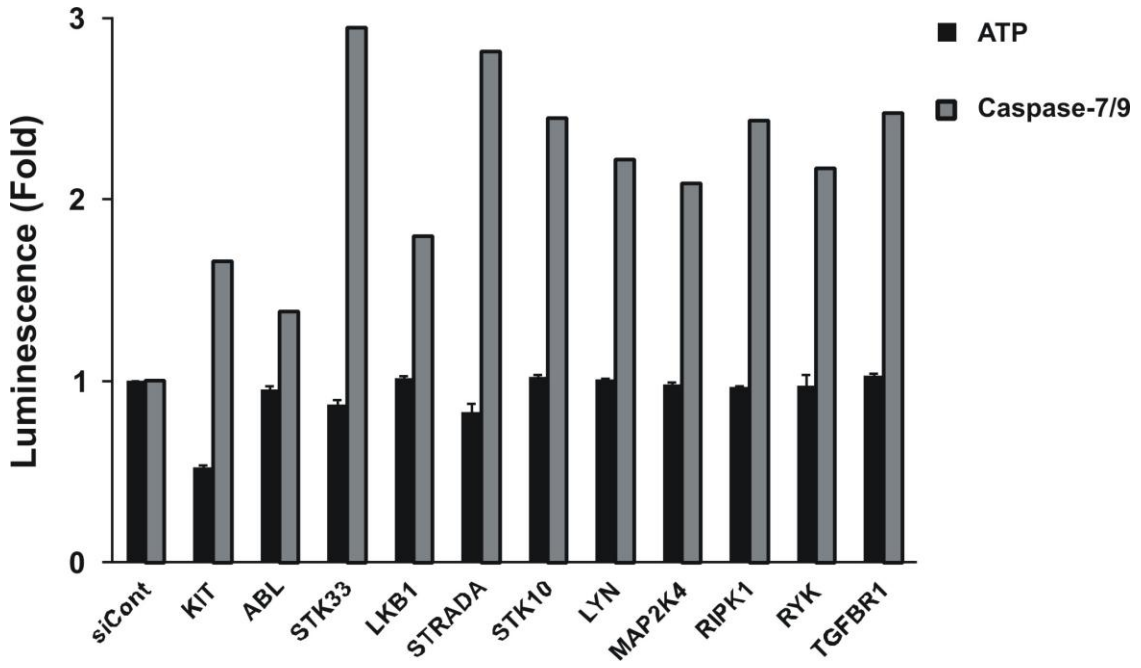

Figure 45: Transient knockdown of 10 hits leads to increased cell death.

Cells were transfected with indicated siRNA using Amaxa nucleofection technology. Cellular proliferation (ATP) and apoptosis (Caspase-7/9) were assessed 72 h and 48h post transfection respectively, using Cell-Titer-GLO and Caspase-GLO, respectively.

C.5 DISCUSSION

Surgical intervention remains the first line of therapy in newly diagnosed GIST patients. In the case of patients with unresectable or metastatic disease where surgical intervention is not an option, Imatinib mesylate is the first line of therapy. [182]. While initial response rates are very promising, nearly half of patients initially responsive to therapy will become resistant to it within 24 months of initial treatment due to secondary mutations in KIT [147]. In light of this we aimed to determine if inhibition of other kinases besides KIT could result in GIST cell death. Following a small preliminary siRNA based screen we identified the SRC family kinase, LYN as a potential therapeutic target. Inhibition of LYN led to reduced cell proliferation and increased cell death levels comparable to KIT inhibition when measured by ATP and caspases based luminescence assays respectively. Furthermore, reduced cell proliferation and increased cell cycle arrest were confirmed by reduced BrdU incorporation and increased $p27^{Kip1}$ expression respectively. Further studies on the role of LYN in GIST cell survival and proliferation will need to be conducted to determine its potential as a therapeutic target.

Following identification of a kinase besides KIT being involved in GIST cell survival and proliferation we aimed to expand our search of new druggable targets by performing a siRNA screen of the entire human kinome. The preliminary screen produced 65 hits, which were verified and reduced to 37 hits through a secondary screen using alternative siRNA sequences. These 37 hits were then reduced to 10 and follow up experiments were performed. The treatment of Imatinib-resistant GIST patients has proven difficult, resulting in abysmal 5-year

survival rates [269]. Identifying potential new therapeutic targets will aid in development of new drugs that could prove invaluable to patients unresponsive to current therapies.

BIBLIOGRAPHY

1. Ferlay, J., et al., *Estimates of worldwide burden of cancer in 2008: GLOBOCAN 2008.* International journal of cancer. Journal international du cancer, 2010. **127**(12): p. 2893-2917.
2. Parkin, D., et al., *Global cancer statistics, 2002.* CA: a cancer journal for clinicians, 2005. **55**(2): p. 74-108.
3. American Cancer Society, I., *Cancer Facts & Figures 2013,* A.C. Society, Editor. 2013: Altanta, GA.
4. American Cancer Society, I. *Colorectal Cancer* 2013 01/17/2013 [cited 2013 07/16/2013]; Colorectal Cancer]. Available from: http://www.cancer.org/cancer/colonandrectumcancer/detailedguide/colorectal-cancer-survival-rates.
5. Brändstedt, J., et al., *Gender, anthropometric factors and risk of colorectal cancer with particular reference to tumour location and TNM stage: a cohort study.* Biology of sex differences, 2012. **3**(1): p. 23.
6. Boyle, T., et al., *Physical activity and risks of proximal and distal colon cancers: a systematic review and meta-analysis.* Journal of the National Cancer Institute, 2012. **104**(20): p. 1548-1561.
7. Kharazmi, E., et al., *Familial risk of early and late onset cancer: nationwide prospective cohort study.* BMJ (Clinical research ed.), 2012. **345**.
8. O'Brien, M.J., et al., *The National Polyp Study. Patient and polyp characteristics associated with high-grade dysplasia in colorectal adenomas.* Gastroenterology, 1990. **98**(2): p. 371-9.
9. Benson, A., *Epidemiology, disease progression, and economic burden of colorectal cancer.* Journal of managed care pharmacy : JMCP, 2007. **13**(6 Suppl C): p. 18.
10. Health, N.I.o. *Genetics of Colorectal Cancer (PDQ®)*. National Cancer Institute at the National Institutes of Health 2013 July 25, 2013 [cited 2013 September 15, 2013].
11. Institute, N.C. *Colon Cancer Genes*. 2013 07/25/2013 08/18/2013].
12. Vogelstein, B. and K. Kinzler, *Cancer genes and the pathways they control.* Nature medicine, 2004. **10**(8): p. 789-799.
13. Liang, J., et al., *APC polymorphisms and the risk of colorectal neoplasia: a HuGE review and meta-analysis.* American journal of epidemiology, 2013. **177**(11): p. 1169-1179.
14. Tomeo, C.A., et al., *Harvard Report on Cancer Prevention. Volume 3: prevention of colon cancer in the United States.* Cancer Causes Control, 1999. **10**(3): p. 167-80.
15. Hanahan, D. and R.A. Weinberg, *Hallmarks of cancer: the next generation.* Cell, 2011. **144**(5): p. 646-74.

16. Taipale, J. and P. Beachy, *The Hedgehog and Wnt signalling pathways in cancer.* Nature, 2001. **411**(6835): p. 349-354.
17. Morin, P.J., et al., *Activation of beta-catenin-Tcf signaling in colon cancer by mutations in beta-catenin or APC.* Science, 1997. **275**(5307): p. 1787-90.
18. Ying, H., et al., *Oncogenic Kras maintains pancreatic tumors through regulation of anabolic glucose metabolism.* Cell, 2012. **149**(3): p. 656-670.
19. Phipps, A., et al., *KRAS-mutation status in relation to colorectal cancer survival: the joint impact of correlated tumour markers.* British journal of cancer, 2013. **108**(8): p. 1757-1764.
20. Misale, S., et al., *Emergence of KRAS mutations and acquired resistance to anti-EGFR therapy in colorectal cancer.* Nature, 2012. **486**(7404): p. 532-536.
21. Arrington, A., et al., *Prognostic and Predictive Roles of KRAS Mutation in Colorectal Cancer.* International journal of molecular sciences, 2012. **13**(10): p. 12153-12168.
22. Tan, C. and X. Du, *KRAS mutation testing in metastatic colorectal cancer.* World journal of gastroenterology : WJG, 2012. **18**(37): p. 5171-5180.
23. Grady, W.M., et al., *Mutational inactivation of transforming growth factor beta receptor type II in microsatellite stable colon cancers.* Cancer Res, 1999. **59**(2): p. 320-4.
24. Parsons, R., et al., *Microsatellite instability and mutations of the transforming growth factor beta type II receptor gene in colorectal cancer.* Cancer Res, 1995. **55**(23): p. 5548-50.
25. Markowitz, S., et al., *Inactivation of the type II TGF-beta receptor in colon cancer cells with microsatellite instability.* Science, 1995. **268**(5215): p. 1336-8.
26. Myeroff, L.L., et al., *A transforming growth factor beta receptor type II gene mutation common in colon and gastric but rare in endometrial cancers with microsatellite instability.* Cancer Res, 1995. **55**(23): p. 5545-7.
27. Hollstein, M., et al., *p53 mutations in human cancers.* Science, 1991. **253**(5015): p. 49-53.
28. el-Deiry, W.S., *Regulation of p53 downstream genes.* Semin Cancer Biol, 1998. **8**(5): p. 345-57.
29. Yu, J. and L. Zhang, *PUMA, a potent killer with or without p53.* Oncogene, 2008. **27 Suppl 1**: p. 83.
30. Iacopetta, B., *TP53 mutation in colorectal cancer.* Hum Mutat, 2003. **21**(3): p. 271-6.
31. Rodrigues, N.R., et al., *p53 mutations in colorectal cancer.* Proc Natl Acad Sci U S A, 1990. **87**(19): p. 7555-9.
32. Goh, H.S., J. Yao, and D.R. Smith, *p53 point mutation and survival in colorectal cancer patients.* Cancer Res, 1995. **55**(22): p. 5217-21.
33. Freed-Pastor, W.A. and C. Prives, *Mutant p53: one name, many proteins.* Genes Dev, 2012. **26**(12): p. 1268-86.
34. Spaderna, S., et al., *A transient, EMT-linked loss of basement membranes indicates metastasis and poor survival in colorectal cancer.* Gastroenterology, 2006. **131**(3): p. 830-40.
35. Mysliwiec, A.G. and D.L. Ornstein, *Matrix metalloproteinases in colorectal cancer.* Clin Colorectal Cancer, 2002. **1**(4): p. 208-19.
36. Gulhati, P., et al., *mTORC1 and mTORC2 regulate EMT, motility, and metastasis of colorectal cancer via RhoA and Rac1 signaling pathways.* Cancer Res, 2011. **71**(9): p. 3246-56.

37. Warburg, O., *On respiratory impairment in cancer cells.* Science, 1956. **124**(3215): p. 269-70.
38. Hsu, P. and D. Sabatini, *Cancer cell metabolism: Warburg and beyond.* Cell, 2008. **134**(5): p. 703-707.
39. Ward, P. and C. Thompson, *Metabolic reprogramming: a cancer hallmark even warburg did not anticipate.* Cancer cell, 2012. **21**(3): p. 297-308.
40. Altenberg, B. and K. Greulich, *Genes of glycolysis are ubiquitously overexpressed in 24 cancer classes.* Genomics, 2004. **84**(6): p. 1014-1020.
41. Wu, W. and S. Zhao, *Metabolic changes in cancer: beyond the Warburg effect.* Acta biochimica et biophysica Sinica, 2013. **45**(1): p. 18-26.
42. Bensaad, K. and K. Vousden, *p53: new roles in metabolism.* Trends in cell biology, 2007. **17**(6): p. 286-291.
43. Wise, D., et al., *Myc regulates a transcriptional program that stimulates mitochondrial glutaminolysis and leads to glutamine addiction.* Proceedings of the National Academy of Sciences of the United States of America, 2008. **105**(48): p. 18782-18787.
44. Dang, C., A. Le, and P. Gao, *MYC-induced cancer cell energy metabolism and therapeutic opportunities.* Clinical cancer research : an official journal of the American Association for Cancer Research, 2009. **15**(21): p. 6479-6483.
45. Dang, C., *Rethinking the Warburg effect with Myc micromanaging glutamine metabolism.* Cancer research, 2010. **70**(3): p. 859-862.
46. Ortega, A., et al., *Glucose avidity of carcinomas.* Cancer letters, 2009. **276**(2): p. 125-135.
47. Wise, D. and C. Thompson, *Glutamine addiction: a new therapeutic target in cancer.* Trends in biochemical sciences, 2010. **35**(8): p. 427-433.
48. Lopez-Rios, F., et al., *Loss of the Mitochondrial Bioenergetic Capacity Underlies the Glucose Avidity of Carcinomas.* Cancer research, 2007. **67**.
49. Kroemer, G. and J. Pouyssegur, *Tumor cell metabolism: cancer's Achilles' heel.* Cancer cell, 2008. **13**(6): p. 472-482.
50. Chatterjee, A., E. Mambo, and D. Sidransky, *Mitochondrial DNA mutations in human cancer.* Oncogene, 2006. **25**(34): p. 4663-74.
51. Brandon, M., P. Baldi, and D. Wallace, *Mitochondrial mutations in cancer.* Oncogene, 2006. **25**(34): p. 4647-4662.
52. Zhou, S., et al., *Frequency and phenotypic implications of mitochondrial DNA mutations in human squamous cell cancers of the head and neck.* Proceedings of the National Academy of Sciences of the United States of America, 2007. **104**(18): p. 7540-7545.
53. Gogvadze, V., S. Orrenius, and B. Zhivotovsky, *Mitochondria in cancer cells: what is so special about them?* Trends in cell biology, 2008. **18**(4): p. 165-173.
54. Pelicano, H., et al., *Mitochondrial respiration defects in cancer cells cause activation of Akt survival pathway through a redox-mediated mechanism.* J Cell Biol, 2006. **175**(6): p. 913-23.
55. Fulda, S. and K.M. Debatin, *Extrinsic versus intrinsic apoptosis pathways in anticancer chemotherapy.* Oncogene, 2006. **25**(34): p. 4798-811.
56. Ashkenazi, A., *Targeting the extrinsic apoptosis pathway in cancer.* Cytokine Growth Factor Rev, 2008. **19**(3-4): p. 325-31.
57. Yu…, J., *Apoptosis in human cancer cells.* Current opinion in oncology, 2004.

58. Adams, J.M. and S. Cory, *The Bcl-2 apoptotic switch in cancer development and therapy.* Oncogene, 2007. **26**(9): p. 1324-37.
59. Yu, J. and L. Zhang, *Apoptosis in human cancer cells.* Curr Opin Oncol, 2004. **16**(1): p. 19-24.
60. Vousden, K.H. and X. Lu, *Live or let die: the cell's response to p53.* Nat Rev Cancer, 2002. **2**(8): p. 594-604.
61. Yu, J. and L. Zhang, *The transcriptional targets of p53 in apoptosis control.* Biochem Biophys Res Commun, 2005. **331**(3): p. 851-8.
62. Chipuk, J.E. and D.R. Green, *How do BCL-2 proteins induce mitochondrial outer membrane permeabilization?* Trends Cell Biol, 2008. **18**(4): p. 157-64.
63. Wang, X., *The expanding role of mitochondria in apoptosis.* Genes Dev, 2001. **15**(22): p. 2922-33.
64. Du, C., et al., *Smac, a mitochondrial protein that promotes cytochrome c-dependent caspase activation by eliminating IAP inhibition.* Cell, 2000. **102**(1): p. 33-42.
65. Suzuki, Y., et al., *A serine protease, HtrA2, is released from the mitochondria and interacts with XIAP, inducing cell death.* Mol Cell, 2001. **8**(3): p. 613-21.
66. Joza, N., et al., *Essential role of the mitochondrial apoptosis-inducing factor in programmed cell death.* Nature, 2001. **410**(6828): p. 549-54.
67. Wang, X., et al., *Mechanisms of AIF-mediated apoptotic DNA degradation in Caenorhabditis elegans.* Science, 2002. **298**(5598): p. 1587-92.
68. Luo, X., et al., *Bid, a Bcl2 interacting protein, mediates cytochrome c release from mitochondria in response to activation of cell surface death receptors.* Cell, 1998. **94**(4): p. 481-90.
69. Li, H., et al., *Cleavage of BID by caspase 8 mediates the mitochondrial damage in the Fas pathway of apoptosis.* Cell, 1998. **94**(4): p. 491-501.
70. Bouillet, P. and A. Strasser, *BH3-only proteins - evolutionarily conserved proapoptotic Bcl-2 family members essential for initiating programmed cell death.* J Cell Sci, 2002. **115**(Pt 8): p. 1567-74.
71. Korsmeyer, S.J., *BCL-2 gene family and the regulation of programmed cell death.* Cancer Res, 1999. **59**(7 Suppl): p. 1693s-1700s.
72. Wyllie, A.H., J.F. Kerr, and A.R. Currie, *Cell death: the significance of apoptosis.* Int Rev Cytol, 1980. **68**: p. 251-306.
73. Kerr, J.F., A.H. Wyllie, and A.R. Currie, *Apoptosis: a basic biological phenomenon with wide-ranging implications in tissue kinetics.* Br J Cancer, 1972. **26**(4): p. 239-57.
74. Kerr, J.F., C.M. Winterford, and B.V. Harmon, *Apoptosis. Its significance in cancer and cancer therapy.* Cancer, 1994. **73**(8): p. 2013-26.
75. Boatright, K. and G. Salvesen, *Mechanisms of caspase activation.* Current opinion in cell biology, 2003. **15**(6): p. 725-731.
76. Renatus, M., et al., *Dimer formation drives the activation of the cell death protease caspase 9.* Proceedings of the National Academy of Sciences of the United States of America, 2001. **98**(25): p. 14250-14255.
77. Pop, C., et al., *Role of proteolysis in caspase-8 activation and stabilization.* Biochemistry, 2007. **46**(14): p. 4398-4407.
78. Pop, C. and G.S. Salvesen, *Human caspases: activation, specificity, and regulation.* J Biol Chem, 2009. **284**(33): p. 21777-81.

79. Slee, E., et al., *Ordering the cytochrome c-initiated caspase cascade: hierarchical activation of caspases-2, -3, -6, -7, -8, and -10 in a caspase-9-dependent manner.* The Journal of cell biology, 1999. **144**(2): p. 281-292.
80. Yang, S., et al., *Caspase-3 mediated feedback activation of apical caspases in doxorubicin and TNF-alpha induced apoptosis.* Apoptosis : an international journal on programmed cell death, 2006. **11**(11): p. 1987-1997.
81. Aouad, S., et al., *Caspase-3 is a component of Fas death-inducing signaling complex in lipid rafts and its activity is required for complete caspase-8 activation during Fas-mediated cell death.* Journal of immunology (Baltimore, Md. : 1950), 2004. **172**(4): p. 2316-2323.
82. Janzen, V., et al., *Hematopoietic stem cell responsiveness to exogenous signals is limited by caspase-3.* Cell stem cell, 2008. **2**(6): p. 584-594.
83. Mukerjee, N., et al., *Caspase-mediated calcineurin activation contributes to IL-2 release during T cell activation.* Biochemical and biophysical research communications, 2001. **285**(5): p. 1192-1199.
84. Acarin, L., et al., *Caspase-3 activation in astrocytes following postnatal excitotoxic damage correlates with cytoskeletal remodeling but not with cell death or proliferation.* Glia, 2007. **55**(9): p. 954-965.
85. Gulyaeva, N., *Non-apoptotic functions of caspase-3 in nervous tissue.* Biochemistry. Biokhimiia, 2003. **68**(11): p. 1171-1180.
86. Naarmann-de Vries, I., et al., *Caspase-3 cleaves hnRNP K in erythroid differentiation.* Cell death & disease, 2013. **4**.
87. LaCasse, E.C., et al., *IAP-targeted therapies for cancer.* Oncogene, 2008. **27**(48): p. 6252-75.
88. Fulda, S. and D. Vucic, *Targeting IAP proteins for therapeutic intervention in cancer.* Nat Rev Drug Discov, 2012. **11**(2): p. 109-24.
89. Keats, J.J., et al., *Promiscuous mutations activate the noncanonical NF-kappaB pathway in multiple myeloma.* Cancer Cell, 2007. **12**(2): p. 131-44.
90. Yuan, S. and C. Akey, *Apoptosome structure, assembly, and procaspase activation.* Structure (London, England : 1993), 2013. **21**(4): p. 501-515.
91. Cain, K., et al., *Apaf-1 oligomerizes into biologically active approximately 700-kDa and inactive approximately 1.4-MDa apoptosome complexes.* The Journal of biological chemistry, 2000. **275**(9): p. 6067-6070.
92. Hughes, M.A., et al., *Reconstitution of the death-inducing signaling complex reveals a substrate switch that determines CD95-mediated death or survival.* Mol Cell, 2009. **35**(3): p. 265-79.
93. Tinel, A. and J. Tschopp, *The PIDDosome, a protein complex implicated in activation of caspase-2 in response to genotoxic stress.* Science (New York, N.Y.), 2004. **304**(5672): p. 843-846.
94. Vakifahmetoglu, H., et al., *Functional connection between p53 and caspase-2 is essential for apoptosis induced by DNA damage.* Oncogene, 2006. **25**(41): p. 5683-92.
95. Mizushima, N., *Methods for monitoring autophagy.* Int J Biochem Cell Biol, 2004. **36**(12): p. 2491-502.
96. Sun, L., et al., *Mixed lineage kinase domain-like protein mediates necrosis signaling downstream of RIP3 kinase.* Cell, 2012. **148**(1-2): p. 213-227.

97. Wang, Z., et al., *The mitochondrial phosphatase PGAM5 functions at the convergence point of multiple necrotic death pathways.* Cell, 2012. **148**(1-2): p. 228-243.
98. Laster, S., J. Wood, and L. Gooding, *Tumor necrosis factor can induce both apoptic and necrotic forms of cell lysis.* Journal of immunology (Baltimore, Md. : 1950), 1988. **141**(8): p. 2629-2634.
99. Vandenabeele, P., et al., *Molecular mechanisms of necroptosis: an ordered cellular explosion.* Nature reviews. Molecular cell biology, 2010. **11**(10): p. 700-714.
100. Hsu, H., et al., *TNF-dependent recruitment of the protein kinase RIP to the TNF receptor-1 signaling complex.* Immunity, 1996. **4**(4): p. 387-96.
101. Holler, N., et al., *Fas triggers an alternative, caspase-8-independent cell death pathway using the kinase RIP as effector molecule.* Nat Immunol, 2000. **1**(6): p. 489-95.
102. Cho, Y.S., et al., *Phosphorylation-driven assembly of the RIP1-RIP3 complex regulates programmed necrosis and virus-induced inflammation.* Cell, 2009. **137**(6): p. 1112-23.
103. He, S., et al., *Receptor interacting protein kinase-3 determines cellular necrotic response to TNF-alpha.* Cell, 2009. **137**(6): p. 1100-1111.
104. Zhang, D.W., et al., *RIP3, an energy metabolism regulator that switches TNF-induced cell death from apoptosis to necrosis.* Science, 2009. **325**(5938): p. 332-6.
105. Goossens, V., et al., *Regulation of tumor necrosis factor-induced, mitochondria- and reactive oxygen species-dependent cell death by the electron flux through the electron transport chain complex I.* Antioxid Redox Signal, 1999. **1**(3): p. 285-95.
106. Kim, Y.S., et al., *TNF-induced activation of the Nox1 NADPH oxidase and its role in the induction of necrotic cell death.* Mol Cell, 2007. **26**(5): p. 675-87.
107. Yazdanpanah, B., et al., *Riboflavin kinase couples TNF receptor 1 to NADPH oxidase.* Nature, 2009. **460**(7259): p. 1159-63.
108. Hitomi, J., et al., *Identification of a molecular signaling network that regulates a cellular necrotic cell death pathway.* Cell, 2008. **135**(7): p. 1311-23.
109. Vercammen, D., et al., *Inhibition of caspases increases the sensitivity of L929 cells to necrosis mediated by tumor necrosis factor.* The Journal of experimental medicine, 1998. **187**(9): p. 1477-1485.
110. He, S., et al., *Receptor interacting protein kinase-3 determines cellular necrotic response to TNF-alpha.* Cell, 2009. **137**(6): p. 1100-11.
111. Goossens, V., J. Grooten, and W. Fiers, *The oxidative metabolism of glutamine. A modulator of reactive oxygen intermediate-mediated cytotoxicity of tumor necrosis factor in L929 fibrosarcoma cells.* J Biol Chem, 1996. **271**(1): p. 192-6.
112. Zong, W.X., et al., *Alkylating DNA damage stimulates a regulated form of necrotic cell death.* Genes Dev, 2004. **18**(11): p. 1272-82.
113. Temkin, V., et al., *Inhibition of ADP/ATP exchange in receptor-interacting protein-mediated necrosis.* Mol Cell Biol, 2006. **26**(6): p. 2215-25.
114. Schinzel, A.C., et al., *Cyclophilin D is a component of mitochondrial permeability transition and mediates neuronal cell death after focal cerebral ischemia.* Proc Natl Acad Sci U S A, 2005. **102**(34): p. 12005-10.
115. Nakagawa, T., et al., *Cyclophilin D-dependent mitochondrial permeability transition regulates some necrotic but not apoptotic cell death.* Nature, 2005. **434**(7033): p. 652-8.
116. Vanden Berghe, T., et al., *Necroptosis, necrosis and secondary necrosis converge on similar cellular disintegration features.* Cell Death Differ, 2010. **17**(6): p. 922-30.

117. Boya, P. and G. Kroemer, *Lysosomal membrane permeabilization in cell death.* Oncogene, 2008. **27**(50): p. 6434-51.
118. Kroemer, G., L. Galluzzi, and C. Brenner, *Mitochondrial membrane permeabilization in cell death.* Physiol Rev, 2007. **87**(1): p. 99-163.
119. Vercammen, D., et al., *Dual signaling of the Fas receptor: initiation of both apoptotic and necrotic cell death pathways.* The Journal of experimental medicine, 1998. **188**(5): p. 919-930.
120. Chan, F.K., et al., *A role for tumor necrosis factor receptor-2 and receptor-interacting protein in programmed necrosis and antiviral responses.* J Biol Chem, 2003. **278**(51): p. 51613-21.
121. Holler, N., et al., *Fas triggers an alternative, caspase-8-independent cell death pathway using the kinase RIP as effector molecule.* Nature immunology, 2000. **1**(6): p. 489-495.
122. Fiers, W., et al., *TNF-induced intracellular signaling leading to gene induction or to cytotoxicity by necrosis or by apoptosis.* J Inflamm, 1995. **47**(1-2): p. 67-75.
123. Martinon, F., et al., *NALP inflammasomes: a central role in innate immunity.* Semin Immunopathol, 2007. **29**(3): p. 213-29.
124. Kalai, M., et al., *Tipping the balance between necrosis and apoptosis in human and murine cells treated with interferon and dsRNA.* Cell death and differentiation, 2002. **9**(9): p. 981-994.
125. Lee, T.H., et al., *The death domain kinase RIP1 is essential for tumor necrosis factor alpha signaling to p38 mitogen-activated protein kinase.* Mol Cell Biol, 2003. **23**(22): p. 8377-85.
126. Zhang, H., et al., *RIP1-mediated AIP1 phosphorylation at a 14-3-3-binding site is critical for tumor necrosis factor-induced ASK1-JNK/p38 activation.* The Journal of biological chemistry, 2007. **282**(20): p. 14788-14796.
127. O'Donnell, M.A., et al., *Ubiquitination of RIP1 regulates an NF-kappaB-independent cell-death switch in TNF signaling.* Curr Biol, 2007. **17**(5): p. 418-24.
128. Meylan, E., et al., *RIP1 is an essential mediator of Toll-like receptor 3-induced NF-kappa B activation.* Nature immunology, 2004. **5**(5): p. 503-507.
129. Lee, T.H., et al., *The kinase activity of Rip1 is not required for tumor necrosis factor-alpha-induced IkappaB kinase or p38 MAP kinase activation or for the ubiquitination of Rip1 by Traf2.* J Biol Chem, 2004. **279**(32): p. 33185-91.
130. Festjens, N., et al., *RIP1, a kinase on the crossroads of a cell's decision to live or die.* Cell death and differentiation, 2007. **14**(3): p. 400-410.
131. Ea, C.K., et al., *Activation of IKK by TNFalpha requires site-specific ubiquitination of RIP1 and polyubiquitin binding by NEMO.* Mol Cell, 2006. **22**(2): p. 245-57.
132. Biton, S. and A. Ashkenazi, *NEMO and RIP1 control cell fate in response to extensive DNA damage via TNF-alpha feedforward signaling.* Cell, 2011. **145**(1): p. 92-103.
133. Yu, P.W., et al., *Identification of RIP3, a RIP-like kinase that activates apoptosis and NFkappaB.* Curr Biol, 1999. **9**(10): p. 539-42.
134. Moriwaki, K. and F.K. Chan, *RIP3: a molecular switch for necrosis and inflammation.* Genes Dev. **27**(15): p. 1640-9.
135. Waris, G. and H. Ahsan, *Reactive oxygen species: role in the development of cancer and various chronic conditions.* Journal of carcinogenesis, 2006. **5**: p. 14.
136. Schumacker, P., *Reactive oxygen species in cancer cells: live by the sword, die by the sword.* Cancer cell, 2006. **10**(3): p. 175-176.

137. Jacobson, M., *Reactive oxygen species and programmed cell death.* Trends in biochemical sciences, 1996.
138. Matthews, N., et al., *Tumour cell killing by tumour necrosis factor: inhibition by anaerobic conditions, free-radical scavengers and inhibitors of arachidonate metabolism.* Immunology, 1987. **62**(1): p. 153-5.
139. Schulze-Osthoff, K., et al., *Cytotoxic activity of tumor necrosis factor is mediated by early damage of mitochondrial functions. Evidence for the involvement of mitochondrial radical generation.* J Biol Chem, 1992. **267**(8): p. 5317-23.
140. Samali, A., et al., *A comparative study of apoptosis and necrosis in HepG2 cells: oxidant-induced caspase inactivation leads to necrosis.* Biochem Biophys Res Commun, 1999. **255**(1): p. 6-11.
141. Festjens, N., T. Vanden Berghe, and P. Vandenabeele, *Necrosis, a well-orchestrated form of cell demise: signalling cascades, important mediators and concomitant immune response.* Biochim Biophys Acta, 2006. **1757**(9-10): p. 1371-87.
142. Vandenabeele, P., et al., *The role of the kinases RIP1 and RIP3 in TNF-induced necrosis.* Science signaling, 2010. **3**(115).
143. Denecker, G., et al., *Death receptor-induced apoptotic and necrotic cell death: differential role of caspases and mitochondria.* Cell Death Differ, 2001. **8**(8): p. 829-40.
144. Tenev, T., et al., *The Ripoptosome, a signaling platform that assembles in response to genotoxic stress and loss of IAPs.* Molecular cell, 2011. **43**(3): p. 432-448.
145. Bertrand, M. and P. Vandenabeele, *The Ripoptosome: death decision in the cytosol.* Molecular cell, 2011. **43**(3): p. 323-325.
146. Feoktistova, M., et al., *Pick your poison: the Ripoptosome, a cell death platform regulating apoptosis and necroptosis.* Cell cycle (Georgetown, Tex.), 2012. **11**(3): p. 460-467.
147. Wang, P., et al., *microRNA-21 negatively regulates Cdc25A and cell cycle progression in colon cancer cells.* Cancer Res, 2009. **69**(20): p. 8157-65.
148. Tang, J., et al., *Bioenergetic Metabolites Regulate Base Excision Repair-Dependent Cell Death in Response to DNA Damage.* Molecular Cancer Research, 2010. **8**(1): p. 67-79.
149. Kohli, M., et al., *SMAC/Diablo-dependent apoptosis induced by nonsteroidal antiinflammatory drugs (NSAIDs) in colon cancer cells.* Proc Natl Acad Sci U S A, 2004. **101**(48): p. 16897-902.
150. Wickline, E., et al., *γ-Catenin at adherens junctions: mechanism and biologic implications in hepatocellular cancer after β-catenin knockdown.* Neoplasia (New York, N.Y.), 2013. **15**(4): p. 421-434.
151. Graves, J., et al., *Mitochondrial structure, function and dynamics are temporally controlled by c-Myc.* PloS one, 2012. **7**(5).
152. Dagda, R.K., et al., *Loss of PINK1 function promotes mitophagy through effects on oxidative stress and mitochondrial fission.* J Biol Chem, 2009. **284**(20): p. 13843-55.
153. Kotas, M.E., et al., *Role of caspase-1 in regulation of triglyceride metabolism.* Proc Natl Acad Sci U S A, 2013. **110**(12): p. 4810-5.
154. Mandal, D., et al., *Caspase 3-mediated proteolysis of the N-terminal cytoplasmic domain of the human erythroid anion exchanger 1 (band 3).* J Biol Chem, 2003. **278**(52): p. 52551-8.

155. Galtieri, A., et al., *Resveratrol treatment induces redox stress in red blood cells: a possible role of caspase 3 in metabolism and anion transport.* Biol Chem, 2010. **391**(9): p. 1057-65.
156. Ngoh, G.A., K.N. Papanicolaou, and K. Walsh, *Loss of mitofusin 2 promotes endoplasmic reticulum stress.* J Biol Chem, 2012. **287**(24): p. 20321-32.
157. Chen, Y. and G. Dorn, *PINK1-phosphorylated mitofusin 2 is a Parkin receptor for culling damaged mitochondria.* Science (New York, N.Y.), 2013. **340**(6131): p. 471-475.
158. Yin, X.-M. and W.-X. Ding, *The reciprocal roles of PARK2 and mitofusins in mitophagy and mitochondrial spheroid formation.* Autophagy, 2013. **9**(11): p. 1687-1692.
159. Tanaka, A., *Parkin-mediated selective mitochondrial autophagy, mitophagy: Parkin purges damaged organelles from the vital mitochondrial network.* FEBS letters, 2010. **584**(7): p. 1386-1392.
160. Yu, J. and L. Zhang, *Apoptosis in human cancer cells.* Current opinion in oncology, 2004.
161. Johnstone, R.W., A.A. Ruefli, and S.W. Lowe, *Apoptosis: a link between cancer genetics and chemotherapy.* Cell, 2002. **108**(2): p. 153-64.
162. Huang, Q., et al., *Caspase 3-mediated stimulation of tumor cell repopulation during cancer radiotherapy.* Nature medicine, 2011. **17**(7): p. 860-866.
163. Laster, S.M., J.G. Wood, and L.R. Gooding, *Tumor necrosis factor can induce both apoptic and necrotic forms of cell lysis.* J Immunol, 1988. **141**(8): p. 2629-34.
164. Cho, Y., et al., *Phosphorylation-driven assembly of the RIP1-RIP3 complex regulates programmed necrosis and virus-induced inflammation.* Cell, 2009. **137**(6): p. 1112-1123.
165. Declercq, W., T. Vanden Berghe, and P. Vandenabeele, *RIP kinases at the crossroads of cell death and survival.* Cell, 2009. **138**(2): p. 229-232.
166. Mocarski, E.S., J.W. Upton, and W.J. Kaiser, *Viral infection and the evolution of caspase 8-regulated apoptotic and necrotic death pathways.* Nat Rev Immunol, 2012. **12**(2): p. 79-88.
167. Kaiser, W., et al., *RIP3 mediates the embryonic lethality of caspase-8-deficient mice.* Nature, 2011. **471**(7338): p. 368-372.
168. Green, D., et al., *RIPK-dependent necrosis and its regulation by caspases: a mystery in five acts.* Molecular cell, 2011. **44**(1): p. 9-16.
169. Zhang, D.W., et al., *RIP3, an Energy Metabolism Regulator That Switches TNF-Induced Cell Death from Apoptosis to Necrosis.* Science, 2009. **325**(5938): p. 332-336.
170. Upton, J., W. Kaiser, and E. Mocarski, *Virus inhibition of RIP3-dependent necrosis.* Cell host & microbe, 2010. **7**(4): p. 302-313.
171. Delavallee, L., et al., *AIF-mediated caspase-independent necroptosis: a new chance for targeted therapeutics.* IUBMB Life, 2011. **63**(4): p. 221-32.
172. Sun, Q., et al., *Chemosensitization of head and neck cancer cells by PUMA.* Mol Cancer Ther, 2007. **6**(12): p. 3180-8.
173. Yu, J., et al., *PUMA mediates the apoptotic response to p53 in colorectal cancer cells.* Proceedings of the National Academy of Sciences of the United States of America, 2003. **100**(4): p. 1931-1936.
174. Ming, L., et al., *PUMA Dissociates Bax and Bcl-X(L) to induce apoptosis in colon cancer cells.* The Journal of biological chemistry, 2006. **281**(23): p. 16034-16042.
175. Sun, Q., et al., *PUMA mediates EGFR tyrosine kinase inhibitor-induced apoptosis in head and neck cancer cells.* Oncogene, 2009. **28**(24): p. 2348-57.

176. Dudgeon, C., et al., *PUMA induction by FoxO3a mediates the anticancer activities of the broad-range kinase inhibitor UCN-01.* Mol Cancer Ther, 2010. **9**(11): p. 2893-902.
177. Leibowitz, B.J., et al., *Uncoupling p53 functions in radiation-induced intestinal damage via PUMA and p21.* Mol Cancer Res, 2011. **9**(5): p. 616-25.
178. Scaffidi, P., T. Misteli, and M.E. Bianchi, *Release of chromatin protein HMGB1 by necrotic cells triggers inflammation.* Nature, 2002. **418**(6894): p. 191-5.
179. Stennicke, H. and G. Salvesen, *Biochemical characteristics of caspases-3, -6, -7, and -8.* The Journal of biological chemistry, 1997. **272**(41): p. 25719-25723.
180. Zhang, D.-W., et al., *Multiple death pathways in TNF-treated fibroblasts: RIP3- and RIP1-dependent and independent routes.* Cell research, 2011. **21**(2): p. 368-371.
181. Khalil, H., et al., *Caspase-3 protects stressed organs against cell death.* Molecular and cellular biology, 2012. **32**(22): p. 4523-4533.
182. O'Donnell, M.A. and A.T. Ting, *RIP1 comes back to life as a cell death regulator in TNFR1 signaling.* FEBS J, 2011. **278**(6): p. 877-87.
183. Xie, T., et al., *Structural basis of RIP1 inhibition by necrostatins.* Structure (London, England : 1993), 2013. **21**(3): p. 493-499.
184. Olsson, M., et al., *DISC-mediated activation of caspase-2 in DNA damage-induced apoptosis.* Oncogene, 2009. **28**(18): p. 1949-59.
185. Bunz, F., et al., *Disruption of p53 in human cancer cells alters the responses to therapeutic agents.* J Clin Invest, 1999. **104**(3): p. 263-9.
186. Xu, R.H., et al., *Inhibition of glycolysis in cancer cells: a novel strategy to overcome drug resistance associated with mitochondrial respiratory defect and hypoxia.* Cancer Res, 2005. **65**(2): p. 613-21.
187. Krebs, H.A. and D. Bellamy, *The interconversion of glutamic acid and aspartic acid in respiring tissues.* Biochem J, 1960. **75**: p. 523-9.
188. Newsholme, E.A., B. Crabtree, and M.S. Ardawi, *The role of high rates of glycolysis and glutamine utilization in rapidly dividing cells.* Biosci Rep, 1985. **5**(5): p. 393-400.
189. DeBerardinis, R.J., et al., *Beyond aerobic glycolysis: transformed cells can engage in glutamine metabolism that exceeds the requirement for protein and nucleotide synthesis.* Proc Natl Acad Sci U S A, 2007. **104**(49): p. 19345-50.
190. Kurokawa, H., et al., *Alteration of caspase-3 (CPP32/Yama/apopain) in wild-type MCF-7, breast cancer cells.* Oncol Rep, 1999. **6**(1): p. 33-7.
191. Janicke, R.U., et al., *Caspase-3 is required for DNA fragmentation and morphological changes associated with apoptosis.* J Biol Chem, 1998. **273**(16): p. 9357-60.
192. Lukens, J., et al., *RIP1-driven autoinflammation targets IL-1α independently of inflammasomes and RIP3.* Nature, 2013.
193. Demetri, G.D., et al., *NCCN Task Force report: management of patients with gastrointestinal stromal tumor (GIST)--update of the NCCN clinical practice guidelines.* J Natl Compr Canc Netw, 2007. **5 Suppl 2**: p. S1-29; quiz S30.
194. Edmonson, J.H., et al., *Contrast of response to dacarbazine, mitomycin, doxorubicin, and cisplatin (DMAP) plus GM-CSF between patients with advanced malignant gastrointestinal stromal tumors and patients with other advanced leiomyosarcomas.* Cancer Invest, 2002. **20**(5-6): p. 605-12.
195. Lehnert, T., *Gastrointestinal sarcoma (GIST)--a review of surgical management.* Ann Chir Gynaecol, 1998. **87**(4): p. 297-305.

196. Emory, T.S., et al., *Prognosis of gastrointestinal smooth-muscle (stromal) tumors: dependence on anatomic site.* Am J Surg Pathol, 1999. **23**(1): p. 82-7.
197. Fletcher, C.D., et al., *Diagnosis of gastrointestinal stromal tumors: A consensus approach.* Hum Pathol, 2002. **33**(5): p. 459-65.
198. Hirota, S., et al., *Gain-of-function mutations of c-kit in human gastrointestinal stromal tumors.* Science, 1998. **279**(5350): p. 577-80.
199. Huizinga, J.D., et al., *W/kit gene required for interstitial cells of Cajal and for intestinal pacemaker activity.* Nature, 1995. **373**(6512): p. 347-9.
200. Robinson, T.L., et al., *Gastrointestinal stromal tumors may originate from a subset of CD34-positive interstitial cells of Cajal.* Am J Pathol, 2000. **156**(4): p. 1157-63.
201. Kindblom, L.G., et al., *Gastrointestinal pacemaker cell tumor (GIPACT): gastrointestinal stromal tumors show phenotypic characteristics of the interstitial cells of Cajal.* Am J Pathol, 1998. **152**(5): p. 1259-69.
202. Ma, Y., et al., *Clustering of activating mutations in c-KIT's juxtamembrane coding region in canine mast cell neoplasms.* J Invest Dermatol, 1999. **112**(2): p. 165-70.
203. Kimura, A., et al., *c-kit Point mutation in patients with myeloproliferative disorders.* Leuk Lymphoma, 1997. **25**(3-4): p. 281-7.
204. Gari, M., et al., *c-kit proto-oncogene exon 8 in-frame deletion plus insertion mutations in acute myeloid leukaemia.* Br J Haematol, 1999. **105**(4): p. 894-900.
205. Nakahara, M., et al., *A novel gain-of-function mutation of c-kit gene in gastrointestinal stromal tumors.* Gastroenterology, 1998. **115**(5): p. 1090-5.
206. Lasota, J., et al., *Mutations in exon 11 of c-Kit occur preferentially in malignant versus benign gastrointestinal stromal tumors and do not occur in leiomyomas or leiomyosarcomas.* Am J Pathol, 1999. **154**(1): p. 53-60.
207. Lasota, J., et al., *Mutations in exons 9 and 13 of KIT gene are rare events in gastrointestinal stromal tumors. A study of 200 cases.* Am J Pathol, 2000. **157**(4): p. 1091-5.
208. Lux, M.L., et al., *KIT extracellular and kinase domain mutations in gastrointestinal stromal tumors.* Am J Pathol, 2000. **156**(3): p. 791-5.
209. Rubin, B.P., et al., *KIT activation is a ubiquitous feature of gastrointestinal stromal tumors.* Cancer Res, 2001. **61**(22): p. 8118-21.
210. Hirota, S., et al., *Gain-of-function mutation at the extracellular domain of KIT in gastrointestinal stromal tumours.* J Pathol, 2001. **193**(4): p. 505-10.
211. Wardelmann, E., et al., *c-kit mutations in gastrointestinal stromal tumors occur preferentially in the spindle rather than in the epithelioid cell variant.* Mod Pathol, 2002. **15**(2): p. 125-36.
212. Stenman, G., A. Eriksson, and L. Claesson-Welsh, *Human PDGFA receptor gene maps to the same region on chromosome 4 as the KIT oncogene.* Genes Chromosomes Cancer, 1989. **1**(2): p. 155-8.
213. Hubbard, S.R., *Juxtamembrane autoinhibition in receptor tyrosine kinases.* Nat Rev Mol Cell Biol, 2004. **5**(6): p. 464-71.
214. Pawson, T., *Regulation and targets of receptor tyrosine kinases.* Eur J Cancer, 2002. **38 Suppl 5**: p. S3-10.
215. Majumder, S., et al., *c-kit protein, a transmembrane kinase: identification in tissues and characterization.* Mol Cell Biol, 1988. **8**(11): p. 4896-903.

216. Nocka, K., et al., *Expression of c-kit gene products in known cellular targets of W mutations in normal and W mutant mice--evidence for an impaired c-kit kinase in mutant mice.* Genes Dev, 1989. **3**(6): p. 816-26.
217. Torihashi, S., et al., *c-kit-dependent development of interstitial cells and electrical activity in the murine gastrointestinal tract.* Cell Tissue Res, 1995. **280**(1): p. 97-111.
218. Ashman, L.K., et al., *Expression of the YB5.B8 antigen (c-kit proto-oncogene product) in normal human bone marrow*. Blood, 1991. **78**(1): p. 30-7.
219. Huang, E., et al., *The hematopoietic growth factor KL is encoded by the Sl locus and is the ligand of the c-kit receptor, the gene product of the W locus.* Cell, 1990. **63**(1): p. 225-33.
220. Nocka, K., et al., *Candidate ligand for the c-kit transmembrane kinase receptor: KL, a fibroblast derived growth factor stimulates mast cells and erythroid progenitors.* EMBO J, 1990. **9**(10): p. 3287-94.
221. Flanagan, J.G. and P. Leder, *The kit ligand: a cell surface molecule altered in steel mutant fibroblasts.* Cell, 1990. **63**(1): p. 185-94.
222. Anderson, D.M., et al., *Molecular cloning of mast cell growth factor, a hematopoietin that is active in both membrane bound and soluble forms.* Cell, 1990. **63**(1): p. 235-43.
223. Blume-Jensen, P., et al., *Activation of the human c-kit product by ligand-induced dimerization mediates circular actin reorganization and chemotaxis.* EMBO J, 1991. **10**(13): p. 4121-8.
224. Serve, H., Y.C. Hsu, and P. Besmer, *Tyrosine residue 719 of the c-kit receptor is essential for binding of the P85 subunit of phosphatidylinositol (PI) 3-kinase and for c-kit-associated PI 3-kinase activity in COS-1 cells.* J Biol Chem, 1994. **269**(8): p. 6026-30.
225. Linnekin, D., *Early signaling pathways activated by c-Kit in hematopoietic cells.* Int J Biochem Cell Biol, 1999. **31**(10): p. 1053-74.
226. Gramza, A.W., C.L. Corless, and M.C. Heinrich, *Resistance to Tyrosine Kinase Inhibitors in Gastrointestinal Stromal Tumors.* Clin Cancer Res, 2009. **15**(24): p. 7510-7518.
227. Ma, Y., et al., *Inhibition of spontaneous receptor phosphorylation by residues in a putative alpha-helix in the KIT intracellular juxtamembrane region.* J Biol Chem, 1999. **274**(19): p. 13399-402.
228. Medeiros, F., et al., *KIT-negative gastrointestinal stromal tumors: proof of concept and therapeutic implications.* Am J Surg Pathol, 2004. **28**(7): p. 889-94.
229. Heinrich, M.C., et al., *PDGFRA activating mutations in gastrointestinal stromal tumors.* Science, 2003. **299**(5607): p. 708-10.
230. Druker, B.J., et al., *Effects of a selective inhibitor of the Abl tyrosine kinase on the growth of Bcr-Abl positive cells.* Nat Med, 1996. **2**(5): p. 561-6.
231. Mol, C.D., et al., *Structural basis for the autoinhibition and STI-571 inhibition of c-Kit tyrosine kinase.* J Biol Chem, 2004. **279**(30): p. 31655-63.
232. Buchdunger, E., et al., *Abl protein-tyrosine kinase inhibitor STI571 inhibits in vitro signal transduction mediated by c-kit and platelet-derived growth factor receptors.* J Pharmacol Exp Ther, 2000. **295**(1): p. 139-45.
233. Joensuu, H., et al., *Effect of the tyrosine kinase inhibitor STI571 in a patient with a metastatic gastrointestinal stromal tumor.* N Engl J Med, 2001. **344**(14): p. 1052-6.
234. van Oosterom, A.T., et al., *Safety and efficacy of imatinib (STI571) in metastatic gastrointestinal stromal tumours: a phase I study.* Lancet, 2001. **358**(9291): p. 1421-3.

235. Demetri, G.D., et al., *Efficacy and safety of imatinib mesylate in advanced gastrointestinal stromal tumors.* N Engl J Med, 2002. **347**(7): p. 472-80.
236. Negri, T., et al., *T670X KIT mutations in gastrointestinal stromal tumors: making sense of missense.* J Natl Cancer Inst, 2009. **101**(3): p. 194-204.
237. Liegl, B., et al., *Heterogeneity of kinase inhibitor resistance mechanisms in GIST.* J Pathol, 2008. **216**(1): p. 64-74.
238. Miselli, F.C., et al., *c-Kit/PDGFRA gene status alterations possibly related to primary imatinib resistance in gastrointestinal stromal tumors.* Clin Cancer Res, 2007. **13**(8): p. 2369-77.
239. Sawyers, C.L., *Disabling Abl-perspectives on Abl kinase regulation and cancer therapeutics.* Cancer Cell, 2002. **1**(1): p. 13-5.
240. Whang, Y.E., et al., *c-Abl is required for development and optimal cell proliferation in the context of p53 deficiency.* Proc Natl Acad Sci U S A, 2000. **97**(10): p. 5486-91.
241. Plattner, R., et al., *c-Abl is activated by growth factors and Src family kinases and has a role in the cellular response to PDGF.* Genes Dev, 1999. **13**(18): p. 2400-11.
242. Cong, F. and S.P. Goff, *c-Abl-induced apoptosis, but not cell cycle arrest, requires mitogen-activated protein kinase kinase 6 activation.* Proc Natl Acad Sci U S A, 1999. **96**(24): p. 13819-24.
243. Nagar, B., et al., *Structural basis for the autoinhibition of c-Abl tyrosine kinase.* Cell, 2003. **112**(6): p. 859-71.
244. Hantschel, O., et al., *A myristoyl/phosphotyrosine switch regulates c-Abl.* Cell, 2003. **112**(6): p. 845-57.
245. Van Etten, R.A., *c-Abl regulation: a tail of two lipids.* Curr Biol, 2003. **13**(15): p. R608-10.
246. Van Etten, R.A., *Cycling, stressed-out and nervous: cellular functions of c-Abl.* Trends Cell Biol, 1999. **9**(5): p. 179-86.
247. Sirvent, A., C. Benistant, and S. Roche, *Cytoplasmic signalling by the c-Abl tyrosine kinase in normal and cancer cells.* Biol Cell, 2008. **100**(11): p. 617-31.
248. Srinivasan, D., D.M. Kaetzel, and R. Plattner, *Reciprocal regulation of Abl and receptor tyrosine kinases.* Cell Signal, 2009. **21**(7): p. 1143-50.
249. Gu, J.J., J.R. Ryu, and A.M. Pendergast, *Abl tyrosine kinases in T-cell signaling.* Immunol Rev, 2009. **228**(1): p. 170-83.
250. Duensing, A., et al., *Mechanisms of oncogenic KIT signal transduction in primary gastrointestinal stromal tumors (GISTs).* Oncogene, 2004. **23**(22): p. 3999-4006.
251. Tuveson, D.A., et al., *STI571 inactivation of the gastrointestinal stromal tumor c-KIT oncoprotein: biological and clinical implications.* Oncogene, 2001. **20**(36): p. 5054-8.
252. Chong, Y.P., et al., *Endogenous and synthetic inhibitors of the Src-family protein tyrosine kinases.* Biochim Biophys Acta, 2005. **1754**(1-2): p. 210-20.
253. Frame, M.C., *Src in cancer: deregulation and consequences for cell behaviour.* Biochim Biophys Acta, 2002. **1602**(2): p. 114-30.
254. Lowell, C.A., *Src-family kinases: rheostats of immune cell signaling.* Mol Immunol, 2004. **41**(6-7): p. 631-43.
255. Xu, Y., et al., *Lyn tyrosine kinase: accentuating the positive and the negative.* Immunity, 2005. **22**(1): p. 9-18.

256. Linnekin, D., C.S. DeBerry, and S. Mou, *Lyn associates with the juxtamembrane region of c-Kit and is activated by stem cell factor in hematopoietic cell lines and normal progenitor cells.* J Biol Chem, 1997. **272**(43): p. 27450-5.
257. Meyn, M.A., 3rd, et al., *Src family kinases phosphorylate the Bcr-Abl SH3-SH2 region and modulate Bcr-Abl transforming activity.* J Biol Chem, 2006. **281**(41): p. 30907-16.
258. Dai, Y., et al., *A Bcr/Abl-independent, Lyn-dependent form of imatinib mesylate (STI-571) resistance is associated with altered expression of Bcl-2.* J Biol Chem, 2004. **279**(33): p. 34227-39.
259. Gamas, P., et al., *Inhibition of imatinib-mediated apoptosis by the caspase-cleaved form of the tyrosine kinase Lyn in chronic myelogenous leukemia cells.* Leukemia, 2009. **23**(8): p. 1500-6.
260. Giroux, V., J. Iovanna, and J.C. Dagorn, *Probing the human kinome for kinases involved in pancreatic cancer cell survival and gemcitabine resistance.* FASEB J, 2006. **20**(12): p. 1982-91.
261. Rikova, K., et al., *Global survey of phosphotyrosine signaling identifies oncogenic kinases in lung cancer.* Cell, 2007. **131**(6): p. 1190-203.
262. Paulson, T.G., et al., *Chromosomal instability and copy number alterations in Barrett's esophagus and esophageal adenocarcinoma.* Clin Cancer Res, 2009. **15**(10): p. 3305-14.
263. Shivakrupa, R. and D. Linnekin, *Lyn contributes to regulation of multiple Kit-dependent signaling pathways in murine bone marrow mast cells.* Cell Signal, 2005. **17**(1): p. 103-9.
264. Ito, T., H. Tanaka, and A. Kimura, *Establishment and characterization of a novel imatinib-sensitive chronic myeloid leukemia cell line MYL, and an imatinib-resistant subline MYL-R showing overexpression of Lyn.* Eur J Haematol, 2007. **78**(5): p. 417-31.
265. Scholl, C., et al., *Synthetic lethal interaction between oncogenic KRAS dependency and STK33 suppression in human cancer cells.* Cell, 2009. **137**(5): p. 821-34.
266. Metzger, R., et al., *CUL2 and STK11 as novel response-predictive genes for neoadjuvant radiochemotherapy in esophageal cancer.* Pharmacogenomics. **11**(8): p. 1105-13.
267. Rosman, D.S., V. Kaklamani, and B. Pasche, *New insights into breast cancer genetics and impact on patient management.* Curr Treat Options Oncol, 2007. **8**(1): p. 61-73.
268. Cheyette, B.N., *Ryk: another heretical Wnt receptor defies the canon.* Sci STKE, 2004. **2004**(263): p. pe54.
269. Linch, M., J. Claus, and C. Benson, *Update on imatinib for gastrointestinal stromal tumors: duration of treatment.* Onco Targets Ther, 2013. **6**: p. 1011-23.